Alex Sagalovych,
Vlad Sagalovych,
Viktor Popov,
Stas Dudnik,
Oleksander Olijnyk

Avinit vacuum-plasma technologies in transport machine building

Monograph

General editorship
Doctor of Technical Sciences, Professor
Vlad Sagalovych

November, 2021

Scientific Route

Tallinn
Estonia

Published in 2021
by «Scientific Route» OÜ
Narva mnt 7-634, Tallin, Harju maakond, Estonia, 10117

DOI: 10.21303/978-9916-9516-7-5

ISBN 978-9916-9516-6-8 (Hardback)
ISBN 978-9916-9516-7-5 (eBook)

Authors

Alex Sagalovych
Academician of Academy of Technological Sciences of Ukraine.
Head of Department of Special Technologies Board.
Leading specialist of Ukraine in the field of the latest technologies for applying functional coatings using the latest physical ion-plasma processes and technologies.
The memder of ASM (Am. Soc. of Materials, USA), TMS (Minerals, Metals & Materials Soc.,USA), SVC (Society of Vacuum Coaters, USA), HTS (Heat Treating Society, USA).
ORCID: https://orcid.org/0000-0003-2136-2740

Vlad Sagalovych
Academician of Academy of Technological Sciences of Ukraine.
Doctor of Technical Sciences, Professor.
Honored Worker of Science and Technology of Ukraine.
Chief Technical Officer.
Well-known scientist in the field of coating physics and chemistry, nonequilibrium plasma chemistry.
ORCID: https://orcid.org/0000-0002-8060-3201

Viktor Popov
Academician of Academy of Technological Sciences of Ukraine.
Doctor of Technical Sciences.
Laureate of the State Prize of Ukraine in the field of science and technology.
Honored Mechanical Engineer of Ukraine.
Chairman of the Management Board.
ORCID: https://orcid.org/0000-0001-7216-2138

Stas Dudnik
PhD.
Head of Technological Department.
Well-known scientist in the field of physics and technology of modern vacuum-plasma coatings.
ORCID: https://orcid.org/0000-0003-2074-4739

Oleksander Olijnyk
PhD.
Leading Process Engineer of the Mechanical Testing and Wear Resistance of the Central Factory Laboratory. State Enterprise «Plant named Malysheva».
Renowned specialist in tribology.
ORCID: https://orcid.org/0000-0002-0115-7697

Abstract

Transport engineering is one of the areas in which coatings for various functional purposes are widely used. Among the many methods used for coating, the group of vacuum-plasma methods occupies one of the leading directions in the field of obtaining coatings with unique characteristics that make it possible to significantly increase the operational characteristics of machines and mechanisms lay down new design solutions for their improvement. The monograph presents the results of the development and practical implementation of new nanomaterials and nanotechnologies for the deposition of Avinit coatings for various functional purposes. A distinctive feature of the presented developments is the integrated use of various vacuum-plasma and plasma-chemical coating methods (vacuum-arc, magnetron), vacuum-plasma processing and diffuse surface saturation. The experimental and technological equipment created for this — the Avinit vacuum-plasma automated cluster — makes it possible to implement various methods of coating deposition, combined into one technological cycle. In the monograph, much attention is paid to the results of experimental studies of obtaining coatings of various compositions and the study of their tribological characteristics in friction pairs with such coatings, as well as other properties. The issues of stability of characteristics of coatings in time are considered, as well as the criteria for such stability. Based on the research carried out, a number of experimental industrial technologies for applying coatings for various functional purposes (reinforcing anti-seize, protective) on parts of transport engineering (pistons and rings of internal combustion engines, fuel equipment, etc.) have been developed, examples of the successful application of the developed technologies in mass production are given. aeronautical and other purposes The monograph also discusses the issues of creating highly efficient tools for processing machine parts and mechanisms, including with precision accuracy, and presents the results of developments in this area.

The book is intended for specialists working in the field of ion-plasma modification of the surface of materials and the application of functional coatings on parts of transport engineering and other industries.

Keywords

Avinit vacuum-plasma coatings, tribological characteristics of coatings, protective and wear-resistant coatings, tools, experimental industrial technologies, transport engineering.

Contents

List of Tables

List of Figures

Preface

The monograph offered to the reader is intended for specialists working in the field of surface modification of materials and the application of functional coatings on parts of transport engineering and other industries. Among the many methods that are used for coating, the group of vacuum-plasma methods occupies one of the leading directions in the field of obtaining coatings with unique characteristics that make it possible to significantly increase the operational characteristics of machines and mechanisms, lay down new design solutions for their improvement. A distinctive feature of the presented developments is the integrated use of various vacuum-plasma and plasma-chemical methods of coating (vacuum-arc, magnetron), vacuum-plasma processing and diffusion surface saturation. The experimental and technological equipment created for these purposes — the Avinit vacuum-plasma automated cluster — makes it possible to implement various methods of coating deposition, combined in one technological cycle. On the basis of the research carried out, a number of experimental and industrial technologies for applying coatings of various functional purposes (strengthening, anti-seize, protective) on parts of transport engineering (pistons and rings of internal combustion engines, fuel equipment, etc.) have been developed. Examples of the successful application of the developed technologies in the mass production of aviation technical and other products are given. The monograph also discusses the issues of creating highly efficient tools for processing machine parts and mechanisms, including with precision accuracy, and presents the results of developments in this area.

The book is intended for specialists working in the field of ion-plasma modification of the surface of materials and the application of functional coatings on parts of transport engineering and other industries.

1

Introduction

Improving the quality of engineering products is one of the main factors in the development of the Ukrainian economy. At present, the restoration and development of the production of internal combustion engines (ICE), which are one of the most complex mechanical engineering products, requires achieving and exceeding the world level of their quality. The high level of competition in the world market, the constant increase in requirements for environmental performance of production and operation, efficiency, overall performance, reliability and service life of internal combustion engines, necessitate the development and development of new design solutions, progressive technologies, materials and coatings with an increased level of technical characteristics [1].

For the reliable operation of the internal combustion engine, materials must have high strength indicators of plasticity, resistance to fatigue and corrosion damage, heat resistance and heat resistance, etc. One of the most important characteristics of materials for parts of friction pairs of internal combustion engines are the characteristics of antifriction properties, seize resistance and wear resistance. These indicators largely determine the technical and economic level, reliability and durability of the internal combustion engine, the ability of highly loaded parts to withstand overloads due to the modern level of forcing.

One of the main causes of wear in metallic materials is the tear of rubbing surfaces. With an unfavorable ratio of materials of parts in contact, their thermodynamic state, structure and mechanical properties, the formation of build-ups, scoring, galling, catastrophic damage to friction surfaces and wear occurs.

Various means are used to prevent tear or reduce damage to an acceptable level [2]:

- choose a combination of materials for rubbing pairs with a minimum adhesion according to the compatibility criteria [3, 4];
- alloying metals in order to reduce the tear ability and increase the extreme pressure properties;
- increase the rigidity of the damaged surfaces by appropriate heat treatment;
- change the composition and condition of the surface layers by chemical-thermal treatment (carburizing, nitriding, sulfiding, etc.) and surface modification (laser, electron-beam hardening, coating);

- a coating of soft metals (In, Cd, Sn, Ag, Cu, brass, etc.) is applied on the friction surface;
- introduce soft components (Pb, Sn) into antifriction alloys;
- use materials that perform the functions of a solid lubricant (graphite, molybdenum disulfide, etc.);
- for the manufacture of rubbing parts, materials are used that have low adhesion relative to the counterbody material (carbon-graphite antifriction materials, ruby, oxide ceramics, diamond).

However, traditional methods of chemical-thermal treatment have significant drawbacks — a significant duration of processes, the need for final machining of hardened surfaces, energy consumption, a negative impact on the environment, the threat of unwanted flooding, and many others, in particular, the need to carry out strengthening treatments in various technological production cycles.

Alloying the base material of the parts is not always advisable, since it leads to their rise in price, while the requirements for the properties of the base materials and working surfaces may differ significantly. In connection with a sharp difference in the requirements for the material properties of parts of friction units in the volume and in a thin surface layer, which determines the parameters of friction and wear, it is more and more important to use new technologies for applying protective, wear-resistant, antifriction and running-in coatings. expanding the possibilities of forming working layers that meet the compatibility criteria, as well as achieving maintenance-free machines with a comprehensive solution to the problem of a sharp multiple increase in the resource of parts with full consideration of all boundary states [5].

Exceeding the permissible wear values of such parts in operation leads to a loss of engine power, an increase in harmful emissions into the atmosphere, noise, vibrations, dynamic loads, excessive losses of fuel, oils and other undesirable consequences.

Methods of creating second protective structures of a dissipative type during the running-in period and the initial stages of testing and operation of machines and mechanisms are of greatest interest from the point of view of achieving the required set of tribotechnical properties for the near-surface layers of parts of friction units. From the point of view of thermodynamics, such structures are nonequilibrium, and practically all processes that increase the tribological compatibility of materials are nonequilibrium. Such non-equilibrium processes also increase the self-organization of the secondary protective structure [6].

The tendencies in the development of engine building indicate that the power and temperature loads in the contact zone of the parts of friction units are constantly increasing. Therefore, for protective coatings, it is advisable to use metal-like carbides, nitrides, borides, silicides of refractory transition metals (Mo, Nb, Ti, Zr, etc.), as well as oxide and oxygen-free compounds

of boron, aluminum, silicon (BN, B_4C, AlN, Al_2O_3, SiC, Si_3N_4, etc.). Due to the high non-technological nature, the manufacture of parts from such compounds in most cases is impractical or economically unprofitable.

This monograph is devoted to solving the problems of modern engine building in the reliability and durability of ICEs produced, which can provide technologies for modifying the surface layers of contacting materials and applying wear-resistant and antifriction coatings to improve the tribotechnical characteristics of friction pairs.

In connection with a sharp difference in the requirements for the material properties of parts of friction units in the volume and in a thin surface layer, which determines the parameters of friction and wear, it is more and more important to use new technologies for applying protective, wear-resistant, antifrictional and running-in coatings. expanding the possibilities of forming working layers that meet the compatibility criteria [3], as well as achieving maintenance-free machines with a comprehensive solution to the problem of a sharp multiple increase in the resource of parts with full consideration of all boundary states [4].

A successful solution to the problems posed is provided by the technologies for modifying the surface layers of contacting materials and the application of wear-resistant and antifriction coatings to improve the tribotechnical characteristics of friction pairs.

2

Methods for creating layers with increased wear resistance

The conflicting requirements for surface (high rigidity and wear resistance, high antifriction properties) and bulk (high strength and toughness) properties can be met by creating compositions with a layer-by-layer arrangement of materials that perform various functions. Due to the fact that the permissible wear of machine parts is small (usually no more than a particle of mm), the thickness of the surface layer with a given set of tribotechnical properties can be small.

The deposition of coatings on one or the other materials not only improves their characteristics, but leads to the formation of a new composite material with a set of parameters inherent in it [7, 8].

Many works are devoted to the study of the wear resistance of various coatings on the working surfaces of machine parts used in friction pairs [7–13].

In order to increase wear resistance and antifriction properties on the working surface of the piston made of G-AlSi (Cu) alloy to the motor of the tractor engine SMD-14, D37-14, etc. anodic oxidizing coatings with a thickness of 20–30 microns were applied, which did not undergo noticeable destruction during engine tests for 2000 hours at an exhaust gas temperature of 530 °C.

In [7], the wear resistance and antifriction properties of anodized coatings on pistons made of the aluminum alloy GK-AlSi12 (Cu) (Si — 12.7 %, Mg — 1.2 %, Cu — 1.1 %, Ni — 1 %) were studied. It is shown that sufficiently high antifriction properties of anodized piston anodic coatings contribute to an increase in the efficiency of a diesel engine and its economy by 1.5 %.

Coatings based on the cermet Cr-Ni-Si-B, which are characterized by high hardness, exhibit good seize resistance. The work [14] provides data on the effect of cermet coatings on the resistance to seize under dry friction conditions. Coatings were applied to X10CrNiTi18-9 steel specimens by surfacing (enameling) in a protective atmosphere (argon, vacuum). The coating thickness was 250—300 microns. The coating of the composition (% weights): 1M — 20 Cr, 70 Ni, 5 Si, 5 B and the coating of BM based on chromium boride with a binder of the previous composition 60 CrB_2 + 40 (Cr-Ni-Si-B) were studied. Stelite surfacing on X10CrNiTi18-9 base was used as a reference. Before testing, the samples were rubbed on

a cast iron plate until the roughness of the rubbing surfaces was obtained according to class 8. The specific load was set to 125 kgf/cm^2. The resulting coatings had a heterogeneous structure in which chromium boride particles are cemented with a metal binder. Chromium beard, distinguished by its very high rigidity, favorably affects the resistance of the coating to seize.

Table 2.1 shows the test results for X10CrNiTi18-9 steel galling with heat-resistant coatings [14].

Table 2.1 Test results for X10CrNiTi18-9 steel galling with coatings

Type of coating of the sample		Test mode		Test results
of the top	of the bottom	Temperature, °C	Specific pressure, kgf/cm^2	
1M	1M	20	50	No burr
		20	100	Burr
stealth G	BM	20	50	–
		20	75	No burr
		20	100	–
stealth C	BM	20	50	–
		20	75	No burr
		20	100	–
stealth C	BM	300	25	stealth

As it is possible to see from the Table 2.1, 1M coating is resistant to seize under normal temperature conditions at specific loads up to 100 kgf/cm^2. Specimens coated with BM, when tested on stelite, showed high resistance to seize. At a temperature of 20 °C and loads of 50, 75, 100 kgf/cm^2, the samples consistently withstood 900 cycles without scoring, at a temperature of 300 °C and a specific load of 25 kgf/cm^2 — 300 cycles, and as a result of these tests, seizes appeared deposited with stelite. The higher galling resistance of the BM samples is, perhaps, due to the higher concentration of chromium boride.

Among the coating methods, a special place is occupied by methods of forming coatings from ionized atomic and molecular flows.

Vacuum ion-plasma methods based on the action on the surface layers of streams of neutral and excited particles (atoms, clusters) with high energy, tens and hundreds of times higher than the energy of thermal atoms and molecules, and ions, the energy of which can vary in wide layers.

When such high-energy particles come into contact with the surface to be coated, conditions are created in microvolumes that ensure the formation of chemical bonds without volumetric heating of parts. In this case, the application of coatings is possible at significantly lower temperatures.

The ability to change the energy of ionized particles of the flow of condensed matter over a wide range (from units to hundreds of thousands of eV) makes it possible to effectively influence most of the practically important characteristics of coatings (density, adhesion, structure, and others) and thereby achieve high values of the corresponding indicators. Another important feature that distinguishes ion-plasma methods is the ability to create multicomponent composite materials under nonequilibrium conditions of their formation. It becomes possible to obtain superhard compounds (carbides, nitrides, oxides and their compounds) by plasma-chemical synthesis at lower temperatures, to form amorphous structures or metastable phases, chemical compounds that cannot be reproduced by other methods. This is a prerequisite for creating materials with higher, sometimes unique, properties compared to existing materials.

Three groups of vacuum ion-plasma methods of coating and surface modification can be distinguished:

- Ion-diffusion saturation (ion nitriding, carbidization, etc.), used to saturate the surface layers with nitrogen, carbon, silicon, obtain carbonitride layers. Due to the radiation stimulation processes, saturation can be performed at lower temperatures and at significantly faster rates than with traditional methods.
- Ion deposition, in which particles of the applied material, converted in one way or another into a gaseous or vapor state, are ionized and accelerated in an electric field — vacuum arc spraying, magnetron sputtering, reactive electron plasma sputtering, atomic ion sputtering, etc. An increase in the energy of particles, set by the accelerating voltage, significantly increases the adhesion and service characteristics of the coatings. With magnetron sputtering carried out in crossed electric and magnetic fields, there is practically no droplet component of the condensed phase, which makes it possible to apply a coating without distorting the original surface quality.
- Ion doping and implantation, based on the phenomenon of the deepest penetration of ions into the crystal lattice at high energies. Due to radiation-stimulated diffusion, surface modification and alloying of surface layers are carried out to a considerable depth.

With reactive methods of ion deposition, plasma-chemical reactions take place with ions of working gases, which are introduced into the reaction chamber, which makes it possible to obtain a coating from various chemical compounds (carbides, nitrides, silicides, etc.). Thus, it is possible to obtain a coating of a complex composition, multilayer, composition varying in thickness, etc. When using reactive plasma-chemical methods of ion deposition, the formation of coatings occurs in non-equilibrium conditions, as a result of which chemical compounds can be formed, which in composition, structure and properties are very different from bulk materials (obtained under equilibrium conditions).

The main characteristics of coatings, which determine its main tribological functions in the process of friction, include wear resistance and coefficient of friction.

A large amount of experimental material on the effect of various vacuum-plasma coatings on tribological characteristics is summarized in [15–17].

Studies of wear resistance and frictional properties of friction surfaces of the most common TiN coating and some others, obtained by vacuum arc spraying on structural and tool steels [18, 19], have shown their high wear resistance and the possibility, at the same time, of obtaining relatively low values of the friction coefficients of coatings paired with some materials, in particular, with gray alloy cast iron used in the manufacture of cylinder liners for diesel locomotives.

Studies of the phase composition of coatings obtained by vacuum ion-plasma methods of titanium deposition in a nitrogen atmosphere reveal the presence of three phases depending on the nitrogen pressure — α-i, ε-i2N and δ-iN. The value of the partial pressure of nitrogen at which is realized and either the other phase, or their combination, depends on the equipment and its characteristics and conditions for the formation of a coating on the substrate, among which the temperature and bias potential have the greatest influence. The partial pressure of nitrogen, at which titanium nitride phases are already found in the coatings, is located at the boundary, about $1 \cdot 10^{-3}$ Pa.

An increase in the partial pressure of nitrogen is accompanied by a transition from the heterophase composition of the coating, followed by the disappearance of the α-Ti, ε-i2N phases, to the single-phase state δ-iN. This transition can occur even when the total nitrogen concentration reaches ~38–40 atm. %, Which is close to the limit of homogeneity δ-iN.

One of the characteristics widely used to assess the strength of coatings is their microhardness.

As studies of coatings with the Si-composition have shown, there is a fairly good correlation between the change in the phase composition of the coatings and the course of the curve of the dependence of the microhardness value on the nitrogen concentration in the coatings or the partial pressure at which the coating was obtained. Although there is a discrepancy in the absolute values of microhardness, which are given by different authors, the maximum microhardness (~28–32 GPa) falls on the range of nitrogen concentrations corresponding to the heterophase composition of the coatings. It is these coatings that show the maximum wear resistance under dry friction conditions, where abrasive wear is the predominant cause of destruction of the contacting surfaces.

In this case, it is also necessary to take into account the structural, orientational and other characteristics that determine the physical and mechanical properties of the coating as a whole.

The application of coatings of TiN, CrN, MoN with a thickness of 2–5 microns makes it possible to increase the durability of the plunger pairs

by 5 times, the service life — by 2–2.5 times, improve the running-in and wear resistance.

Promising results were obtained when working coatings of TiN, CrN, MoN with a counterbody of gray cast iron, bronze CuAl8Fe3.

When friction with steel, single-layer TiN, TiCN, MoN coatings have high wear resistance.

The development of plasma technologies made it possible to control with a high degree of accuracy the pressure and composition of the reaction gas, the degree of focusing of the plasma flow and its separation from the droplet phase. All this contributed to the development of technologies for obtaining composite coatings.

Controlling the technological process of coating molding makes it possible to obtain compositions with variable properties depending on the percentage of components. A change in the composition of the coating leads to a change in stiffness, coefficient of friction, surface roughness, etc. characteristics, allowing to achieve optimal coating properties for solving specific problems.

A coating of multicomponent nitrides shows good results [19]. Such systems (TiCrN, TiMoN, NbZrN) have high thermodynamic stability, acceptable values of hardness and toughness, significantly exceeding brittle oxides, carbides, borides.

Multicomponent nitride coatings containing aluminum show a significant increase in performance [20, 21].

One of the types of such coatings is TiAlN. This coating has high rigidity and temperature resistance. The coating is characterized by increased elasticity, which significantly reduces the possibility of chipping from the working surface.

During the formation of functional wear-resistant, antifriction and other layers that are in direct contact with the counterbody during operation, recently, composite coatings such as (TiAl) N, (TiCr) N, (MoAl) N have been intensively studied [22–25].

Low friction coefficients give two-layer, multilayer and composite coatings TiN + Mo, TiN + Ti, TiN + bronze.

In order to clarify the possibility of using composite coatings in friction units, the tribotechnical properties of composite coatings Ti-Cu-N, Ti-Al-N, Mo-Al-N, obtained by the vacuum arc method, have been investigated.

The coatings were applied to samples made of nitrided steel 1.8509. The tests were carried out on friction machine in M14B2 oil, temperature 340K, load 1.0 kN, test time 1 hour. Roughness of coatings Ra = 0.32–0.64 microns. **Table 2.2** shows the values of volumetric and weight wear «coating-bronze Br 012 (Sn 12 %)».

As can be seen from the data presented, all the studied composite coatings significantly increase the wear resistance of the sample — shoes, in addition, provide a low wear capacity of the coating.

Table 2.2 Results of studying the wear of a «coating-bronze Br 012» pair

The composition of the coating	The thickness of the coating, μm	The average weight wear of the coating V_p, g	The average weight wear of the shoe V_k, g	The coefficient of friction F_{fr}
Ti-Al-N	10	0.0001	0.0099	0.008
Ti-Cu-N	10	0.0001	0.0055	0.032
Mo-Al-N	10	0.0001	0.0015	0.03
without coating	—	0.010	0.0072	0.07

The aluminum concentration in the Ti-Al-N coating has a significant effect on the coefficient of friction F_{fr}. The smallest values of the coefficient of friction are realized when the concentration of aluminum in the coating is 10–15 % (**Fig. 2.1**).

The use of composite coatings paired with bronze Br 0.12 leads to a decrease in the coefficient of friction, in addition, provides a low wear capacity of the coating.

A good set of properties is realized on TiN-bronze coated specimens. They turn out to be practically wear-resistant, like TiN, but have several times lower wear capacity. Multilayer TiN-α-Ti coatings are characterized by a more stable coefficient of friction.

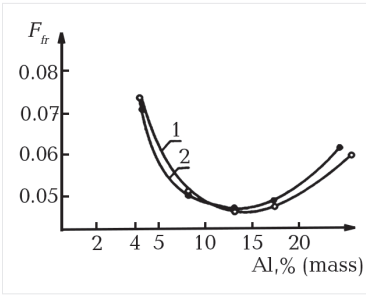

Fig. 2.1 Dependence of F_{fr} on the aluminum content at loads: 1–0.6 kN, 2–1.8 kN

Table 2.3 shows the values of the friction coefficients F_{fr}, averaged for each coating over all loads, the average weight wear of the coating V_c during the test, the maximum depth of the wear groove h, as well as the highest specific load in the friction zone (lubricant M14B2, V=1.3 m/s, friction pair «coating-sleeve cast iron», test time 1 hour).

Comparison of the above results shows that composite coatings have the highest wear resistance. These coatings are also characterized by a minimum measurable wear value. During testing, they wear out to a depth of 0.7–0.9 microns. Composite coatings are also characterized by a more stable coefficient of friction.

Coatings of the Ti-Al-N system have higher values of rigidity and temperature resistance than Ti-N. Such coatings as TiCrN, TiMoN, NbZrN are characterized by high thermodynamic stability, rather high values of stiffness and toughness, significantly exceeding the corresponding brittle oxides, carbides, borides.

Table 2.3 Results of studying the friction and wear of composite coatings

Coating	Chrome (galvan)	TiN	Ti-Al-N	Ti-Cu-N	Mo-Al-N
Thickness, μm	10	10	10	10	10
F_{fr}	0.10	0.11	0.05	0.064	0.067
h, μm	2.5	1.8	0.7	0.9	0.8
V_c, g	0.019	0.008	0.003	0.003	0.004
Maximum specific load in the friction zone, MPa	18100	25000	30760	28570	26700

Coatings of the Ti-Al-N system have higher values of rigidity and temperature resistance than Ti-N. Such coatings as TiCrN, TiMoN, NbZrN are characterized by high thermodynamic stability, rather high values of stiffness and toughness, significantly exceeding the corresponding brittle oxides, carbides, borides.

Vacuum-arc coatings, which have found wide application for increasing the durability of cutting tools, possessing high hardness, wear resistance and thermal stability, are practically not used in friction units of machine parts, mainly due to the high level of wear of the counterbody.

Studies in the field of creating new materials with record characteristics in terms of wear resistance, the ability to work in extreme conditions show the high prospects of composite coatings, which are multilayer and nanolayer coatings — a number of alternating different compositions and thicknesses with structural elements that have sizes from several hundred. to units of nanometers.

Such materials, in comparison with materials of the same composition with a conventional structure, can have several times higher corresponding characteristics in terms of tribological and other properties. With the correct choice of the layer design, one can hope for the creation of coatings that combine the high wear resistance of the coating and the low wear of the counterbody.

An example of such composite coatings is, for example, TiN-AlN-TiAlN. The thickness of each layer can vary from a few nanometers to a few microns.

When microdesigning multilayer coatings, it is advisable to create soft interlayers before applying hard coatings. The soft layer increases the adhesion of the coating to the substrate, ensures the presence of a large positive gradient of mechanical properties in the coating, which is a good condition for normal operation under friction conditions. Such layers prevent the propagation of cracks that occur during operation. Usually chromium, molybdenum, α-Ti are used as soft sublayers.

The creation of composite coatings with intermittent layers makes it possible to increase the rigidity and reduce the abrasive wear of the resulting coating.

Multilayer composite coatings have advantages in some cases over mono coatings, for example, in friction units. Yes, vacuum-arc TiN coatings, although they have high wear resistance and thermal stability, often cause increased wear of the counterbody. At the same time, composite coatings of the CrxN-TiN type can be combined with increased rigidity with low wear of the counterbody.

The work [22] shows the possibility of increasing the wear resistance of samples made of NiCrMoV6 55 steel with a low tempering temperature by applying a vacuum-arc method of multilayer CrxN-TiN coatings followed by heat treatment. Multilayer CrxN-TiN coatings [22–25] combine high wear resistance of the coating and low wear of the counterbody.

Application of multilayer CrxN-TiN coatings containing up to 20 alternating layers (thickness ratio CrxN:TiN=5:1) with a total thickness of up to 3 microns with preliminary treatment of the coated surface with chromium ions. The wear of such coatings is 2...2.5 times less compared to single-layer CrxN coatings.

In [24, 25], it is noted that the rigidity and strength of a multilayer coating increases with a decrease in the thickness of individual layers. So, if single-layer TiAlCrN coatings have a hardness of 24 GPa, then multilayer TiAlN-CrN coatings with layer thicknesses of 15 and 6 nm, respectively, have a hardness of 35 GPa.

A very promising method is duplex treatment, which combines in a single technological cycle plasma nitriding in a two-stage vacuum arc discharge (TVAD) with the formation of sufficiently thick nitride layers with high hardness, heat resistance and crack resistance, followed by deposition [26, 27].

Thus, in terms of the totality of properties, composite coatings are the most interesting and promising for industrial applications.

3

Experimental studies of Avinit technologies

3.1 Experimental equipment – Avinit vacuum-plasma cluster

All experimental-research and pilot-industrial developments on the application of functional multilayer composite coatings on parts with surfaces of various geometries with precision processing were carried out by us on the developed and created experimental-technological equipment — the automated vacuum-plasma cluster Avinit, which makes it possible to implement complex methods. coating and ionic surface treatment combined in one technological cycle.

Vapor deposition methods (CVD and PECVD):

- Vacuum arc coating method.
- Magnetron coating method.
- Electron beam coating method.
- Plasma diffuse saturation methods.
- Ion-plasma cleaning methods.

A detailed technological vacuum-plasma automated cluster Avinit with high energy saturation with power sources of various types (gas-phase and vacuum-arc evaporators) for obtaining multicomponent multilayer coatings is described in [28–31].

It consists of several functional blocks (**Fig. 3.1**):

1. Avinit C block (methods of modernized vacuum-arc coating) for obtaining hard and superhard multilayer and layered functional coatings from metals, alloys and their compounds with nitrogen, carbon, oxygen.

When obtaining Avinit C coatings, it is possible to switch to the nano-range for the implementation of the processes of controlled formation of multicomponent nano- and microstructured coatings with a nanolayer thickness from units to hundreds of nanometers.

2. Avinit V block (methods of vapor deposition (CVD and PECVD)), designed for vacuum-plasma and plasma-chemical surface treatment and the application of functional metal and metal-carbide coatings based on molybdenum, tungsten, chromium by thermal decomposition of organometallic compounds, in mainly hexacarbonyl Mo, W, Cr and their compounds with nitrogen, carbon, etc. on the inner and outer surfaces of parts.

The use of gas-phase and plasma-chemical methods in combination with other methods of coating and surface modification (methods of ion doping, implantation, vacuum-plasma, diffusion, vacuum-thermal methods, etc.) significantly expands the possibilities of creating fundamentally new materials.

Among the known methods of applying high quality coatings, the CVD and PECVD methods are out of competition in most cases when it is necessary:

- Apply high-density coatings of uniform thickness to products of complex shape with a developed surface, including blind holes, internal cavities and pipes made of $L/d \gg 1$ (L is the length of the pipe, d is its diameter).
- Realize high productivity of coating processes in which the growth rate can reach from several hundred microns per hour to several millimeters per hour.
- Obtain a coating of refractory, hard-to-machine metals, alloys and compounds with a density close to theoretical and high purity, form from them self-supporting products of different geometries with a wall thickness of up to 10 mm or more from various materials, including difficult to machine (for example, W) materials and unique alloys from immiscible components (for example, Mo-Cu) (vapor-phase metallurgy.

3. Avinit M block for applying coatings (monolayer, multilayer, nanolayer and nanostructured) of metals and their various compounds by magnetron sputtering methods.

4. Avinit E block for ion-plasma surface treatment of materials in high-density plasma in various gas media of various compositions (argon, nitrogen, carbon-containing gases and mixtures of these gases), including internal cavities and channels of certain sizes, providing high values of coating adhesion.

In the implementation of technological processes for the application of functional hardening and protective coatings Avinit, a very thorough ionic treatment (cleaning) of the surface of products using a glow discharge is provided; using a gas plasma generator of the Avinit cluster; using metal ions.

5. Avinit N block for carrying out processes of ion-plasma surface modification, in particular, for ion-plasma surface treatment, plasma diffusion saturation (nitriding, nitrocarburizing, etc.) of parts made of steels and alloys in high-density low-temperature nonequilibrium plasma, precision nitriding, processes diffuse and saturation in plasma with a hollow cathode.

Avinit N block provides nitriding processes for the surface of parts made of steels and alloys in a high-density non-equilibrium plasma of a non-self-sustaining glow discharge. with a density several orders of magnitude higher than with ion nitriding in a conventional glow discharge, as a result of which the formation of a nitrided layer is intensified by 2–5 times in comparison with the processing by the traditional method of ion nitriding in a glow discharge and 5–10 times compared with gas nitriding.

6. Avinit T block for thermal and thermochemical treatment.

7. Avinit S block for electron-beam coating.

Fig. 3.1 Elements of the Avinit vacuum-plasma cluster

The multipurpose automated cluster Avinit provides an operation mode when using any evaporative devices, systems and control devices included in its composition, while simultaneous operation of all evaporators of the same type or alternate (in any sequence) of different types of evaporation devices is allowed.

The use of the developed automated system makes it possible to select the most optimal modes and methods of surface treatment and coating or their combination to achieve the maximum technical and economic effect in solving specific problems, to achieve strict adherence to certified technological regimes and to achieve the best high quality indicators when applying functional coatings in the conditions of serial production.

3.2 Research methods and techniques

The development of processes for the deposition of multifunctional multilayer composite coatings was carried out on an automated vacuum-

plasma cluster Avinit according to a given program using one-component cathodes in a reaction gas medium and without it. All the main characteristics of the coating process were monitored automatically.

3.2.1 Methods of sample preparation

The prototypes were placed in the technological equipment and could move, depending on the selected technological scheme, around their axis, move around the axis passing through the center of the vacuum chamber, or perform planetary motion with rotation around its axis and the axis of the chamber simultaneously.

Movable shutters were placed between the cathode (targets) and technological equipment with prototypes, which made it possible to «cut off» the initial uncontrolled stage of the technical process and establish a stationary mode of ionization and condensation.

The setting of the optimal stationary mode depends to a large extent on the homogeneity of the target structure (with magnetron sputtering) or cathodes (with vacuum-arc sputtering). These factors determine the required stability of the temperature regimes of deposition and the continuity of the structural-phase state and chemical composition of the coating.

The deposition of multicomponent or composite coatings was carried out using single-component cathodes with simultaneous operation of several sputtering sources in a pulsed or continuous mode with or without the use of reaction gases. The samples were placed in a rotary or planetary tooling, which ensured the rotation of the samples simultaneously around its axis and the center of the chamber.

Titanium Ti2, aluminum Al0, molybdenum Mo99.9 vacuum-melted, Cu, Cr were used as cathode (target) materials. Argon, nitrogen, and benzene served as plasma-forming and reaction gases. The main impurity in nitrogen was oxygen, the level of which did not exceed 0.04 at. %. The composition of residual gases and impurities in the reaction gas was monitored using an MX-7304A technological mass spectrometer.

Structural steel X155CrVMo12-1 and heat-resistant steel X155CrVMo12-1, widely used in the production of many precision friction units, were chosen as samples. Samples of steel 1.773 with dimensions of 20×10×5 mm were polished to a roughness of class 8 (Ra=0.32 μm). Microhardness HB~900. Specimens of steel X155CrVMo12-1 56...61HRC, 10×10×10 mm in size, were polished to a roughness of class 10 (Ra=0.063 microns) according to factory technologies to the required geometric parameters.

A feature of the preparation of samples is that their preliminary heat treatment was carried out in full compliance with the technological regulations for the processing of end products adopted in production. As the studies have shown, this has a significant effect on the quality of the resulting coating.

3.2.2 Technique of coating application

The development of processes for the deposition of new multifunctional multilayer composite coatings was carried out on the Avinit vacuum cluster created for the implementation of complex coating methods (plasma-chemical CVD, vacuum-plasma PVD (vacuum arc, magnetron), ion saturation and ion surface treatment).

Hardware and technological developments have been completed (the use of improved separation devices, improved diagnostics of plasma and gas flows, improvement of IR measurements (in the infrared range) of temperature fields of coated products, improvement of mechanical and electronic systems for protection against micro-arcs and modernization of cathodes. Possibilities of technological equipment and ensuring the deposition of high-quality coatings on precision surfaces.

Avinit coatings adhere to precision surfaces of high cleanliness class up to 12 — 13 class without reducing the class of surface cleanliness. This is achieved by using effective methods of surface cleaning in the technologies being developed — cleaning in Ar glow discharge, cleaning in a two-stage vacuum-arc discharge and cleaning with metal ions at a voltage above the zero growth point, as well as preventing surface damage by micro-arcs, for which the Avin installation has an arc extinguishing system providing high quality cleaning of the surface from oxides and other contaminants without the occurrence of electrical breakdowns. Deposition occurs at low temperatures, not exceeding the tempering temperatures of the base, ensuring the preservation of the mechanical characteristics and the absence of curvature of the coated products.

To implement the processes of controlled formation of multicomponent nano- and microstructural coatings with a controlled composition using vacuum-plasma and plasma-chemical processes, a through synchronization technology has been developed using a computer to control the technological processes of coating deposition. It allows to control the operation of the spraying sources, the admission of the reaction gas and other systems of the installation according to a given program and to keep records of the parameters of the installation during the entire technological cycle.

Before applying the coatings, the vacuum chamber was evacuated to a residual gas pressure of $(2–3)\cdot10^{-3}$ Pa. Then the substrates were cleaned in a glow discharge plasma at Ar pressure of $\sim1\cdot10^{-1}$ Pa and a potential on the substrate of 1300 V for 10 min. and a transition was made to cleaning with metal ions in the plasma of a vacuum-arc discharge with a current of 90–100 A with a closed curtain, which was in front of the samples, in order to reduce the likelihood of micro-arc discharges when the arc plasma source was turned on. After operating the plasma source in this mode for 1–3 minutes. there was a «passivation» of the vacuum environment due to the binding of chemically active components with a film on the surfaces of

the vacuum chamber and its additional disinfection, as a result of which the pressure of residual gases decreased to values ≤ $(0.7–1)\cdot10^{-3}$ Pa.

Glow discharge processing. Glow discharge occurs as a result of electrical breakdown of the interelectrode gap at a relatively low pressure of the gaseous medium and a sufficiently low resistance of the external circuit. Basically, all processes leading to the formation and maintenance of a glow discharge are concentrated in the immediate vicinity of the cathode surface. The gas pressure and the interelectrode distance determine the discharge ignition voltage. When a glow discharge is inflamed, excitation and ionization of the gas occur. The density of charged particles (electrons, ions) can reach significant values; in general, the plasma of a glow discharge is electrically neutral.

The required pressure of the working medium (residual atmosphere, nitrogen, or neutral gas — Ar) was set using a gas leak. The rectified voltage was controlled in the range U=(0...6) kV, the discharge current was I_p=(0...100) mA.

The workpiece to be processed was mounted on a support-holder — a cathode, and thus, in the case of irradiation of conductive materials, they were bombarded with accelerated positively charged ions of the elements of the medium, in the atmosphere of which the glow discharge was burning. The ion energy is proportional to the accelerating potential of the cathode and the multiplicity of the ion charge.

Ionic bombardment of the surface. All experiments using ion bombardment of the surface were carried out at an ion current density of ~ 10 mA/cm, a chamber pressure of ~10–5 mm Hg. Ti, Mo were used as plasma-forming materials (cathodes). Lining material — X162CrMoV12 steel. The temperature of the samples during the experiments was ~150–200 °C, the time of exposure to the plasma flow was 1.5–3.0 min, in order to maintain the set temperature (T_n), the process was carried out in a pulsed mode.

The results indicate the dependence of the rate of condensation and sputtering on the cathode material and ion energy, which is determined by the accelerating potential of the substrate. As the ion energy increases, the contribution of sputtering increases. For each type of ion, there is a value (U_n) at which equilibrium occurs to the process of condensation and sputtering.

On samples made of X162CrMoV12 steel, the change in the phase composition of the surface subjected to bombardment with molybdenum ions with an average energy of ~3 keV (U_n=–1.1 kV) (bombardment time 3 min) at temperatures of 150–200 °C was studied. Depending on the experimental conditions, the formation of monolayers of molybdenum compounds with steel components was observed: FeMo, Fe_2Mo, $FeNi_3$, MoN, Mo_2N, Mo_2C, $FeMoC_2$.

An increase in sample temperature during ion bombardment enhances the surface digestion effect. Traces of machining (surface cleanliness class ~6–8) can be completely destroyed (smoothed) at 600 °C for 1.5 minutes or 3.0 minutes at 400 °C.

With an increase in the bombardment time (dose) with Mo ions at a temperature of 200 °C and 500 °C, the depth of digestion increases, and the roughness increases. In this case, the class of surface cleanliness is determined by the micro- and macrostructure of the bombarded material.

The microhardness of the materials under study does not change noticeably if the temperature of the samples during bombardment with molybdenum ions does not exceed the characteristic temperatures of phase transitions. In the case when the temperature during bombardment exceeds the tempering temperature, corresponding changes in hardness and microhardness are observed.

The transition to the deposition of the coating was carried out by lowering the potential of the substrate, admitting the reaction gas to a predetermined pressure, which was then maintained automatically, and opening the shutter in front of the samples.

The energy of ions directed to the substrate changed in accordance with the change in the applied potential in the range from –30 to –1000 V.

The substrate temperature was monitored using reference samples and Marathon and Raytek IR pyrometers. In some cases, the temperature of the substrate was controlled by a chromel-alumel thermocouple, which was fixed on the back side of the witness sample, which was fixed next to the prototype on the substrate. In most experiments, it did not go beyond 200–450 °C.

The distribution of the ion flux density in the plane of the substrate and their value were estimated from the ion current data obtained using a single shielded probe. The change in the density of the ion flux to the substrate was achieved by varying the arc discharge current or the distance from the cathode of the metal plasma source.

Mo-C coatings were obtained in the Avinit V block by thermal decomposition of a metal-containing compound, molybdenum hexacarbonyl $Mo(CO)_6$.

The Mo-C coating was also applied to the internal calibrated surfaces of 12×20 tubes with a class of cleanliness of the treated surface — 9a.

3.2.3 Methods for studying the properties of samples

Obtaining information about the entire complex of properties of functional materials is a rather complex and voluminous task, especially when it comes to studying thin-film compositions. In these studies, the main attention was focused on the study of the reproduction of the composition of the compositions during their formation by vacuum-plasma methods, adhesion of film materials, structural state and some other properties.

The study of the structure and properties of working surfaces (microsection, coating hardness, determination of the surface geometry after coating) and determination of material parameters (layer thickness, uniformity,

defectiveness, and structure of the material itself) were carried out using the methods of metallographic, chemical, X-ray diffraction and micro-X-ray spectral analyzes.

The metallographic characteristics of the coatings were studied on microsections made from the samples under study. To prepare a thin section, the sample was pressed into a special powder on an automatic assembly press «SIMPLIMET 2000». Grinding and polishing was carried out in automatic mode on a device of the EKOMET 3+AUTOMET 2 model by BUEHLER.

The roughness of the surface of the samples before and after the deposition of coatings was measured on a JENOPTIK nanoscan 855 profilometer-profilograph.

The microhardness of the layers was measured using a LECO AMN-43 microhardness tester, in an automatic mode at a load of 50 g. Measurement of microhardness and Young's modulus in many layer and nanolayer coatings of Avinit type with a thickness of 1...3 μm, performed using a nanohardness measuring device from CSM (Switzerland) (loading speed 20.00 mH/min, maximum depth 100.00 nm at 6 nan D processing of results in the Oliver — Fahr model).

The looseness of the films was judged on the basis of potentiostatic measurements (on the witness samples obtained on metal substrates), as well as on the basis of the data of structural studies.

The degree of reproduction of the composition of the films was evaluated according to the data of X-ray (X-ray diffractometer DRON-3, filtered Cu-K_α radiation) and spectral (spectrograph ISP-30) studies, comparing the spectra of the starting materials (targets) and condensed films.

The study of the functional areas of the surface of the samples was carried out using scanning electron microscopy (SEM).

The volume distribution of chemical elements was recorded using electron probe X-ray microanalysis (EPMA):

- along the plane of the coated samples;
- in the area of the surface areas of the samples, on which the friction tests were carried out.

The profiles of changes in the chemical identity and the nanolayer of functional coatings were recorded using the secondary ion mass spectrometry (SIMS) method on an MS 7201M secondary emission mass spectrometer. The maximum profiling depth is 5 microns. For sputtering, an Ar^+ ion beam with an energy of 5–7 keV was used.

The metallophysical measurements of the coatings obtained on the prototype parts were carried out using a JSM T-300 scanning electron microscope.

To measure the characteristics of the geometric dimensions of the control samples, the involute surfaces were measured on a Wenzel LH65 control and measuring machine by means of surface points applied to the 3-D model of the part with an accuracy of 0.5 μm.

For the purposes of technological control, the composition of residual or working gases in the vacuum volume of the vacuum-plasma equipment, a technological quadrupole mass spectrometer of the MX-7304A type was used, capable of monitoring the composition of the gas phase in the range up to 350 amu. in real time and track 6 predefined peaks from the mass spectrum up to 350 amu. The mass spectrometer was connected to an external computer and operated in a unified system of automated control and management of technological processes.

Plasma parameters (ion current, ion density, current-voltage characteristics, spectral characteristics) were continuously monitored and archived using a PlasmaMeter plasmometer and a PlasmaSpectr spectrometer.

3.2.4 Methods for studying the characteristics of friction and wear

Tribological tests of coated samples were carried out on friction machines in order to determine the critical values of the load parameters leading to a burr, i.e. finding the boundaries of application of the studied friction pairs, determining the coefficients of friction and wear and their change in the process of friction to predict the compatibility of materials.

The tests were carried out according to the following basic schemes — «cube (main sample) — roller (counterbody)» and «ring-ring» (for wear tests).

Test modes, the total number of samples for testing was determined taking into account the operating conditions of the planned friction pairs in real operating conditions and were refined in the course of the work.

Tribological tests of antifriction, wear properties and setting of samples with coatings were carried out in the Central laboratory of the Malyshev plant (Kharkiv) on a friction machine 2070 SMT-1 according to the «cube-roller» scheme with a step load in the load range of 1 — 20 MPa.

The tests were carried out in a TS-1 fuel environment and in a diesel fuel environment. To determine the tear of the surface layers of materials of friction pairs, the load was made from $P_{\min}$ to the critical point P_{cr}, at which tear occurs.

Tribological tests for friction and wear of samples with coatings according to the «ring-ring» scheme were carried out on an improved serial friction machine 2070 SMT-1 according to a standardized test procedure at the Kharkiv National University of Air Force named after Kozhedub.

To reproduce the results of wear tests, the coincidence of the end surfaces was controlled by the value of the contact plane: not less than 90 % of the working surface of each sample.

In the process of tribological tests, the following were recorded:

- the value of the friction force F_{fr}, normal load N, contact pressure P, according to the value of which the mechanical losses in tribosystems were estimated;

- the temperature of the elements was continuously recorded in real time of tests in a direct approximation (1 mm) from the friction zone using a «moving» thermocouple.

The friction coefficients were determined as $f=F_{fr}/N$.

To determine the tear of the surface layers of materials of friction pairs, the load was made from $P_{min}=200$ N through 200 N to the critical value P_{cr}, at which tear occurs.

Additionally, the wear rate was measured by the acoustic emission method. After the selection of the best coating materials for friction pairs based on the results of tribological tests, the technologies for applying coatings for specific units were tested and serial parts were obtained for full-scale life tests. The tests were carried out at the stands of the Malyshev plant (Kharkiv) and Kharkiv Engine Engineering Design Bureau (KEEDB).

3.3 Properties of Avinit multifunctional multicomponent coatings

The main focus of our work on the creation of new structures of functional coatings is associated with the development of new materials and industrial technologies for the deposition of multilayer and nanolayer ion-plasma and plasma-chemical coatings and their introduction into mass production to increase the resources of products and the reliability of their operation by using the developed nanotechnologies.

As a preliminary consideration shows, the most promising for industrial applications are vacuum-plasma composite coatings based on nitrides and carbides of titanium, molybdenum, aluminum, chromium.

Therefore, the main efforts were focused on the development of such coatings using Avinit technologies.

In order to work out the technologies for obtaining multi-layer composite nanolayer functional coatings Avinit, it was necessary to study the process of deposition of vacuum-arc coatings to determine the optimal parameters of the process of obtaining high-quality coatings in the conditions of specific technological equipment Avinit.

In [32–54], numerous experimental studies were carried out on the development of processes for the deposition of multicomponent multilayer and nanolayer Avinit coatings based on metal nitrides and carbides and their metallophysical, mechanical and tribological characteristics.

A detailed analysis of the developed Avinit technologies for obtaining Avinit coatings was carried out in [29–31].

Here we briefly present only some of the parameters of the Avinit processes and the metallophysical and tribological characteristics of multifunctional multilayer and nanolayer coatings with improved mechanical and tribological properties for friction pairs in transport engineering.

3.3.1 Properties of Avinit C coatings (nitride-based)

The influence of the main parameters on the change in the properties of the obtained coatings based on molybdenum, titanium and their compounds with nitrogen has been studied.

3.3.1.1 Avinit C 100 coating (based on titanium nitrides)

The composition of the coatings and their microhardness are important characteristics.

The microhardness of Avinit C 100 coatings obtained by vacuum-arc deposition in titanium-nitrogen plasma in a vacuum $P=10^{-3}$ mm·Hg is $4\cdot10^3$ MPa.

With an increase in the partial pressure of nitrogen, the phases α-i, ε-i2N gradually disappear and a transition to the formation of a single-phase iN coating occurs.

At nitrogen pressures $P=5\cdot10^{-3}$ mm Hg. microhardness of coatings reaches values of 30.103 MPa, which correlates well with the literature data [55–57].

Study of the influence of ion energy on the properties of Si-coatings on X162CrMoV12 steel samples at a nitrogen pressure $P=6\cdot10^{-3}$ mm·Hg and $P=1.5\cdot10^{-3}$ mm·Hg. and the values of the accelerating potential from –50 V to –300 V and the temperature of the samples 200...600 °C shows. Changes in these condensation conditions have practically no effect on the microhardness of the resulting coatings.

The roughness of the samples with coatings is determined both by the roughness of the initial substrate surface and by the modes of coating.

When the initial surface was treated to a cleanliness corresponding to class 6–7, the application of coatings did not reduce the cleanliness class and, depending on the application mode, could even increase it by several units. When applying and coatings in the mode of formation of a layered structure on the original surface of the sample of steel treated to 7 cleanliness class, the value of roughness Ra had a value that corresponds to 10 cleanliness class.

A decrease in the ion current density during condensation, the use of a straight-line separator to get rid of the droplet phase increases the uniformity of the coating structure and helps to maintain the surface cleanliness class at the level of 13.

3.3.1.2 Avinit C 200 coating (based on molybdenum nitrides)

The coatings were obtained at an ion current density $I=10$ mA/cm^2, substrate potential $U_n=-25$ V, and substrate temperature $T_n<200$ °C. Nitrogen pressure during condensation $2.5\cdot10^{-3}$ mm Hg.

During the deposition of molybdenum nitride coatings without the use of separating devices, the microhardness of a coating with a thickness of 12 μm is 30890 MPa and decreases to 19613 MPa with an increase in the substrate temperature. The roughness of the surface of the coatings corresponds to V 7–8 class when deposited on the surface of steel X162CrMoV12 polished to V 12 cleanliness class.

A characteristic feature of the surface morphology is its cellular structure, the presence of inclusions in the form of metal (Mo) drops.

The transition zone of the steel-condensate interface is of interest from the point of view of ensuring the adhesion of these materials. The experiments were carried out on samples of X162CrMoV12 steel with pure molybdenum coatings applied at different values of U_n (–25...–200 V) at T_n=(90...150 °C).

For some grains, the heat affected zone during the condensation of molybdenum with a relatively high energy (U_n=–200 V) is characterized by the formation of pores or precipitates of the second phase.

Their magnitude and depth distribution indicate the presence of a temperature gradient in the near-surface layers during ion bombardment and condensation. The length of the zone can reach ~3 μm. The microstructure of the condensate inherits the features of the substrate structure, the interface has a form characteristic of the diffusion interaction of materials.

Structural changes in steel in the zone of thermal action of the ion flow during bombardment and condensation correlate with changes in microhardness; after bombardment, it decreases by 20 % and after condensation (within 1 h) — by 50 %. With a decrease in the time of ion bombardment to 1 min. and condensation up to 20 min the heat-affected zone is reduced to ~1 μm.

Thus, the experimental results confirm the possibility of low-temperature deposition of high-hard wear-resistant Avinit coatings based on molybdenum nitrides in modes that provide good adhesion to the substrate materials (X162CrMoV12 steel) without a significant decrease in steel strength (<200 °C) and without deterioration of the purity class.

3.3.1.3 Composite coating Avinit C110 and Avinit C210

Table 3.1 shows the program of experiments on the development of the process of applying composite coatings Avinit C110 (TiN-Ti) and Avinit C210 (Mo_2N-Mo) on samples of steel X162CrMoV12) and the parameters of the initial samples.

Coatings of compounds were formed by letting nitrogen into the chamber synchronously with the operation of one or another vacuum-arc sputtering source with different cathodes. The nitrogen pressure was chosen so as to obtain typical values of microhardness for the corresponding compounds of the studied metals with nitrogen.

Table 3.1 Technological parameters and characteristics of the original samples

No.	Cathode	NN	Composition	Process parameters		Initial Parameters		
				Time, hours	Pressure. Nitrogen mm	HRC	Class	Rough
1	Ti	1 2 3¤	TiN	1.5 2.5 4.0	$(1.5–2)\cdot10^{-3}$	60–62	13 12c 12c	0.018 0.021 0.020
2	Ti	*5¤ 6 7¤	Ti_2N	5.0	$5\cdot10^{-4}$	60–62	12c 13 13	0.020 0.015 0.017
3	Ti	*8¤ 9¤ 10	Microlayers TiN-Ti	4.0	$(1.5–2)\cdot10^{-3}$ Work 12 min, Pause 12 min	60–62	13 13 13	0.015 0.015 0.016
4	Ti	17¤ *18¤ 19	Nanolayers TiN-Ti	4.0	$5\cdot10^{-4}$ Work 48 s, Pause 48 s	60–62	12c 12c 12c	0.020 0.021 0.020
5	Mo	11¤ *12¤ 13	Microlayers Mo_2N-Mo	2.0	$1.8\cdot10^{-3}$ Work 12 min, Pause 12 min	60–62	12c 12c 12c	0.020 0.021 0.020
6	Mo	14¤ *15¤ 16	Nanolayers Mo_2N-Mo	2.0	$5\cdot10^{-4}$ Work 48 s, Pause 48 s	60–62	12c 12c 12c	0.020 0.021 0.020
7	Ti	20 21¤ *22¤	TiN	4.0	$(1.5–2)\cdot10^{-3}$ without separator	60–62	12c 12c 12c	0.020 0.021 0.020
8	Ti	4	TiN	1.0	$(1.5–2)\cdot10^{-3}$ without separator	60–62	12c	0.020

Studies have shown that for the formation of compounds based on Ti, the nitrogen pressure should be $3...4\cdot10^{-1}$ Pa, and for compounds based on Mo — $1...1.3\cdot10^{-1}$ Pa.

The study of the formation processes of coatings of different compositions was carried out under conditions that did not lead to an increase in the temperature of the samples above 200 °C. At the stage of vacuum-plasma cleaning, this was achieved through the use of a pulsed processing mode and the choice of the ratio of the intervals of operation and pause of arc sources, as well as the total processing time. When forming coatings using a titanium cathode, as experiments showed, the operating mode of the arc source was 2 seconds and a pause of 4 seconds with a total processing time of 3–5 minutes with a gradual increase in the accelerating potential from 30...50 V to a maximum value of 1000 V. When working with a molybdenum cathode, the pause increased to 6 seconds. At the stage of deposition of coatings based on titanium and its compounds with nitrogen, it was possible to keep the temperature in the range of 180–200 °C in the mode of conti-

nuous operation of the vacuum-arc source at a potential on the samples of 30–40 V. In the case of deposition of coatings based on molybdenum and their compounds even at a potential of 25 V, it was impossible to keep the temperature of the samples within the specified limits with the constant operation of the vacuum-arc source, therefore, a pulsed mode of operation with a cycle of 6 seconds (work), 4 seconds (pause) was applied.

Metallographic studies of the samples after the deposition of coatings of different compositions show that the worked out regimes ensured the formation of high-quality coatings. **Table 3.2** shows data on the rigidity, microhardness and roughness of the investigated coatings.

Table 3.2 Characteristics of the studied samples with coatings

No.	Composition	Finite. Parameters				
		Thickness, μm	Hard., $H_{v(5\ kg)}$	Microhard., $H_{v(50\ g)}$	Class	Rough
1	TiN (continuous)	–	710 710	1145 1000	11c 10c	0.040 0.10
2	Ti_2N (continuous)	1	710 710	1145 1550	10c	0.10
3	Microlayers TiN-Ti	0.6	710 710	894 894	11c	0.040
4	Nanolayers TiN-Ti	0.2	710 710	894 894	12a	0.036
5	Microlayers Mo_2N-Mo	0.5	660 710	894 800	12b	0.026
6	Nanolayers Mo_2N-Mo	0.2	710 690	570 650	12b	0.025
7	TiN (continuous without separator)	0.25–0.28	690–710 690	–	7c	0.70

The hardness and microhardness of the base material according to the selected modes of coating application practically do not decrease in comparison with the initial state.

The microhardness of the coatings was in the range of 10,000–15,000 MPa, depending on the composition of the coating. The coatings had good adhesion to the backing material. No cases of peeling of the coatings were observed during the application of the mesh of scratches.

The nanocomposite coatings had a layered structure of layers of the corresponding composition ~15 nm thick.

After coating samples with roughness corresponding to 12–13 cleanliness class, the surface roughness of the samples practically does not change, or the surface cleanliness class deteriorates slightly (by one or two units).

Without the use of a rectilinear separating device, the quality of the coating surface, as shown by the results of profilographic studies, significantly

deteriorates. A large number of macroparticles appear on the surface of the coatings (mainly metal droplets, which, depending on the time of their appearance on the growing surface, are covered with subsequent layers), characteristic of condensation from unseparated plasma streams. Their number, size, shape depend on the technological parameters of the deposition process.

3.3.1.4 Avinit C 300 coating (based on Ti-Al-N)

Even a relatively simple Ti-system, when viewed from the point of view of multicomponent systems, can have different heterostructures and, accordingly, different properties and different areas of application. Naturally, an even greater variety of properties and an expansion of the scope of application can be expected from more complex systems.

Properties of coatings Ti-Al-N, Ti-Cr-N, Ti-Mo-N, Nb-Zr-N significantly depend on the content of alloying elements - aluminum, chromium, molybdenum, zirconium. With an increase in the content of alloying elements, such coatings have higher values of rigidity and toughness, temperature resistance, heat resistance, and better tribotechnical characteristics in comparison with one-component nitrides.

Our main efforts were focused on the development of processes for obtaining coatings Avinit C 300 (based on Ti-Al-N) and the study of their properties.

Due to the high heat resistance of Ti-Al-N coatings [58], the upper temperature limit of their operation is much higher than that of TiN coatings and reaches temperatures of 800–900 °C. These coatings have significantly preferred tribological characteristics, which is extremely important for their use as materials for promising tribological pairs [22, 23, 58, 59].

We have carried out a number of experimental studies on the development of processes for multilayer and nanolayer ion-plasma coatings Avinit C based on the Ti-Al-N system [32–38].

As it is known, the characteristics of coatings (Ti-Al-N) significantly depend on the aluminum content. With an increase in the aluminum content, the hardness of the coating increases from values typical for TiN coatings to values close to 40 GPa at an aluminum concentration of 40–50 at % with respect to titanium N [60].

The structure of multilayer coatings is a series of alternating layers of various compositions and thicknesses with a thickness of each layer from several nanometers to several microns.

It is determined by the distance *L* from the cathode to the surface, the density of the ion current of the arc sources, the speed of rotation of the rotary device and is provided by the time the coated surface is sequentially located in the zone of action of each of the cathodes.

The hardness and strength of the layer coating increases with decreasing thickness of the individual layers.

Based on the experiments carried out to determine the growth rate of coatings obtained on substrates in planetary motion, the Avinit cluster control program was created to obtain TiN-AlN nanolayer coatings.

The protocols of the automated control system for these processes are shown in **Fig. 3.2**.

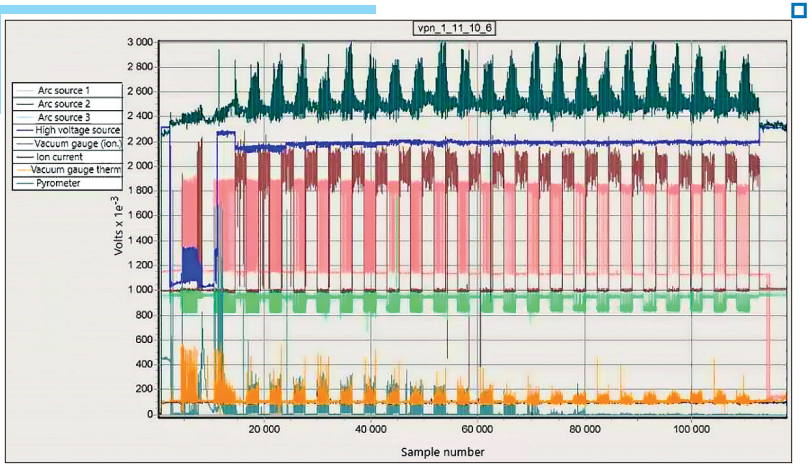

Fig 3.2 Fragment of the protocol of the automated control system of the technological process of applying the TiN-AlN nanocoating: *a* — TiN-AlN (50/50) nanocoating with a repetition period of 20 nm and the same thickness of individual nanolayers; *b* — TiN-AlN (30/70) nanocoating with a repetition period of 12 nm and a thickness of individual nanolayers of 4 and 8 nm

The composition and some characteristics of the investigated coatings are given in **Table 3.3**.

Table 3.3 Characteristics of the samples

No.	Coating composition	Base hardness, HRC	Technological parameters			Coating properties		
			Programmable composition	*T*, °C	Nitrogen pressure, *P*, Pa	Thickness, μm	Microhardness, Hv, (MPa)	Roughness Ra, μm
Coating based on Ti-Al-N (TiN-AlN)								
1	Avinit C/P 300	59–60	Multilayer	200	$3 \cdot 10^{-1}$	10.0	26000–30000	0.040 (11b)
2	Avinit C/P 310	59–60	Nanolayer with a repeatability period of 12 nm and a thickness of individual nanolayers 4 and 8 nm	200	$3 \cdot 10^{-1}$	1.5	‡ 3000–3200 HV_{100} † 2500–3000 HV	0.036 (12a)
3	Avinit C/P 320	59–60	Nanolayer with a repeatability period of 12 nm and a thickness of individual nanolayers — 8 nm and 4 nm	200	$3 \cdot 10^{-1}$	1.5	‡ 3000–3500 HV_{100} † 3000–3500 HV	0.036 (12a)

‡ Measurement of HV_{100} microhardness on reference specimens using a microhardness tester.
† Measurement of nanohardness with a nanohardness tester

The choice of the mode and design of intermediate layers. are very important for obtaining strong adhesion coatings on precision surfaces, since even minor deviations from the optimal technology can lead to curvature of the parts to be coated.

The coatings were applied at temperatures not exceeding 200 °C, which ensures the preservation of the mechanical properties of the substrate and does not lead to a decrease in the rigidity of the base — steel X155CrVMo12-1 (**Table 3.3**). Moreover, the coatings have good adhesion to the substrate. After coating samples with a roughness of 12–13 cleanliness classes, the surface roughness practically does not change.

The results of metallophysical measurements of the Avinit C/P 310-n1 coating on a JSM T-300 scanning electron microscope are shown in **Fig. 3.3, 3.4**.

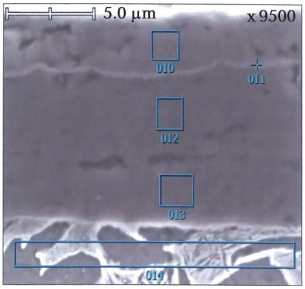

a

No.	N	Al	Ti	Mo	Summ, %
010	9.10	27.93	62.96	–	100
011	6.89	16.73	76.38	–	100
012	10.7	45.87	43.44	–	100
013	10.71	42.22	42.07	–	100
014	–	3.64	88.94	7.41	100

b

Fig. 3.3 Appearance of the coating Avinit C/P 310-n1 (cross-section) with the indicated zones of analysis (*a*); the approximate chemical composition of the analyzed zones (*b*). Coating thickness ~9 microns

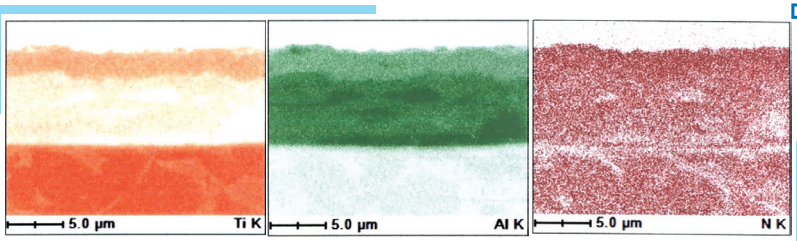

Fig. 3.4 Appearance of Avinit C/P 310-n1 coating (cross-section) in the coverage area mapping mode. The larger the content of the element corresponds to the more intense coloring

To determine the microhardness of thin coatings (<4 µm), the nanohardness was measured using a CSM nanohardness tester (Switzerland). The measurements of the microhardness and Young's modulus in Avinit C/P 320 coatings with a thickness of 1.4 µm gave the value H_v=1600–2300 kg/mm^2, E=250–300 GPa, Poisson's ratio K=0.30.

Metallographic studies of Avinit-type coatings were carried out using the methods of secondary ion mass spectrometry (SIMS), electron probe X-ray microanalysis (EPMA), scanning electron microscopy (SEM).

Fig. 3.5 for the Avinit C/P coating shows the dependences of the currents of the secondary ions Al^+, Ti^+ on the sputtering time and, accordingly, on the depth of the distribution profile of the components.

Thus, the experimental results confirm the possibility of low-temperature deposition of wear-resistant high-hard coatings Avinit C based on metal nitrides in modes providing good adhesion to the substrate materials (steel with a precision surface Ra=0.025 µm) without a significant decrease in the strength characteristics of steel (<200 °C) without deterioration of the cleanliness class of the original surface.

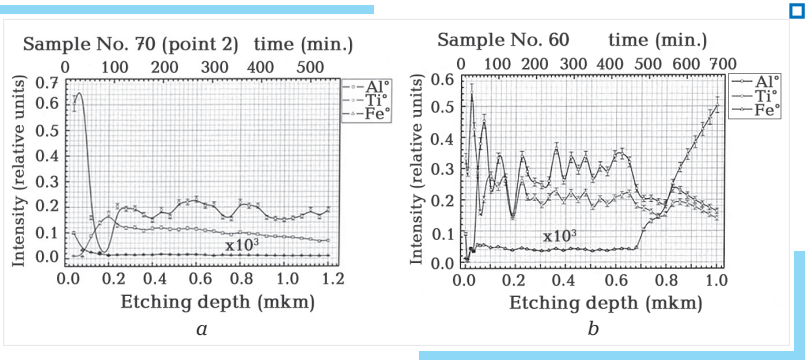

Fig. 3.5 Dependences of the currents of secondary ions Al^+, Ti^+ on the sputtering time: *a* — coating Avinit C/P 320; *b* — coating Avinit C/P 310

The studies carried out made it possible to select the temperature-time parameters for obtaining reinforcing Avinit C coatings to increase the wear resistance of the working surfaces of precision friction pairs, ensuring the production of coatings of a given composition with a thickness of 1–3 microns, and to develop software products for obtaining such coatings on the Avinit cluster. multicomponent multilayer coatings for real serial parts.

3.3.2 Properties of Avinit D functional coatings (based on carbide)

Many authors [61—66] note that nano- and microlayer multicomponent coatings with very high hardness and temperature resistance are most promising for solving problems of creating new designs of functional multilayer coatings with improved tribological characteristics. In this regard, coatings in metal-carbon systems, in particular, Avinit D coating based on Ti-C and Mo-C, are of great interest for use as antifriction wear-resistant coatings for friction pairs.

The results of developments on obtaining Avinit D coatings based on metal carbides and their metallophysical and tribological properties are given in [44, 46–48].

New processes (PVD and hybrid PVD + CVD) have been developed for the controlled formation of multicomponent nano- and microstructural Avinit D coatings in metal-carbon systems using vacuum-plasma (PVD) and plasma-chemical (CVD) processes for the deposition of multicomponent multilayer and nanolayer coatings — carbon «(MeC, MeC:H, Me-CN, MeC-C) (Me-Ti, Mo).

Multicomponent nano- and microlayer coatings of metal-carbon systems (TiC; TiC-N, TiC-C) and (MoC, MoC-C, Mo-C-N) were selected as candidate coatings for research.

When developing new promising nanocoatings:

- new designs of antifriction, wear-resistant coatings Avinit D have been created for working in friction pairs with heat-hardened steel and with steel coated with a microstructural or nanostructured coating of the Avinit type;
- proven processes of applying anti-friction wear-resistant coatings on steel samples with precision surfaces for metal-physical and tribological studies;
- tribological studies of «coated steel — steel» pairs were carried out;
- selected tribopairs from different pairs based on the results of tribological tests of optimal designs of tribopairs in the «coating-steel» and «coating-Avinit-type coating» systems;
- selected, according to the research results, the optimal combinations of the coating material for the subsequent development of the application of the selected coating on full-scale products.

1. Avinit D/P coating. The testing of the PVD technological parameters of the processes of applying multilayer and nanolayer coatings in the Ti-C and Mo-C systems was carried out in the Avinit C block of the Avinit installation. Titanium Ti2, molybdenum Mo99.9 vacuum-melted, and antifriction graphite GG365 (Electrocarbon Topolcany) were used as cathode materials.

To obtain carbide-containing layers, benzene C6H8 was used as the reaction gas.

To carry out metallographic studies, coating was carried out on witness samples made of X155CrVMo12-1 steel with a hardness of 56...61 HRC with precision surfaces used in the production of parts. For this, the working planes of the samples were processed according to factory technologies to a roughness of 0.016–0.021 microns (12–13 roughness class).

With the use of modernized PVD deposition, the processes of applying monolayer and multilayer Avinit D/P 100 coatings (TiC, Ti-CN, TiC-C) and Avinit D/P 200 coatings (MoC, MoC-C, Mo-CN) have been worked out.

For the deposition of multilayer coatings (TiC-Ti) and (MoC-Mo), built on a sequence of metal and carbide layers, a two-cathode scheme was used with the simultaneous operation of one-component cathodes (Me and C), located towards each other, in an environment of residual gases with rotation samples around their axis with continuous or pulsed (periodic) operation of sputtering sources.

Obtaining high-quality coatings in such a scheme became possible due to the provision of stable combustion of a controlled graphite cathode due to the modernization of the cathode assemblies and the control system.

At the same time, the following coatings in the «metal-carbon» systems have been worked out — monolayer TiC, monolayer TiC-N, nanolayer TiC-TiN, nanolayer TiC-C, MoC monolayer structures, monolayer Mo-C-N, nanolayer MoC-C structures.

According to this scheme, multilayer coatings of different composition and structure were obtained to study their properties, in particular, tribological

characteristics in various friction pairs (depending on the composition and ratio of layers) and the possibility of their use as wear-resistant and antifriction coatings.

2. Avinit D/C coating. In the Avinit C block, by deposition from plasma metal flows (Ti, Mo, Zr, Cr, Nb) in an atmosphere of benzene vapors C_6H_8, we have developed new processes for the controlled formation of multicomponent nano- and microstructural carbide-containing multilayer coatings in metal-carbon systems of the type (TiC-Ti) and (MoC-Mo), built on a sequence of metal and carbide layers in a single-cathode circuit mode with continuous operation of the sputtering source (Ti, Mo, Zr, Cr, Nb) and pulsed (periodic) supply of the reaction gas (benzene vapor C_6H_8), namely, Avinit D/C 100 coatings — monolayer TiC:H, nanolayer TiC:H-TiN, nanolayer TiC-C:H, Avinit D/C 200 coatings — monolayer MoC:H, nanolayer MoC:H-TiN, nanolayer MoC:H (with different carbon content).

The results of examining samples (coating thickness, coating hardness, determination of the surface geometry after coating) with some of the obtained coatings are given in **Table 3.4**.

Table 3.4 Characteristics of samples with carbide-containing coatings

No.	Samples	Microhardness H_v, kg/mm^2	Thickness H, μm	Roughness Ra, μm
1	Avinit D/P 100 based on Ti-C	2 300	1...2	0.036
2	Avinit D/P 100 based on Ti-C	2500	12	1.45 — 1.15
3	Avinit D/P 100 based on Ti-C:H	2500	8...10	—
4	Avinit D/C 100 based on Ti-C:H	1700	1...5	—
5	Avinit D/C 100 based on T-C:H	2000	1	—
6	Avinit D/P 200 based on (Mo-C)	1800	1	—
7	Avinit D/P 200 based on (Mo-C)	2200	8 — 10	1.15 — 1.05
8	Avinit D/C 230 based on Mo-C:H	2300	1.5	—
9	Avinit D/C 240 based on Mo-C:H	2500	8 — 10	1.15 — 1.05
10	Avinit D/C 120 based on Ti-C:H	2000	1	—
11	Avinit D/P 100 based on Ti-C	2500	12	1.45 — 1.15
12	Avinit D/P 200 based on Mo-C	2300	8 — 10	1.15 — 1.05

Metallophysical measurements of Avinit D/P 100 and Avinit D/P 200 coatings (**Fig. 3.6, 3.7**). on a scanning electron microscope JSM T-300 give the following results — the thickness of the coating is ~6–9 microns, the carbon content is ~10–15 %, sufficiently evenly distributed in the structure of the coating in accordance with its design. The quality of adhesion is high — no delamination of the coating from the base was found on all investigated coatings.

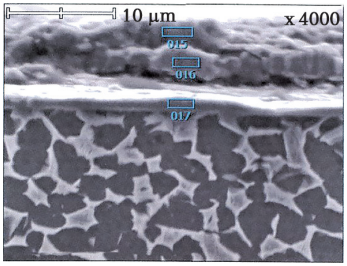

a

No.	C	Ti	Summ, %
015	12.72	87.28	100
016	6.54	93.46	100
017	5.02	94.98	100

b

Fig. 3.6 Appearance of Avinit D/P 100 coating (based on the Ti-C system) (cross-section) with the indicated analysis zones — (*a*); the approximate chemical composition of the analyzed zones — (*b*). Coating thickness ~3.5 microns

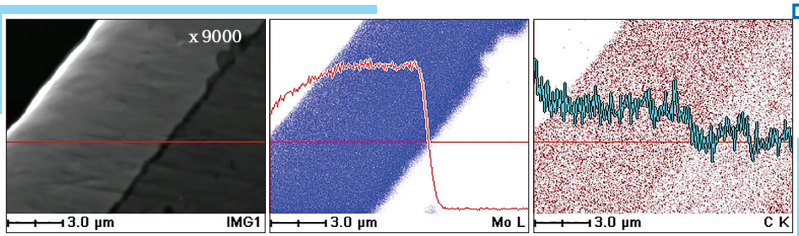

Fig. 3.7 Appearance of Avinit D/P 200 coating (based on the Mo-C system) in line analysis mode. Coating thickness ~6 microns

Thus, the worked out modes make it possible to obtain high-quality uniform coatings with high adhesion, while maintaining the stiffness of the steel base within the specified limits — the stiffness and microhardness of the base material according to the selected modes of coating application practically do not decrease in comparison with the initial state. The roughness of the surface of samples 12–13 of the cleanliness class practically does not change.

3.3.3 Properties of Avinit V coatings

The works [45–51] are devoted to the study of the process of deposition of metal and metal-carbide coatings by gas-phase deposition using organometallic compounds (carbonyls of chromium, molybdenum, tungsten), in particular, Mo coatings by thermal decomposition of molybdenum hexacarbonyl $Mo(CO)_6$ into a complex profile and the study of tribological characteristics of multilayer Mo-C coatings

The development of Mo coatings was carried out on an Avinit V gas-phase block at temperatures of 350 — 450 °C on pre-heat-treated speci-

mens of steel 1.773 with a size of 20×10×5 mm, polished to a roughness of class 8 (Ra=0.32 μm) and samples made of steel X155CrVMo12-1 with 56...61 HRC with a size of 10×10×10 mm, polished according to factory technologies up to grade 10 roughness (R_a=0.063 microns).

The characteristics of the coatings differ sharply in a given temperature range. At 350 °C and 450 °C, a consistently uniform coating with a high microhardness is observed: HB=2200 at 350 °C, HB=1700 at 450 °C (**Fig. 3.8**). The coating thickness is linearly dependent on the holding time. At 450 °C, the coating has good adhesion to the base; at lower temperatures, poor adhesion to the original sample is observed.

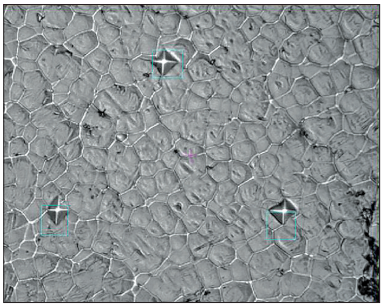

a

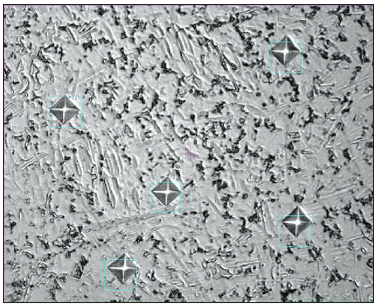

b

Fig. 3.8 The structure of the surface of the Mo coating obtained at *T*: *a* — 350 °C; *b* — 450 °C

The performed X-ray studies reveal a significant amount of the Mo2C carbide phase, which is responsible for the increased microhardness of Mo coatings.

At higher temperatures (surface temperature above 500—700 °C, *P*=0.1 mm Hg), Mo coatings with a significantly lower carbon content (up to 0.11 wt. %) Ca be obtained, which significantly the lowest microhardness of the obtained Mo coatings HB100=400 and even less.

Therefore, it seems appropriate to call the obtained coatings molybdenum-carbide coatings or, by analogy with solid electrolytic chromium, solid gas-phase molybdenum.

The average coating speed is 50...70 microns/hour.

The technologies of multistage actions were developed during several technological cycles to obtain thick coatings. Coatings with a thickness of 100 μm were obtained. No delamination of the coating was observed.

A JSM T-300 scanning electron microscope was used to study the composition of the obtained coatings on X155CrVMo12-1 steel samples in the mapping mode and in different zones along the coating thickness.

Metallographic studies confirm the possibility of low-temperature deposition of high-quality coatings of solid gas-phase molybdenum in the developed CVD process, while providing good adhesion to the substrate materials (steel X155CrVMo12-1, 1.773) without reducing the strength of the steel and without deteriorating the purity class of the initial surface.

Thus, on the gas-phase block of the Avinit installation, a process has been developed for applying coatings of «hard» molybdenum (molybdenum carbide coatings with a high carbon content) by pyrolysis of molybdenum carbonyl at a rate of up to 90 microns per hour. Optimization of the processes of applying high-quality fortress coatings on prototypes has been made. Measured characteristics of coatings (microhardness, phase composition, roughness, stiffness of the base). The studies carried out indicate that the development of pilot-industrial technologies is promising for the selection of optimal designs of tribopairs for precision assemblies. The good reproducibility of the coatings obtained makes it possible in the future to develop technologies for mass production.

3.4 Investigation of the characteristics of friction and wear of coatings

3.4.1 Tribological characteristics of Avinit C coatings

To expand the comparative base, «basic tests» were carried out according to the «cube-roller» scheme on samples of «uncoated steel — bronze».

Materials, chemical-thermal and mechanical processing of samples for these tests were selected as one of the best currently existing options for the operation of friction pairs in aviation fuel. X155CrVMo12-1 steel («raw», nitrided, cemented and heat-treated) was used as steel samples, and Br.O10C2N3 bronze (Sn 9–11 %, Pb 2–2.35 %, Ni 3–4 %), VB-23NTS (Pd 18–22 %, Ni 3–4 %, Zn 3–4 %, Sb 3–4 %, P 0.15–0.3), VB-24 (Sb 4.7–6, 2 %, P 0.4–0.9), as well as the same bronzes, processed according to the factory technology, with VAP-2 coatings (67 % MoS_2 and 33 % epoxy binder).

As shown by preliminary tests according to the «cube-roller» scheme, seize was not observed at the maximum possible loads (2 kN), which, when converted to PV, is > 2600 kgm/s, which unnecessarily overlaps the real PV values in most cases of real operating conditions of friction pairs. Therefore, in subsequent tests, the loads were limited to 1.6 kN (8 degrees of loading).

«Basic tests» established that the friction pair (bronze BVB-23NTS/nitrided steel 1.7361) is characterized by:

- high constancy to seize;
- secondary running-in — with an increase in the load, which at the initial moment causes an increase in the coefficient of friction, which, during further work at a new stage of the load, basically decreases. However,

on a «straight pair» (a more rigid specimen is a movable one) at loads of 1400 and 1600 N, there was an increase in the coefficient of friction;

- a sufficiently high stability in time of the coefficient of friction when operating at a constant load;
- a significant difference between the «direct» and «reverse» (stationary — more rigid sample) pairs in terms of the values of the coefficient of friction and wear of the samples.

«Direct» steam during long-term operation has:

a) lower values of the coefficient of friction;

b) lower values of wear, mainly due to less wear of the soft (bronze) sample.

Fig. 3.9 shows the data for the initial friction pair «steel X155CrVMo121 — bronze Br 10S2N3» by the value of the friction coefficient, its dependence on the value of the load to a value at which the contacting friction surfaces do not seize yet with the formation of damage in the form of scoring and a catastrophic increase in the coefficient of friction.

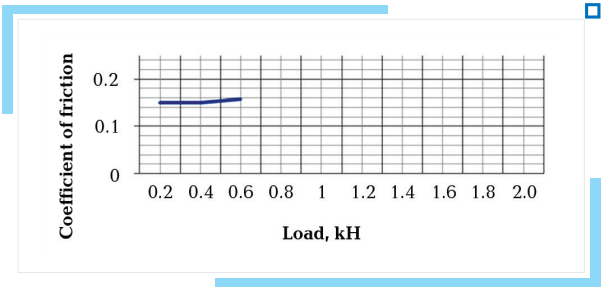

Fig. 3.9 Dependence of F_{fr} on loading for the friction pair «steel X155CrVMo12-1 — bronze Br.O10C2N3»

With an increase in the load over 0.6 kN, the friction force sharply increased, and then the exam was stopped, i.e. this pair showed a rather low P_{cr} value. In this case, this can be considered the main defect of the friction pair. Thus, when applying coatings, an increase in Pcr for the test pair will be considered a positive result, while maintaining the value of the friction coefficient at an acceptable level or decreasing it.

Fig. 3.10 shows the results of examinations for friction pairs «steel X155CrVMo12-1 with TiN coating — bronze Br.O10C2N3» and «steel X155CrVMo12-1 with MoN coating — bronze Br.O10C2N3».

Apparently, the deposition of a TiN coating did not lead to positive changes in the tribological characteristics of such a friction pair as compared to the initial uncoated pair. In contrast, the application of the MoN coating increased the P_{cr} value from 0.6 kN to 1.0 kN compared to the original uncoated one. The friction coefficient with increasing load decreased to 0.16 and then did not change significantly, which is also

a positive moment for this friction pair. Such a difference in the behavior of the MoN coating from TiN can be associated with its ability, upon reaching certain loads and, accordingly, contact temperatures at local points where these loads are highest, to decompose with the release of Mo, and, thus, due to the lower hardness of the latter, to contribute to a decrease in local load peaks on microroughnesses to a level that still does not lead to the tear of the contacting friction surfaces. Confirmation of the increase in Pcr due to just such a mechanism for reducing local load peaks can be the results of tests of friction pairs with layered TiN-Ti and MoN-Mo coatings (**Fig. 3.11**), obtained in accordance with Scheme 2 and already having metal layers of lower hardness compared to the rigidity of their compounds with nitrogen.

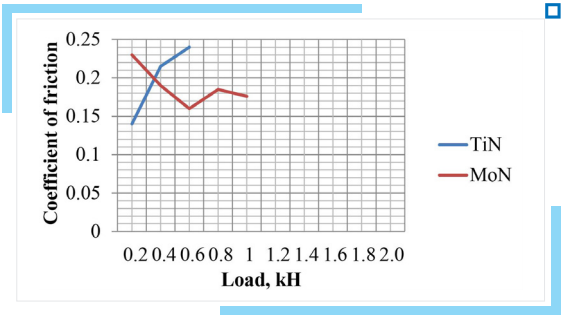

Fig. 3.10 Dependence of F_{fr} on loading for pairs «coating — bronze Br.O10S2N3» on loading for friction pairs «steel X155CrVMo12-1 with TiN coating — bronze Br.O10C2N3» and «steel X155CrVMo12-1 with MoN coating — bronze Br.O»

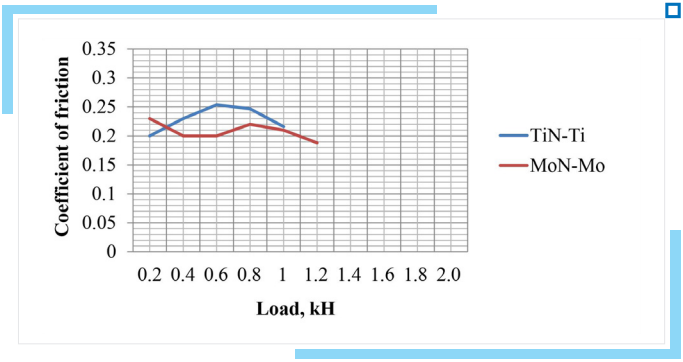

Fig. 3.11 Dependence of the coefficient of friction on the load for friction pairs «steel X155CrVMo12-1 coated (TiN-Ti) — bronze Br.O10C2N3» and «steel X155CrVMo12-1 coated (MoN-Mo) — bronze Br.O10C2»

It can be seen that, in contrast to the TiN coating, the deposition of a layered TiN-Ti coating led to an increase in P_{cr} from 0.6 kN to 1.0 kN,

and starting from a load of 0.6 kN, the friction coefficient decreased with increasing load. In general, the behavior of this pair was similar to the pair with the MoN coating, and the increase in P_{cr} can be explained from the same standpoint, only in this case the soft phase was introduced into the composition of the coating already during its formation.

Modification of the MoN coating with molybdenum additionally increased P_{cr} by another 0.2 kN, that is, it has already become twice as large as compared to uncoated steam, and had a positive effect on the stabilization of the friction coefficient in the entire range of loads. True, the value of the friction coefficient itself slightly increased, including the same for the TiN-Ti coating. Thus, as these studies have shown, an increase only in the stiffness of the material in contact with the bronze Br.O10S2N3 in friction pair does not improve the tribological characteristics of the steam under the selected exam conditions.

Reducing the coefficient of friction can be achieved in different ways. When friction pairs work in liquids, the friction coefficient can be reduced, for example, by mechanical surface treatment in order to create an optimal microrelief for keeping the liquid film in the contact zone of the friction surfaces or by other methods. One of these methods is the modification of the bronze surface by processing it with abrasive dispersed materials using factory technology. In **Fig. 3.12** shows the results of examinations for the pair «steel X155CrVMo12-1 — bronze Br.O10C2N3 with processing according to the factory technology».

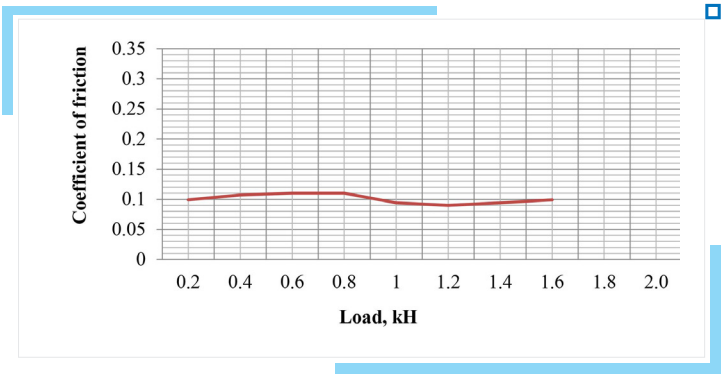

Fig. 3.12 Dependence of the friction coefficient on loading for the friction pair «steel X155CrVMo12-1 — bronze Br.O10S2N3 with processing according to the factory technology»

The processing of the bronze surface using the factory technology significantly influenced both the value of the friction coefficient (in the direction of its decrease) and the value of P_{cr} in comparison with the parameters

for the steam «steel X155CrVMo12-1-bronze Br.O10S2N3», increasing the latter by more than 2.5 times. But at the same time, as the review of the friction surfaces after the exams showed, the wear of the steel sample increased many times. No bronze wear was recorded. **Fig. 3.13** shows a comparative diagram of the wear of friction pairs of steel X155CrVMo12-1 with bronze, processed and without processing.

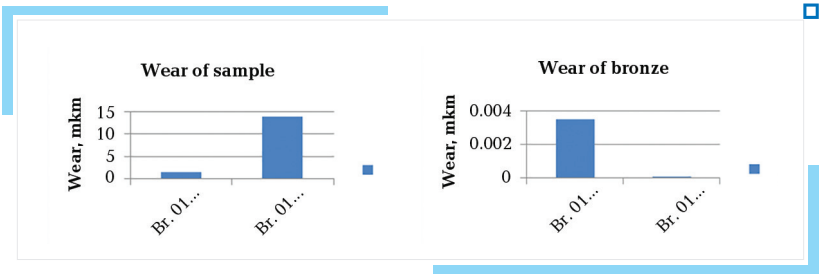

Fig. 3.13 Histograms of wear: steel sample and bronze Br.O10S2N3 without processing and processing from the factory technology

Thus, the main disadvantage of such a pair is the unacceptably high wear of one of the contacting materials, namely steel X155CrVMo12-1, which exceeded 20 times the wear that was recorded in exams with unmodified bronze. The appearance of the friction surfaces and the amount of wear itself indicated that it was abrasive. In such a case, the application of high hardness reinforcement coatings is an effective means of reducing frictional wear on the surface and therefore it was interesting to expand the range of exam coatings to include higher hardness TiN-AlN coatings. **Fig. 3.14** shows the test results of friction pairs «steel X155CrVMo12-1 with TiN coating — bronze Br.O10S2N3 with processing according to the factory technology», «steel X155CrVMo12-1 with MoN coating — bronze Br.O10C2N3 with processing according to the factory technology 1 with coating TiN-AlN — bronze Br.O10S2N3 with finishing according to the factory technology».

It can be seen that the TiN and MoN coatings when working with bronze Br.O10C2N3, which have undergone processing according to the factory technology, also have more preferable indicators in terms of the coefficient of friction than when working in tandem with bronze Br.O10C2N3 without treatment, as in the case with a steel sample. But, in contrast to the case of the operation of the pair «steel 12KhF1-bronze Br.O10S2N3 with processing according to the factory technology», with the values of the friction coefficient at the level of values for the steel sample and the same value of P_{cr}, the wear of the coatings did not exceed 0.6–0.8 μm, that is, it was ~20 times less than for an uncoated sample. The TiN-AlN coating showed even better performance both in terms of the coefficient of friction, which

was lower than 0.1 in the entire load range, and in terms of the amount of wear, which did not exceed 0.4–0.6 microns. No wear of bronze, as in the previous case, was recorded.

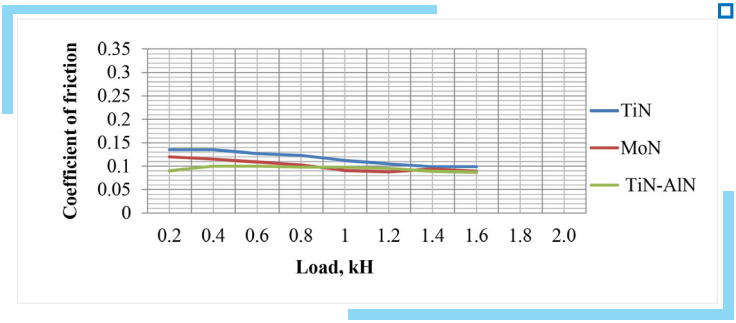

Fig. 3.14 Dependence of the friction coefficient on the load for pairs with TiN, MoN and TiN-AlN coatings and, accordingly, bronze Br.O10S2N3, which has been processed according to the factory technology

The tests, on the one hand, clearly showed the high sensitivity of the studied tribological characteristics of friction pairs to the composition and state of the contacting surfaces, and, on the other hand, demonstrated that the methods of applying functional coatings using various technological schemes of their formation can effectively improve the tribological characteristics of friction pairs in the case of proper selection of starting parts and layouts and formation characteristics of such coatings.

Subsequently, in-depth tribological tests were carried out of the improved multicomponent multilayer coatings obtained at the Avinit installation according to the developed technological schemes for the formation of multilayer coatings in order to clarify the possibilities of their use as wear-resistant and antifriction coatings and for further performance of wear and aggregate tests on specific parts in full-scale friction units of aircraft units.

Investigation of samples with Avinit C. To study the tribological characteristics of friction pairs with nanocoatings during friction and wear tests according to the «cube-roller» scheme, the following samples were obtained:

- cubes made of X155CrVMo12-1 steel with a hardness of 56...61 HRC with working surfaces ground with diamond paste to the required geometric parameters according to the factory technology (non-flatness — ≤ 0.001 mm, roughness — Ra 0.08 μm (▼11));
- rollers (counterbodies) made of steel X155CrVMo12-1 with a hardness of 56...61 HRC, with working surfaces ground in with KT10/7 paste (titanium carbide with grain size of 7–10 microns).

The characteristics of Avinit C coatings are given in **Table 3.5**.

Table 3.5 Characteristics of Avinit C coatings

Samples	Type of coating	Coating composition	Properties
Cubes	microlayer coatings Avinit C/P 310	Ti-Al-N separated	H_v=3000 kg/mm^2, h=1–3 μm
	multilayer coatings Avinit C/P 300	Ti-Al-N unseparated	H_v=3000 kg/mm^2, h=1–3 μm
	multilayer coatings Avinit C/P 210	Mo-N separated	H_v=2300 kg/mm^2, h=1–2 μm
	multilayer coatings Avinit C/P 100	Ti-N	H_v=2000 kg/mm^2, h=10–15 μm
	microlayer coatings Avinit C/P 510	Zr- Al-N separated	–
	nanolayer coatings Avinit C/P 320	Ti-Al-N separated	H_v=3500 kg/mm^2, h=1–2 μm
	multilayer coatings Avinit C/P 350	Ti-Al-N unseparated	H_v=3500 kg/mm^2, h=20 μm
Rollers	multilayer coatings Avinit C/P 210	Mo-N unseparated	H_v=2300 kg/mm^2, h=1–3 μm
	multilayer coatings Avinit C/P 220	Mo-N unseparated	H_v=2300 kg/mm^2, h=10...15 μm
	multilayer coatings Avinit C/P 100	Ti-N unseparated	H_v=2000 kg/mm^2, h=10–15 μm
	monolayer coatings Avinit A/P 200	Mo-N unseparated	H_v=3100 kg/mm^2, h=12 μm
	monolayer coatings Avinit A/P 300	Ti-Al-N unseparated	H_v=2800...3300 kg/mm^2, h=12 μm

Table 3.6 shows the absolute loads, kN, estimates of the running-in marks on the samples after testing, as well as the values of the coefficients at different values of the load for all investigated friction pairs. In **Fig. 3.15**, the results of these tests are presented in graphical form.

The surface morphology, roughness, the amount of production after testing (geometric properties of the running-in traces) are given in **Table 3.7**.

The performed in-depth metallophysical studies make it possible to more fully judge the dynamics of the wear process over the thickness of the coating and to more reasonably approach the choice of technological parameters for the deposition of nanolayer coatings with different thicknesses.

The parameters of Avinit multilayer and layered coatings during tribological tests for seize resistance and wear are given in **Table 3.8**.

Table 3.6 Results of tribological tests of samples coated with Avinit C

No.	No. cube (coating) No. roller (coating)	1st load, stage (load, kN)				2nd load, stage (load, kN)						
		1 0.2	2 0.4	3 0.6	4 0.8	1 0.2	2 0.4	3 0.6	4 0.8	5 1.0	6 1.2	7 1.4
8	072 [Avinit C/P 510] $7_{8/1}$ Avinit C/P 220	0.06	0.07	0.1	–	0.03	0.07	0.113	0.122	0.128	Burr	–
9	072 [Avinit C/P 510] 7_1 30Cr3MoWV, cemented)	0.04	0.05	0.08	–	0.12	0.12	0.12	0.128	0.132	0.127	0.121
10	057 [Avinit C/P 320] $7_{4/1}$ (20Cr3MoWV, cemented)	0.03	0.05	0.063	–	0.05	0.09	0.087	0.09	0.092	0.097	0.106
11	057 [Avinit C/P 320] $7_{9/1}$ Avinit C/P 220	0.03	0.03	0.03	–	0.012	0.011	0.02	0.03	0.03	0.03	0.03
		3rd load				0.01	0.009	0.007	0.011	0.014	–	–
		4th load				0.01	0.01	0.01	0.015	0.018	–	–
12	057 [Avinit C/P 320] $7_{б/No.}$ (Avinit C/P 110)	0.08	0.085	0.087	–	0.07	0.09	0.093	0.105	0.12	0.117	0.113
13	062 [Avinit C/P 320] $7_{6/1}$ Avinit C/P 220	0.1	0.115	0.13	–	0.06	0.13	0.13	0.11	0.102	0.1	0.097
14	067 [Avinit C/P 320] $7_{7/1}$ Avinit C/P 220	0.05	0.05	0.073	–	0.03	0.05	0.067	0.09	Burr	–	–
16	б/No. (X155CrVMo12-1) 7_3 (Avinit C/P 110)	0.09	0.095	0.11	–	0.06	0.1	0.13	0.13	0.132	0.127	0.129
17	057 [Avinit C/P 320] $7_{10/1}$ Avinit C/P 220	0.01	0.013	–	–	0.01	0.01	0.01	0.012	0.018	0.02	0.024

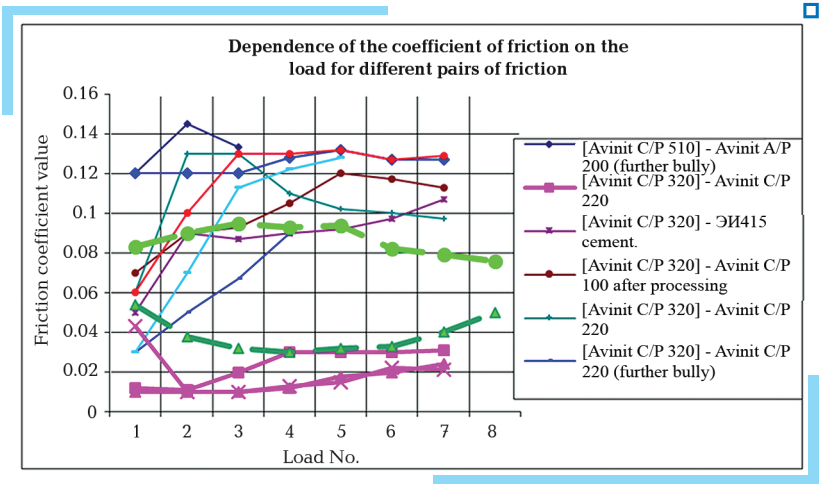

Fig. 3.15 Dependence of the coefficient of friction of samples with Avinit C coating on the load

Table 3.7 Evaluation of running-in traces on samples after tribological tests

Absolute load, kN	Coef. friction	No. sample	Geometric characteristics of traces of running-in		
1	2	3	4		
0.2...0.8 then tear	0.1...011	Main 056 Avinit C/P 320,	Height of adhesions, μm	Width, mm	Rough-ness
			110 max	2	–
		Contrtilo 6_1 Avinit A/P 200	Depth of working out, μm		
			Up to 3		
0.2 tear	–	Main 056 Avinit C/P 320	Depth, μm	Width, mm	Rough-ness
			Up to 12 damage	2.5	–
		Contrtilo $6_{7/1}$ Avinit A/P 300	Depth of working out, μm		
			Up to 0.7		
0.2...0.4 then tear	0.1...0.12	Main 066 Avinit C/P 330	Depth, μm	Width, mm	Rough-ness
			Up to 0.8	0.8	–
		Contrtilo 6_3 Avinit A/P 200	Depth of working out, μm		
			Up to 2.5		

Continuation of Table 3.7

1	2	3	4		
0.2...0.6 then tear	0.1...0.123	Main 061 Avinit C/P 330	Height of adhesions, μm	Width, mm	Rough-ness
			Up to 50	2	–
		Contrtilo 6_4 Avinit A/P 200	Depth of working out, μm		
			Up to 3.5		
0.2...1.0 then tear	0.12...0.1145	Main 071 Avinit C/P 510	Depth, μm	Width, mm	Rough-ness
			12	1.7	–
		Contrtilo 6_2 Avinit A/P 200	Depth of working out, μm	Width, mm	Rough-ness
			Up to 2	0.8	Ra 0.12 (▼10б)
0.2...0.8 then tear	0.03...0.09	Main 067 Avinit C/P 510	Depth, μm	Width, mm	Rough-ness
			Up to 5	2.3	–
		Contrtilo $7_{7/1}$ Avinit C/P 220	Depth of working out, μm		
			Up to 2.5		
0.2	tear	Main 072 Avinit C/P 510	Depth, μm	Width, mm	Rough-ness
			–	–	–
		Contrtilo $6_{8/1}$ Avinit A/P 300	Depth of working out, μm	Width, mm	Rough-ness
			–	–	–
0.2	tear	Main 067 Avinit C/P 320	Depth, μm	Width, mm	Rough-ness
			–	–	–
		Contrtilo $6_{9/1}$ Avinit A/P 300	Depth of working out, μm		
			–		
0.2	tear	Main 062 Avinit C/P 320	Depth, μm	Width, mm	Rough-ness
			–	–	–
		Contrtilo $6_{10/1}$ Avinit A/P 300	Depth of working out, μm	Width, mm	Rough-ness
			–	–	–
0.2...1.4	0.06...0.09 0.13	Main 062 Avinit C/P 320	Depth, μm	Width, mm	Rough-ness
			8	1.4	–
		Contrtilo $7_{6/1}$ Avinit C/P 220	Depth of working out, μm		
			Up to 5		
0.2...1.0 then tear	0.03...0.12	Main 072 Avinit C/P 510	Depth, μm	Width, mm	Rough-ness
			Up to 10	2	–
		Contrtilo $7_{8/1}$ Avinit C/P 220	Depth of working out, μm	Width, mm	Rough-ness
			–	–	–

Continuation of Table 3.7

1	2	3	4		
0.2...1.4	0.12...0.12 0.132	Main 072 Avinit C/P 510	Depth, μm	Width, mm	Roughness
			Up to 1	0.8	Ra 0.032 (▼12a)
		Contrtilo 7_1 without coating	Depth of working out, μm		Roughness
			–		–
0.2...1.4	0.06...0.12 0.132	Main б/№ without coating	Depth, μm	Width, mm	Roughness
			Up to 3	1	Ra 0.08 (▼11a)
		Contrtilo 7_3 Avinit C/P 110	Depth of working out, μm		Roughness
			–		Ra 0.023 (▼12c)
0.2...1.4	0.05...0.10	Main 057 Avinit C/P 320	Depth, μm	Width, mm	Roughness
			1.8	0.8	–
		Contrtilo $7_{4/1}$ without coating	Depth of working out, μm		Roughness
			–		–
0.2...1.4	0.012 0.03	Main 057 Avinit C/P 320	Depth, μm	Width	Roughness
			Up to 0.3	0.5	Ra 0.023 (▼12c)
		Contrtilo $7_{9/1}$ Avinit C/P 220	Depth of working out, μm	Roughness	
				Ra 0.02 (▼12c)	
0.2...1.4	0.01...0.024	Main 057 Avinit C/P 320	Depth, μm	Width,	Roughness
			Up to 0.1	Up to 0.5	Ra 0.025 (▼12c)
		Contrtilo $7_{10/1}$ Avinit C/P 220	Depth of working out, μm	Roughness	
				Ra 0.02 (▼12c)	
0.2...1.4	0.043...0.02 0.01	Main 057 Avinit C/P 320	Depth, μm	Width, mm	Roughness
			Up to 0.1	Up to 0.5	Ra 0.025 (▼12c)
		Contrtilo $7_{11/1}$ Avinit C/P 220	Depth of working out, μm	Roughness	
			there is no production	Ra 0.01	
0.2...1.4	0.07...0.113 0.12	Main 057 Avinit C/P 320	Depth, μm	Width, mm	Roughness
			Up to 0.3	Up to 0.6	–
		Contrtilo $7_{b/No.}$ Avinit C/P 110	Depth of working out, μm	Roughness	
			there is no production	Ra 0.032 (▼12a)	

Table 3.8 Parameters of Avinit multilayer and layered coatings during tribological tests for seize resistance and wear

microlayer coatings Avinit C/P 320	H_v=3500 kg/mm^2, h=1–2 μm
multilayer coatings Avinit C/P 210	H_v=2300 kg/mm^2, h=1–2 μm
multilayer coatings Avinit C/P 220	H_v=2300 kg/mm^2, h=20 μm
multilayer coatings Avinit C/P 220	H_v=2300 kg/mm^2, h=16 μm
nanolayer coatings Avinit C/P 320	H_v=3500 kg/mm^2, h=1–2 μm
multilayer coatings Avinit C/P 350	H_v=3500 kg/mm^2, h=20 μm

The values of the coefficient of friction in a friction pair (Avinit C/P 210/ Avinit C/P 320), recorded during tests for seize resistance and wear (during wear tests, average) are shown in **Fig. 3.16**.

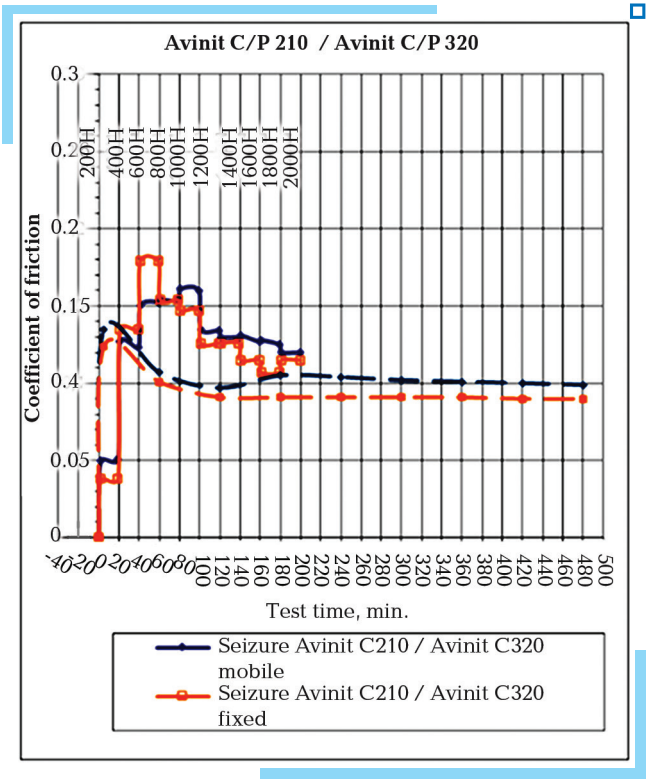

Fig. 3.16 Coefficients of friction in a pair of friction (Avinit C/P 210/ Avinit C/P 320)

During wear tests during the entire test period, the recorded parameters were at the same level, and the wear rate was characterized by 20...40 information units of acoustic emission, however, periodic bursts of the wear rate up to 140...160 information units of acoustic emission were observed. Fractographic studies of these samples revealed pitting damage on the contact surface of the sample (**Fig. 3.17**), the state of the contact surface of the reverse sample has no comments.

After testing all friction pairs, there are no signs of increased wear, tear of the working surfaces of samples coated with Avinit C/P 320-ms1 and Avinit C/P 210-m1, except for the above pitting damage.

Fig. 3.18 shows the values of the coefficient of friction in friction pairs (▼ 8, Avinit C/P 220, ▼ 10/Avinit C/P 320), recorded during tests for seize resistance and wear (during wear tests — average).

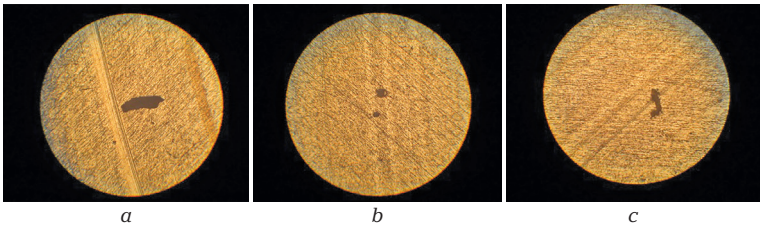

Fig. 3.17 Fractography of surface No. 6 at three points along the line of contact: *a* — outer surface; *b* — the middle part; *c* — inner surface

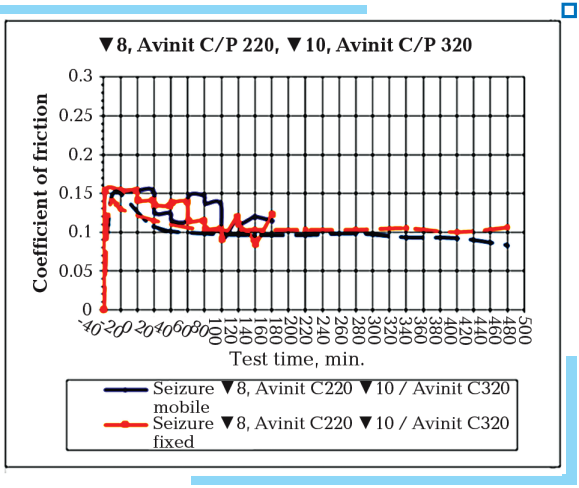

Fig. 3.18 Coefficients of friction in a pair of friction (▼8, Avinit C/P 220, ▼10 / Avinit C/P 320)

After testing all friction pairs, there are no signs of increased wear, tear of the working surfaces of specimens with coatings Avinit C/P 320 and ▼ 8, Avinit C/P 220, ▼ 10.

The nature of the change in the steam wear rate is shown in **Fig. 3.19**.

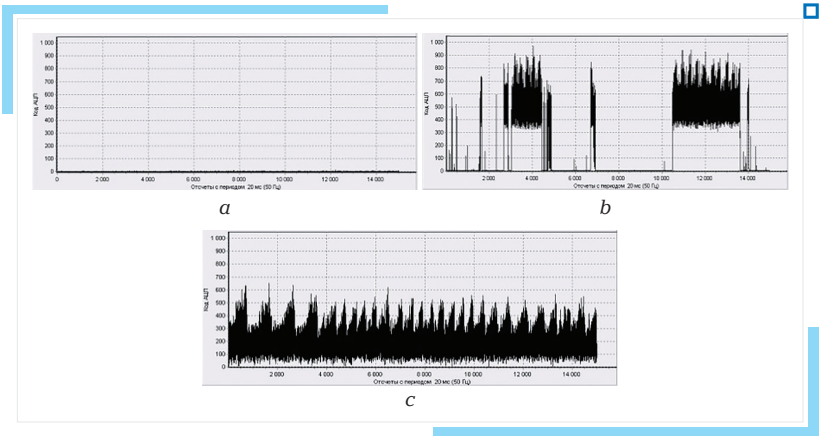

Fig. 3.19 The nature of the change in the rate of wear of steam No. 3/No. 3: *a* — up to the 90th miniline of tests; *b* — 90th miniline of tests; *c* — during the time until the end of the tests

Traces of mutual running-in on the contacting ends of the samples are more pronounced.

The traces of running-in on the samples shine and do not have traces of adhesion, and even more so, catastrophic damage to the coatings.

During wear tests of steam from the 120th minute, the friction coefficient began to decrease and reached abnormally low values (0.0048), followed by a transition to periodic fluctuations from 0.02 to 0.1. Mutual traces of running-in on the working ends of the samples are practically absent.

No noticeable difference was found in the work of friction pairs, which include samples with different surface preparation for Avinit C/P 220 coating.

The results of testing coatings in friction pairs Avinit C/P 220, ▼ 10/ Avinit C/P 350, ▼ 10) are given in **Table 3.9**.

After testing all friction pairs, there are no signs of increased wear, tear of the working surfaces of samples with coatings Avinit C/P 350 ▼ 10 and Avinit C/P 220 ▼ 10.

Operating time of Avinit C/P 350 ▼ 10 and Avinit C/P 220 ▼ 10 under conditions: load 1600N, 500 rpm, lubrication — TC-1 fuel, both direct and reverse friction pair after tests according to this section 40 hours on each specified sample.

When testing coatings in friction pairs (Avinit C/P 220, ▼ 10/ Avinit C/P 320), tested specimens were used as reverse parts making up the friction pairs and externally did not have any damage.

Table 3.9 Values of specimen wear during wear tests for 8 hours of friction pair Avinit C/P 350 ▼ 10 and Avinit C/P 220 ▼ 10

Friction pair	Wear, gr					
	Avinit C220, ▼10	Average	Avinit C350, ▼10	Average	Total	Average total
	stationary		mobile		«direct» pair	
No. 1/No. 1	0.0005		0		0.0005	
No. 2/No. 2	0.0002	0.00032	0	0	0.0002	0 .00032
No. 3/No. 6	0.00025		0		0.00025	
	mobile		stationary		«reverse» pair	
No. 4/No. 1	0.0006		0.0001		0.0007	
No. 5/No. 2	0.00035	0.00038	0.00015	0.00013	0.0005	0.00051
No. 6/No. 6	0.0002		0.00015		0.00035	

The values of specimen wear during 8 hours of testing of the friction pair Avinit C/P 220, ▼ 10 / Avinit C/P 320 are given in **Table 3.10**.

Table 3.10 Values of specimen wear during 8 hours of testing friction pair Avinit C/P 220, ▼ 10 / Avinit C/P 320

Friction pair	Wear, gr.					
	Avinit C210	Average	Avinit C320	Average	Total	Average total
	stationary		mobile		«direct» pair	
No. 1/No. 1	0.0043		0.00115		0.00545	
No. 2/No. 2	0	0.03618	0	0.00072	0	0.0369
No. 4/No. 4	0.10425 (pitting destruction)		0.001		0.10525	
	mobile		stationary		«reverse» pair	
No. 3/No. 3	0.0586		0		0.0586	
No. 5/No. 5	0.0028	0 .02092	0.0021	0.00148	0.0049	0.0224
No. 6/No. 6	0.00135 (pitting destruction)		0.00215		0.0035	

After tribological tests in friction pairs (▼ 10, Avinit C/P 220, ▼ 10/ Avinit C/P 320), the working surfaces of the samples with Avinit C/P 220 coatings were machined with a 5...6 μm allowance to the geometric one. parameters: no plane ≤0.001 mm; roughness Ra 0.16 μm (▼ class 10). As a result, a coating Avinit C/P 220, ▼ 10, 5...10 μm thick, was created, which was tested together with a coating that had already passed tribological tests Avinit C/P 320 and was not subjected to any modification after preliminary tests. After testing all friction pairs, there are no signs of increased wear, tear of the working surfaces of samples with Avinit C/P 220 and Avinit C/P 320 coatings. The Avinit C/P 320 coating operating time under the following conditions: load 1600N, 500 rpm, lubricant — TC-1 fuel, both direct and reverse friction pair after tests according to this section was 24 hours on each specified sample.

3.4.2 Tribological characteristics of Avinit D coatings

The results in the form of tables and graphs for *Avinit* D/P 100 coatings (Ti-C; Ti-C: H, Ti-C-N, Ti-C-C) are shown in **Fig. 3.20** and **Table 3.11**, and for Avinit D/P 200 coatings (MoC, MoC-C, Mo-C-N, Mo-C: H) — in **Table 3.12**.

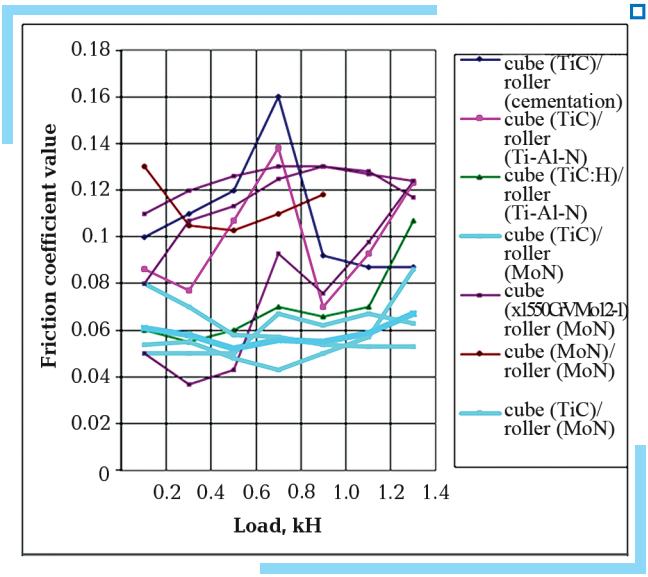

Fig. 3.20 Dependence of the coefficient of friction on the load for friction pairs, that worked without wear and tear

Table 3.11 Tribological test results of Avinit D/P 100 coatings

No.	Cube (coating)	Roller (coating)	Test results	
1	2	3	4	
1	X155CrVMo12-1. 56...61 HRC	Avinit D/P 120 Ti-C-C (6) t=12 µm, 1800...2200HV	Operating time ≈ 2...5 sec: burr in the process of increasing the load from 0 to ≈ 100 N max	Metal deposits on the cube, the corresponding grooves on the roller
2		Avinit C/P 110 Ti-N (5) t=8 µm, 600...900 HV	200 H (2.5 min), F_{fr}=0.22; 400 H (2...3 sec), the beginning of the tear	The cube has a wear mark width ≈5mm, on a roller initial traces of transfer of material of a cube
3		Avinit D/P 130 TiN-TiC (4) t=12µm, 1890 HV	Operating time ≈ 2...5 sec: burr in the process of increasing the load from 0 to ≈ 100 N max	Metal deposits on the cube, the corresponding grooves on the roller
4	Avinit D/P 100 TiC (15) t=8...10 µm, 2000 HV; removed allowance 3...4 microns, layer thickness t=6...7 µm	20Cr3MoWV, cementation, ≥88HRN15	200 H (2.5 min), F_{fr}=0.10; 400 H (2.5 min), F_{fr}=0.11; 600 H (2.5 min), F_{fr}=0.12; 800 H (2.5 min), F_{fr}=0.16; 1000 H (2.5 min), F_{fr}=0.092; 1200 H (2.5 min), F_{fr}=0.087; 1400 H (2.5 min), F_{fr}=0.087; in the first second after increasing the load more than 1400 N — the beginning of burrs. $(pV)_{max}$=303 Wt/mm^2	The cube has two traces: ■ one trace of running-in, at loads of 200...1400 H; ■ the second trace of wear ≈2 mm wide, which appeared, due to burr. Options for running-in: ■ depth — 0.7 microns; ■ width — 0.6 mm; ■ area — 6 mm^2. The video shows the initial traces of the transfer of the cube material that appeared after the tear
5	Avinit D/C 100 TiC:H (19) t=1.5 µm, 1700 H_{50}		200 H (2.5 min), F_{fr}=0.10; 400 H (2.5 min), F_{fr}=0.11; 600 H (2.5 min), F_{fr}=0.12; 800 H (5...10 sec), beginning of burrs	The cube has a wear mark width ≈5mm, on a roller traces of transfer of material of a cube
6	Avinit C/P 110 TiN (18) t=10µm, 2000...2200HV		200 H (2.5 min), F_{fr}=0.16; 400 H (2.5 min), F_{fr}=0.15; 600 H (2.5 min), F_{fr}=0.157; at ≈700H burr	Minor deposits of metal on the cube, the corresponding scratches on the roller

Continuation of Table 3.11

1	2	3	4	
7	Avinit C/P 330 n(Ti-Al-N) (5) t=1.5μm, 3500HV	Avinit D/P 120 Ti-C-C (6) t=12 μm, 1800...2200 HV	200 H (≈2.5 min), F_{fr}=0.14 at the end of the mode — the beginning of the tear	
8		Avinit D/P 130 TiN-TiC (4) t=12 μm, 1890 HV	Operating time ≈ 1...3 sec: burr when going to load 200 H	The cube has a wear mark ≈2 mm wide with metal deposits
8a		Avinit D/P 130 TiN-TiC (4) t=12 μm, 1890 HV	200 H (2.5 min), F_{fr}=0.14 400 H (2.5 min), F_{fr}=0.138 600 H (2.5 min), F_{fr}=0.143 800 H (2.5 min), F_{fr}=0.148 1000 H (2.5 min), F_{fr}=0.146 1200 H (2.5 min), F_{fr}=0.143 1400 H (2.5 min), F_{fr}=0.140	The cube has a wear mark width ≈4 mm. The roller has a normal trace of running-in, visually there are no signs of wear
9		Avinit D/P 100 TiC (7) t=12 μm, 2054 HV	200 H (2.5 min), F_{fr}=0.160 400 H (2.5 min), F_{fr}=0.155 600 H (2.5 min), F_{fr}=0.150 800 H(2.5 min), F_{fr}=0.150 1000 H (2.5 min), F_{fr}=0.140 1200 H (2.5 min), F_{fr}=0.130 1400 H (2.5 min), F_{fr}=0.119	The cube has a wear mark width ≈6 mm. The roller has a normal trace of running-in, visually there are no signs of wear
10	Avinit D/P 100 TiC (15) t=8...10 μm, 2000 HV; an allowance of 3...4 μm is removed, the layer thickness is t=6...7 μm	Avinit C/P 330 n(Ti-Al-N) (13) t=1.5 μm, 3500 HV	20 0H (2.5 min), F_{fr}=0.086 400 H (2.5 min), F_{fr}=0.077 600 H (2.5 min), F_{fr}=0.107 800 H (2.5 min), F_{fr}=0.138 1000 H (2.5 min), F_{fr}=0.070 1200 H (2.5 min), F_{fr}=0.093 1400 H (2.5 min), F_{fr}=0.123 $(pV)_{max}$=152 W/mm^2	The cube has a trace of running-in with the parameters: ▪ depth — 4.1 microns; ▪ width — 1.2 mm; ▪ area — 12 mm^2. The roller has a normal trace of running-in, visually there are no signs of wear

Continuation of Table 3.11

1	2	3	4	
11	Avinit D/C 100 TiC:H (19) t=1.5 µm, 1700 H_{50}	Avinit C/P 330 n(Ti-Al-N) (13) t=1.5 µm, 3500 HV	200 H (2.5 min), F_{fr}=0.060 400 H (2.5 min), F_{fr}=0.055 600 H (2.5 min), F_{fr}=0.060 800 H (2.5 min), F_{fr}=0.070 1000 H (2.5 min), F_{fr}=0.066 1200 H (2.5 min), F_{fr}=0.070 1400 H (2.5 min), F_{fr}=0.107 $(pV)_{max}$=182 W/mm^2	The cube has a trace of running-in with the parameters: ▪ depth — 3.1 microns; ▪ width — 1 mm; ▪ area — 10 mm^2. The roller has a normal trace of running-in, visually there are no signs of wear
12	X155CrVMo12-1, 56...61 HRC	Avinit D/P 100 TiC (7) t=12 µm, 2054 HV	Operating time ≈ 1...2 sec at a load of 200 N: burr	The cube has a wear mark width ≈2 mm, with metal deposits in the center; corresponding furrow on the roller
12a		Avinit D/P 100 TiC (7)	Operating time ≈ 2...5 sec at a load of 200 N: burr	The cube has a wear mark width ≈2 mm, with metal deposits in the center; corresponding furrow on the rolle
12b		Avinit D/P 130 TiN-TiC (4)	200 H (2.5 min), F_{fr}=0.140 400 H (2.4 min), F_{fr}=0.140, at the end of the mode — a tear	The cube has a wear mark width ≈2 mm, with metal deposits, the corresponding groove on the roller
13	Avinit C/P 210 MoN (17) t=1.5 µm, 2200 HV	20Cr3MoWV, cementation, ≥88HRN15	200 H (2.5 min), F_{fr}=0.140 400 H (2.5 min), F_{fr}=0.123 600 H (2.5 min), F_{fr}=0.127 at the beginning of loading 800 N: burr	Traces of setting, both on the cube and on the roller
14	Avinit *D/P 100* TiC (15) t=8...10 µm, 2000 HV; removed allowance 3...4 microns, layer thickness t=6...7 µm	Avinit C/P 210 MoN (12) t=1.5 µm, 2200 HV	200 H (2.5 min), F_{fr}=0.050 400 H (2.5 min), F_{fr}=0.050 600 H (2.5 min), F_{fr}=0.050 800 H (2.5 min), F_{fr}=0.067 1000 H (2.5 min), F_{fr}=0.062 1200 H (2.5 min), F_{fr}=0.067 1400 H (2.5 min), F_{fr}=0.063 $(pV)_{max}$=260 W/mm^2	On a cube and on a roller the normal trace of running-in, visually there are no signs of wear. It is necessary to work on a cube with parameters: ▪ depth — 0.8 microns; ▪ width — 0.7 mm; ▪ area — 7 mm^2

Continuation of Table 3.11

1	2	3	4	
15	Avinit D/C 100 TiC:H (19) t=1.5 µm, 1700 H_{50}	Avinit C/P 210 MoN (12) t=1.5 µm, 2200 HV	200 H (2.5 min), F_{fr}=0.110 400 H (2.5 min), F_{fr}=0.095 600 H (2.5 min), F_{fr}=0.100 800 H(2.5 min), F_{fr}=0.090 1000 H(2.5 min), F_{fr}=0.096 at 1200 N operating time ≈2...5 sec: tear	The cube has a normal trace of running-in with metal deposits in the center; corresponding furrow on the roller
16	X155CrVMo12-1, 56...61 HRC		200 H (2.5 min), F_{fr}=0.050 400 H (2.5 min), F_{fr}=0.037 600 H (2.5 min), F_{fr}=0.043 800 H (2.5 min), F_{fr}=0.093 1000 H (2.5 min), F_{fr}=0.076 1200 H (2.5 min), F_{fr}=0.098 1400 H (2.5 min), F_{fr}=0.124 $(pV)_{max}$=182 W/mm^2	The cube has a trace of running-in with the parameters: ▪ depth — 2.7 microns; ▪ width — 1 mm ▪ area — 10 mm^2. The roller has a normal trace of running-in, visually there are no signs of wear
17	Avinit C/P 210 MoN (17) t=1.5 µm, 2200 HV	Avinit C/P 210 MoN (12)	200 H (2.5 min), F_{fr}=0.130 400 H (2.5 min), F_{fr}=0.105 600 H (2.5 min), F_{fr}=0.103 800 H (2.5 min), F_{fr}=0.110 1000 H (2.5 min), F_{fr}=0.118 then the load was not increased $(pV)_{max}$=260 W/mm^2	The cube has a trace of running-in with the parameters: ▪ depth — 0.2 microns; ▪ width — 0.5 mm; ▪ area — 5 mm^2. The roller has a normal trace of running-in, visually there are no signs of wear
18	Avinit D/P 100 TiC (15) t=8...10 µm, 2000 HV; removed allowance 3...4 microns, layer thickness t=6...7 µm	Avinit C/P 210 MoN (12) t=1.5 µm, 2200 HV	200 H (2.5 min), F_{fr}=0.054 400 H (2.5 min), F_{fr}=0.055 600 H (2.5 min), F_{fr}=0.048 800 H (2.5 min), F_{fr}=0.043 1000 H (2.5 min), F_{fr}=0.050 1200 H (2.5 min), F_{fr}=0.057 1400 H (2.5 min), F_{fr}=0.086	The cube has a trace of running-in with the parameters: ▪ depth — 1.7 microns; ▪ width — 1.1 mm; ▪ area — 11 mm^2. The roller has a normal trace of running-in, visually there are no signs of wear

Continuation of Table 3.11

1	2	3	4	
19	Avinit D/P 100 TiC (15) t=8...10 µm, 2000 HV; removed allowance 3...4 microns, layer thickness t=6...7 µm	Avinit C/P 210 MoN (12) t=1.5 µm, 2200 HV	200 H (2.5 min), F_{fr}=0.080 400 H (2.5 min), F_{fr}=0.070 600 H (2.5 min), F_{fr}=0.058 800 H (2.5 min), F_{fr}=0.057 1000 H (2.5 min), F_{fr}=0.054 1200 H (2.5 min), F_{fr}=0.053 1400 H (2.5 min), F_{fr}=0.053	The cube has a trace of running-in with the parameters: ■ depth — 0.5 microns; ■ width — 1.5 mm; ■ area — 15 mm^2. The roller has a normal trace of running-in, visually there are no signs of wear
20	Avinit D/C 100 TiC:H (19) t=1.5 µm, 1700 H_{50}	Avinit D/C 320 n(Ti-Al-N) (13) t=1.5 µm, 3500 HV (analogue of factory technology)	200 H (2.5 min), F_{fr}=0.066 400 H (2.5 min), F_{fr}=0.062 600 H (2.5 min), F_{fr}=0.073 800 H (2.5 min), F_{fr}=0.087 1000 H (2.5 min), F_{fr}=0.092 1200 H (2.5 min), F_{fr}=0.098 1400 H (2.5 min), F_{fr}=0.106	The cube has a trace of running-in with the parameters: ■ depth — 3 microns; ■ width — 1 mm; ■ area — 10 mm^2. The coating is completely worn in thickness. The roller has a normal trace of running-in, visually there are no signs of wear
21	Avinit D/C 100 TiC:H (19) t=1.5 µm, 1700 H_{50}	Avinit D/C 320 n(Ti-Al-N) (13) t=1.5 µm, 3500 HV (analogue of factory technology)	200 H (2.5 min), F_{fr}=0.074 400 H (2.5 min), F_{fr}=0.073 600 H (2.5 min), F_{fr}=0.087 800 H (2.5 min), F_{fr}=0.092 1000 H (2.5 min), F_{fr}=0.104 1200 H (2.5 min), F_{fr}=0.105 1400 H (2.5 min), F_{fr}=0.110	The cube has a trace of running-in with the parameters: ■ depth — 3.4 microns; ■ width — 1 mm; ■ area — 1 0mm^2. The coating is completely worn in thickness. The roller has a normal trace of running-in, visually there are no signs of wear
22	X155CrVMo12-1, 56...61 HRC	Avinit C/P 210 MoN (12) t=1.5 µm, 2200 HV	200 H (2.5 min), F_{fr}=0.080 400 H (2.5 min), F_{fr}=0.107 600 H (2.5 min), F_{fr}=0.113 800 H (2.5 min), F_{fr}=0.125 1000 H (2.5 min), F_{fr}=0.130 1200 H (2.5 min), F_{fr}=0.128 1400 H (2.5 min), F_{fr}=0.117	The Cube has a trace of running-in with the parameters: ■ depth — 3.8 microns; ■ width — 1 mm; ■ area — 10 mm^2. The roller has a normal trace of running-in, visually there are no signs of wear

Continuation of Table 3.11

1	2	3	4	
23	X155CrVMo12-1, 56...61 HRC	Avinit C/P 210 MoN (12) t=1.5 µm, 2200 HV Earned in experiments 1 and 5	200 H (2.5 min), F_{fr}=0.110 400 H (2.5 min), F_{fr}=0.120 600 H (2.5 min), F_{fr}=0.126 800 H (2.5 min), F_{fr}=0.130 1000 H (2.5 min), F_{fr}=0.130 1200 H (2.5 min), F_{fr}=0.127 1400 H (2.5 min), F_{fr}=0.124	The cube has a trace of running-in with the parameters: ▪ depth — 3.2 microns; ▪ width — 1 mm; ▪ area — 10 mm^2. The roller has a normal trace of running-in, visually there are no signs of wear
24	Avinit C/P 210 MoN (22) t=1.5 µm, 2200 HV	20Cr3MoWV, nitriding, >800 HV. Earned with a load of 200N max	200 H (2.5 min), F_{fr}=0.146 400 H (2.5 min), F_{fr}=0.143 600 H (2.5 min), F_{fr}=0.130 800 H (2.5 min), F_{fr}=0.130 1000 H Operating time ≈ 2...5 sec: burr.	The cube has a wear mark width ≈5mm, on a roller traces of transfer of material of a cube
25	Avinit D/C 230 Mo-Al-C:H (20)	Avinit C/P 210 MoN (12) t=1.5 µm, 2200 HV	200 H (2.5 min), F_{fr}=0.046 400 H (2.5 min), F_{fr}=0.073 600 H (2.5 min), F_{fr}=0.092 800 H (2.5 min), F_{fr}=0.108 1000 H Operating time ≈ 1 min: burr	Stick of metal on the cube in the center of the initial trace of running-in
26	Avinit C/P 210 MoN (17) t=1.5 µm, 2200 HV	Avinit C/P 110 Ti N	When reaching the level of 200 N: burr	Stick of metal on the cube in the center of the initial trace of running-in

Table 3.12 Tribological test results of Avinit D/P 200 coatings

No.	Cube (coating)	Roller (coating)	Test results	
1	MoC:H (26) $t \leq 2$ µm	20Cr3MoWV, cementation, ≥88HRN15	200 H (2.5 min), F_{fr}=0.140 400 H (2.5 min), F_{fr}=0.110 600 H (2.5 min), F_{fr}=0.123 800 H (2.5 min), F_{fr}=0.123 1000 H (2.5 min), F_{fr}=0.132 when the load increases by more than 1000N — the beginning of the tear	Initial traces of mutual transfer of material on the cube and roller. Parameters of a trace of running-in on a cube: ▪ depth — 11 microns; ▪ width — 1.2 mm
2		Avinit C/P 210 MoN (16) t=1.5 µm, 2200 HV	200 H (2.5 min), F_{fr}=0.160 400 H (2.5 min), F_{fr}=0.145 600 H (2.5 min), F_{fr}=0.143 800 H(2.5 min), F_{fr}=0.147 1000 H (2.5 min), F_{fr}=0.150 1200 H (2.5 min), F_{fr}=0.148 1400 H (2.5 min), F_{fr}=0.147	The cube has a trace of running-in with the parameters: ▪ depth — 14 microns; ▪ width — 1.6 mm. The roller has a normal trace of running-in, visually there are no signs of wear
3		Avinit D/C 320 n(Ti-Al-N) (14) t=1.5 µm, 3500 HV (analog of factory technology)	200 H (2.5 min), F_{fr}=0.09 400 H (2.5 min), F_{fr}=0.09 600 H (2.5 min), F_{fr}=0.097 800 H (2.5 min), F_{fr}=0.105 1000 H (2.5 min), F_{fr}=0.102 at the output of 1200N jump on the moment, the test is stopped	The cube has a trace of running-in with the parameters: ▪ depth — 16 microns; ▪ width — 1.7 mm. The roller has a normal trace of running-in, visually there are no signs of wear

Analysis of the results. The entire obtained array of tribological data for the investigated coatings is shown in the middle form in **Fig. 3.21**.

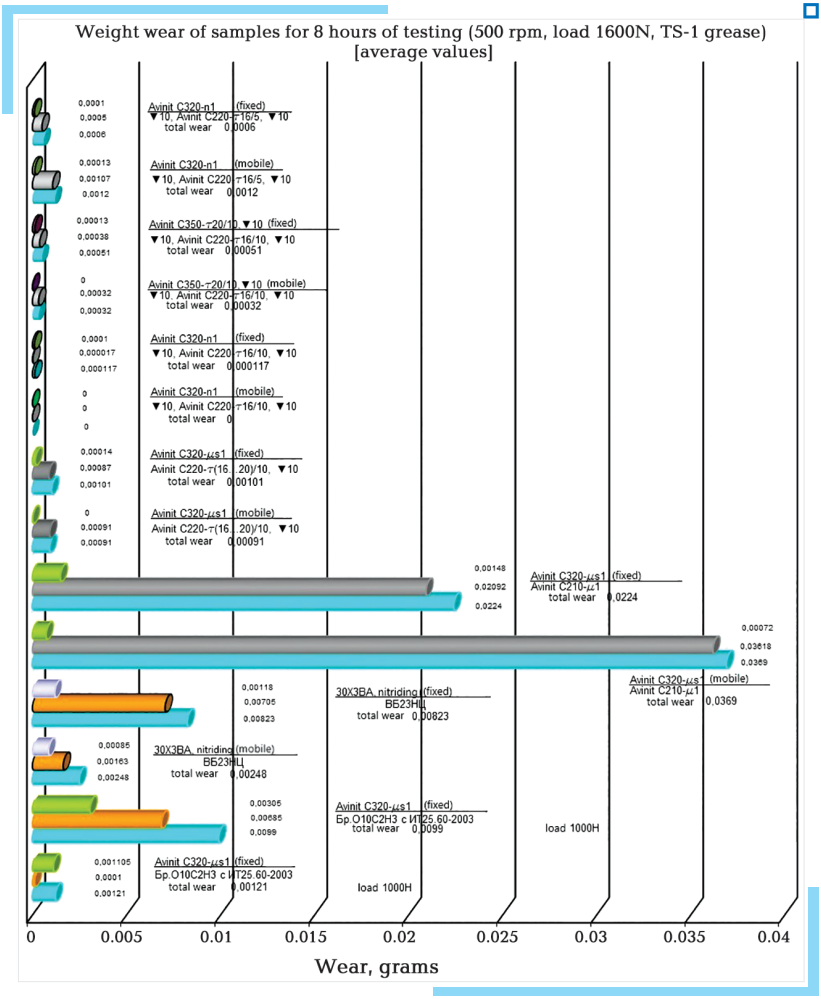

Fig. 3.21 Generalized array of tribological data

Comparison with the test results «coated steel — bronze Br.010C2N3, processed according to the factory technology», as well as with bronzes Br.010C2N3, VB-23, VB-24 with uncoated steel shows that the presence of the developed coatings significantly increases the resistance of tribopairs to seize, increasing the seize value P_{cr} and practically preventing seize.

Tribological studies of improved Avinit coatings have shown that coating deposition effectively improves steam seize resistance by increasing the seize value Pcr. The use of multilayer coatings (for example Avinit C/P 110 of the TiN-Ti type) leads to an increase in Pcr in comparison with monolayer coatings (for example, Avinit C/P 100 of the TiN type). Particularly effective are coatings based on Avinit C/P 220, which have the highest P_{cr} values.

All of the improved coatings had low coefficients of friction at loads up to 2.0 kN. This is evidenced not only by an increase in the load during tests to the limit, but also by the course of the dependence of the friction coefficients on the load, after a certain rise with an increase in the load to 0.6–0.8 kN, it decreased to a maximum load of 2 kN.

The values of the friction coefficients for all types of coatings have fairly close values and at loads over 1.0 kN they are in the range from 0.06 to 0.1.

The smallest coefficient of friction small steam — Avinit C/P320 coating — Avinit C/P220 coating. The value of the coefficient of friction of the steam did not exceed 0.095 in the entire range of loads, and at the maximum load it was 0.065, which corresponds to the minimum value obtained for the pairs of friction with the investigated coatings.

All coatings in the tests showed high wear resistance, the value of which did not exceed 0.8 μm.

Friction pairs, the working surfaces of which have micro- and nanolayer coatings Avinit C/P 320, Avinit C/P 320, Avinit C/P 350, Avinit C/P 220, Avinit C/P 220, Avinit C/P 220, have been tested in limiting lubrication conditions are characterized by:

- high constancy to seize;
- lack of secondary running-in;
- a sufficiently high stability in time of the coefficient of friction when operating at a constant load;
- significantly less difference between «direct» and «reverse» pairs, in comparison with the «base» pair VB23NS bronze/nitrided steel 30X3VA.

All tested friction pairs with nanocoatings have a clearly defined running-in period of 60 minutes, after which the values of the friction coefficients stabilize and, with a constant load of 1600N, are within 0.09...0.132.

Comparison of the bronze surface after testing with different types of coatings showed that Avinit C/P 320 coatings provide the best roller running-in among the tested friction pairs. On the other hand, the amount of wear of this type of coating has minimum values, which in general allows to consider this pair as the best according to the results of the tests performed.

The best combination of wear resistance and tribological properties was shown by a friction pair composed of Avinit C/P 220 coatings (16...20 μm thick), followed by machining by grinding to a thickness of 10...15 μm, and Avinit C/P 320-n1 μm), without further machining.

This pair had the smallest coefficient of friction (F_{fr}=0.095 in the entire load range, and at maximum load F_{fr}=0.075) and practically zero wear in

8 hours tests. Wear resistance significantly exceeds the pair VB23NS/nitride steel 30X3VA (selected as one of the best options that exist at present for the operation of friction pairs):

a) 12 times minimum for the couple as a whole:

b) 2.5 times the minimum for a harder steam sample;

c) 44 times the minimum for a softer steam sample;

d) on «straight» steam after testing for 8 hours, no weight wear by the applied control methods was found.

Weight wear detected after 8 hours of wear tests is less than that of the «base» pair:

- 2.7 times for a «straight» pair;
- 8.1 times for the «reverse» pair.

Based on the tribological tests carried out, the choice of improved coatings based on the Ti-Al-N system was made to increase the wear resistance and reduce the coefficient of friction of pairs.

The best combination of wear resistance and tribological properties was shown by a friction pair composed of Avinit C/P 220 coatings (16...20 μm thick), followed by machining by grinding to a thickness of 10...15 μm, and Avinit C/P 320, without further machining. It had the lowest coefficient of friction and practically zero wear in 8 hours tests.

To increase wear resistance and reduce friction coefficients, Avinit multicomponent multilayer coatings based on carbide systems — Avinit D/P 100 (Ti-C; Ti-C:H, Ti-CN, Ti-CC) and Avinit D/P 200 (Mo-C, MoC-C, Mo-CN, Mo-C:H).

At present, the processes of applying such coatings to specific parts in full-scale friction units are being tested for carrying out resource and aggregate tests.

Summing up the results of in-depth metallophysical and tribological studies, it is possible to formulate the features of Avinit coatings that make them extremely attractive for industrial implementation, primarily in precision friction pairs:

1. A significant increase in the spectrum of sources, provided by the complexity of the methods used, makes it possible to obtain a coating from almost any elements and alloys, refractory oxides, carbides, nitrides, cermet compositions based on refractory metals and oxides, which significantly expands the possibilities of creating fundamentally new materials and coatings of assemblies and parts for various purposes operating under extreme conditions in terms of temperature, exposure to aggressive media, mechanical stress.

When obtaining Avinit coatings, it is possible to switch to the nanorange for the implementation of the processes of controlled formation of multicomponent nano- and microstructural coatings with specified characteristics, containing a large number of layers of various chemical compositions (metal, nitride, carbide, oxide, etc.) with a thickness from units to hundreds of nanometers.

The correct choice of individual layer materials, deposition methods and optimization of technological parameters create the preconditions for the synthesis of materials with a set of unique properties, including extremely high rigidity, strength, chemical stability, low friction coefficient and increased wear resistance.

The developed software products make it possible to move to the microdesign of functional coatings and ensure the production of specified nano- and microlayer multicomponent coatings and reach a qualitatively new level of further modification and improvement of Avinit coatings designs, technology stability and improved quality control when applying such coatings.

2. For the formation of reinforcing superhard and wear-resistant and antifriction nanostructured coatings by complex methods of vacuum-plasma and plasma-chemical deposition from the gas and vapor phases using nonequilibrium low-temperature plasma, technological schemes and their variations have been worked out depending on the type of substrate and application features, taking into account the requirements for ensuring the necessary properties coatings depending on their functional purpose.

3. Avinit coatings are deposited on precision surfaces of high cleanliness class up to 12–13 class without reducing the class of surface cleanliness. This is achieved by the possibility of using effective technologies for surface cleaning in the technologies being developed — cleaning in Ar glow discharge, cleaning in a two-stage vacuum-arc discharge (TVAD) and cleaning with metal ions, as well as preventing surface damage by micro-arcs due to an improved three-level (mechanical, electrical and electronic) arc extinguishing system, providing high quality surface cleaning from oxides and other contaminants without the occurrence of electrical breakdowns.

The deposition is carried out at low temperatures, not exceeding the tempering temperatures of the base material, which ensures the preservation of the mechanical characteristics of the coated products.

4. Avinit coatings have a nanolayer and multilayer structure and contain a large number of layers of different chemical composition (metal, nitride, carbide, oxide, etc.) with a thickness from units to hundreds of nanometers.

Layers of different chemical composition are applied using combined methods — PVD (vacuum arc and magnetron sputtering) and CVD (gas phase and plasma chemical deposition).

The layer structure is provided by programmable coordinated modes of operation of plasma sources (both PVD and CVD), working gases (argon, nitrogen, carbon- and oxygen-containing gases) and high potential applied to the substrate.

The conducted studies allowed to select the temperature-time parameters of obtaining Avinit reinforcing coatings to increase the wear resistance of the working surfaces of precision friction pairs, ensuring the production of coatings of a given composition with a thickness of 1–3 μm, and to develop software products for obtaining such coatings on Avinit equipment and

development of technologies for applying multifunctional multicomponent multilayer coatings on real parts of serial units.

Based on the concept of nanolayer coatings, the proven technological parameters of the processes (PVD and hybrid PVD + CVD) for the deposition of multilayer and nanolayer coatings in metal-nitrogen and metal-carbon systems using vacuum plasma (PVD) and plasma-chemical (CVD):

a) «hard and superhard coatings»:

- nitride-based in metal-nitrogen systems — monolayer and multilayer (Ti, Mo, Zr, Cr) N, Ti-Al-N, Ti-Mo-N, Zr-Ti-N, etc.;
- carbide-based in metal-carbon systems — monolayer and multilayer TiC, monolayer Ti-CN, nanolayer TiC-TiN, nanolayer TiC-C, MoC monolayer structures, monolayer Mo-CN, nanolayer MoC-C, monolayer TiC:H , nanolayer TiC: H-TiN, nanolayer and multilayer TiC-C: H, monolayer MoC: H, nanolayer MoC: H-TiN, nanolayer MoC: H structures;

b) «metal-metal coatings» — metal multilayer PVD coatings of Mo, Ti, Zr, Nb, Cr, Ni; multilayer PVD coating based on Cu-Mo-N; multilayer PVD coating based on (Cu-C) (with different carbon content).

Experimental results confirm the possibility of low-temperature deposition of high-hard wear-resistant Avinit coatings based on metal nitrides and carbides in modes that provide good adhesion to substrate materials (X162CrMoV12 steel with a precision surface Ra=0.025 μm) without a significant decrease in the strength characteristics of steel (<200 °C) and the initial surface cleanliness class.

Multicomponent multilayer nanolayer coatings have been developed that have high wear resistance and tribological characteristics.

The combination of high hardness, wear resistance and low values of the coefficient of friction in hard and superhard Avinit coatings is important when used in friction pairs to prevent tear.

The obtained results of metallophysical and tribological studies are the basis for the selection of coating materials and the development of new designs of wear-resistant antifriction coatings to increase the performance of friction pairs in the «coating-steel» and «coating-coating» systems, as well as to develop the processes of their application.

3.5 Plasma precision nitriding of Avinit N

In mechanical engineering, very common special technological processes to improve the performance of parts and structures are the methods of chemical thermal treatment (CTO) (carburizing, nitriding, nitrocarburizing, etc.) [67–71].

A new method of vacuum-plasma precision nitriding of metals and alloys Avinit N in high-density low-temperature nonequilibrium nitrogen plasma has been developed and patented in the research and production corporation FED JSC [72–74].

This method is described in detail in [29, 30, 75].

Plasma burns evenly in large volumes, providing uniform heating of parts to the required temperature and nitriding of complex-shaped products of various shapes and sizes, including through and blind holes. Its density is several orders of magnitude higher than during ionic nitriding in a conventional glow discharge, as a result of which the formation of the nitrided layer is intensified.

Compared to widely used nitriding methods (ionic, liquid and gas), vacuum-plasma precision nitriding of Avinit N has the following main advantages:

- the method of plasma nitriding ensures the absence of deformation of the part (distortion) while maintaining the original geometric dimensions after nitriding with an accuracy of 1–2 μm. After precision plasma nitriding of Avinit N, the original dimensions of the parts are retained. There is no brittle surface layer typical for traditional nitriding methods. This allows an accurate «to size» nitriding operation to be obtained;
- the formation of a nitrided layer is significantly accelerated by 2–5 times compared with the traditional method of ion nitriding in a glow discharge and 5–10 times compared with gas nitriding;
- the hardness of the nitrided layer increases due to obtaining a uniform hardened nitrided layer, which increases the fatigue limit and wear resistance of the processed parts [76];
- stable processing quality is ensured. Nitriding of geometrically complex products of various shapes and sizes, including through and blind holes, is possible;
- it is possible to carry out nitriding and apply superhard Avinit coatings in a single technological process.

Plasma nitriding Avinit N provides:

- reducing the processing time by 10–50 times, both by reducing the processing time by 85 %, and by eliminating the final high-precision proof;
- absence of ammonia and hydrogen-containing compounds in working gases, reducing the consumption of working gases by 80 %; reduction of electricity consumption by 70–75 %;
- reduction of deformation of parts, excluding finishing grinding.

Plasma precision nitriding processes eliminate the disadvantages of traditional industrial nitriding processes (traditional ion nitriding, liquid and gas nitriding), increase the performance properties of parts, and expand the range of processed materials.

Plasma precision nitriding of Avinit N is widely used by FED JSC in the serial production of aviation products instead of traditional methods of ion nitriding, liquid and gas nitriding.

Considering the significant advantages that provide new vacuum-plasma technologies for chemical and thermal treatment of Avinit, these technologies using high-density low-temperature nonequilibrium plasma will find industrial application in transport engineering, in particular, to improve

the performance of diesel engines and create new materials using plasma precision nitriding processes. Avinit N.

Examples of plasma nitriding Avinit N:

1. Full-size high-precision gear wheel of an aircraft engine (SE «Ivchenko-Progress», Zaporizhzhia) [77].

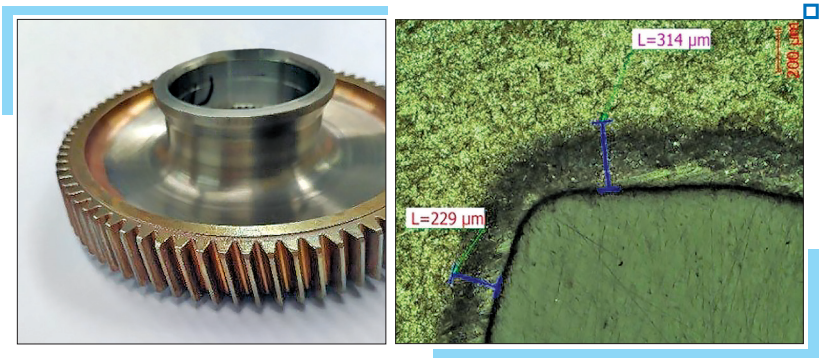

Fig. 3.22 Plasma nitriding of Avinit N gear (steel 34NiCrMoV14-5)

The gear is made in 4 degrees of accuracy (up to 1 µm). Plasma nitriding of Avinit N. The depth of the nitrided rat is 0.3 mm. Microhardness Hµ=730–930.

The original geometric dimensions before and after nitriding are preserved with an accuracy of 1–2 m. No changes in the geometry of the teeth of the wheels and wear of the coating were found after tests in the engine gearbox.

2. Separator for helicopter freewheel clutch (Motor Sich JSC, Zaporizhzhia) [43].

The depth of the nitrided layer is 0.2 mm. Microhardness Hµ=730–830. Coating thickness Avinit C 1.5 µm. Microhardness Hµ=3000.

Fig. 3.23 Helicopter freewheel separator (plasma nitriding Avinit N+Avinit nanocoating)

Avinit Plasma Nitriding, combined with subsequent application of Avinit Super Hard Coatings, eliminates the fretting wear of the sliding surfaces common in commercial separators.

Fig. 3.24 Serial parts of aviation hydraulic units nitrided with precision plasma nitriding Avinit N [29, 30]

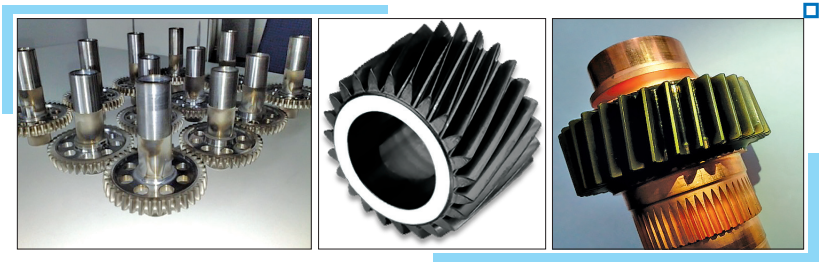

Fig. 3.25 Serial plasma precision nitriding of Avinit N gears [29, 30]

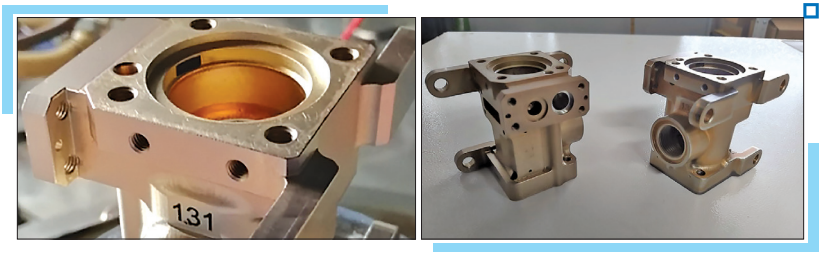

Fig. 3.26 Serial nitriding of aircraft unit bodies made of BT6 titanium alloy [29, 30]

3.6 Metallic coatings for corrosion protection in hydrogen-containing environments

It is known that hydrogen intensively interacts with a number of metals, changing their properties. The most dangerous from the point of view of deterioration of operational characteristics is the process of formation of brittle hydrides and the development of gas porosity in the bulk of the

material, which sharply reduces the strength and often leads to premature destruction of products.

Hundreds of publications are devoted to this issue every year. The main regularities of the interaction of hydrogen with metals have been studied in sufficient detail, however, the problem of suppressing the harmful effects of hydrogen on the properties of materials under real operating conditions remains relevant. This is due to the following circumstances:

1) the criteria that determine the maximum permissible concentration of hydrogen in the material, as a rule, are established when conducting research on microsamples and do not guarantee the absence of fragility in complexly stressed large-sized structures;

2) the forms of manifestation of hydrogen embrittlement and the corresponding mechanisms causing it are quite diverse. Therefore, it is not always possible to foresee all the options for the effect of hydrogen on materials and, accordingly, prevent the harmful consequences of such an effect;

3) hydrogen in metals under «normal» operating conditions (room temperatures and above) is quite mobile. Therefore, under the influence of gradients of temperatures, voltages, electric and magnetic fields, local significant hydrogen saturation of individual regions of the material is possible.

An effective way to prevent the harmful effects of hydrogen on materials can be the application of protective coatings that impede the penetration of gas into the product and ensure the concentration of H_2 in the metal is below the maximum permissible during the entire service life.

This section presents the results of studies of the mechanisms of interaction of hydrogen with materials due to coating and the effect on these processes of the characteristics of coatings and some external factors of their operation:

1. Physical mechanisms of molecular hydrogen penetration into metals.

Schematically, the process of hydrogen penetration from the gas phase into the metal is usually represented [88] consisting of several stages:

1. Physical adsorption of hydrogen on the metal surface, in the first approximation, depends only on the P and T gas.

2. Chemisorption processes — the interaction of an adsorbed molecule with active centers of the surface, the transition of a molecule to a higher energy state, in the limit — its chemical dissociation and saturation with «hydrogen atoms» of the «surface» layer of the metal.

3. Diffusion of hydrogen «atoms» from the surface layer into the bulk of the matrix with the formation of a solid solution.

4. Strengthening of the solid solution at the moment of its «saturation» and the formation of hydride.

A diagram of the change in the energy of gas particles dissolved in the metal lattice can be presented in the form (**Fig. 3.27**).

Here E — potential energy of the metal-hydrogen system. The energy of a diatomic molecule that does not interact with the metal is taken as zero.

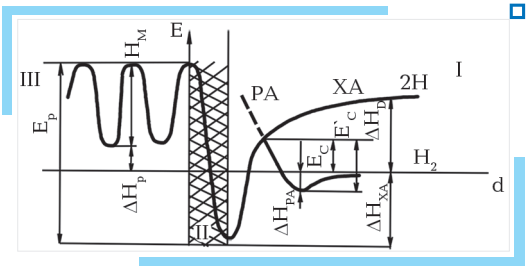

Fig. 3.27 Diagram of the change in the energy of hydrogen when interacting with a metal. I — gas; II — surface layer; III — metal

The PA curve describes physical adsorption and is characterized by a wide potential minimum of shallow depth (NFA).

The *XA* curve refers to the chemical adsorption of a dissociated gas (HD is the dissociation energy of a molecule) and is characterized by a narrow deep minimum ΔH_{XA} (ΔH_{XA} heat of chemisorption).

The transition from the physically adsorbed state to the chemically adsorbed state is associated with overcoming the activation energy E_c', and from the molecular state to the chemisorbed state, the energy E_c.

The activation energy of chemisorption depends on the relative position of the potential curves of FA and CA, in particular, ES can vary from zero to the dissociation energy of the molecule ΔHD (431 kJ/mol). The dissolution of hydrogen from a chemisorbed state is characterized by the activation energy E_r. Finally, the diffusion of hydrogen atoms from the surface layer into the bulk of the matrix is associated with the activation energy of migration E_m.

If to consider such a phenomenon as the permeability of metal membranes from the standpoint of using protective coatings, then it is also necessary to take into account the process of hydrogen penetration through the boundary from the side of the membrane outlet. In the future, since this aspect of the problem of the interaction of gaseous hydrogen with metals is of the greatest interest, it is advisable to define the very concept of water impermeability.

The rate of hydrogen penetration is measured by the amount of gas (kg, g, mol, cm^3, cm^3/100 g) passing per unit time through a flat metal membrane of thickness l and area S in a steady state at a given temperature T and a pressure difference P_1 and P_2, called flow J through a single membrane area: $j=J/S$. The penetration coefficient or permeability is defined as a value numerically equal to the rate of penetration through a membrane of unit thickness at $P_1=1$ atm and $P_2=0$.

Thus, for a given membrane thickness and external pressure, to estimate water penetration, it is sufficient to know the steady-state flux density j, which is obviously determined by the slowest of the above stages of hydrogen penetration.

In this regard, an approximate estimate of the characteristic times of the processes occurring during water penetration may be useful.

The characteristic time of the change in the hydrogen concentration along the length l due to diffusion is estimated by the formula:

$$\tau D \sim l^2/D.$$

Formally, it is possible to introduce the characteristic times of the change in the hydrogen concentration in the «surface» layer of the metal from the side of the entrance due to the processes of hydrogen penetration through the metal-protected material interface. Then the following cases can take place: τ_{sec}, $\tau_D \ll \tau_{ag}$ — the water impermeability process is controlled by adsorption processes. In this case, a uniform distribution of hydrogen throughout the entire thickness of the metal membrane is ensured, as well as thermodynamic equilibrium at the «metal-protected material» interface.

The flux density will be determined by the supply of hydrogen to the surface layer of the coating. Strictly speaking, in this case, two stages must be distinguished: (1) directly chemisorption or activated adsorption, and (2) the transition of atoms from the chemisorbed layer to the crystal lattice.

Each of them has its own characteristic time and can be controlled when the surface layer of the metal is saturated with hydrogen. The contribution of surface processes to water impermeability is usually formulated in terms of the steady-state flux density *j*.

Calculating *j* is a tricky task. In general, *j* can be represented as:

$$j = k_1(Cp_2 - c_2) \text{ for stage (1);}$$

$$j = k_2(C_p - C) \text{ for stage (2),}$$

where C_p — equilibrium concentration obtained from Sieverts' law; $C_p = \sqrt{P} \cdot \text{const}$; C — concentration of gas in the metal.

Both expressions do not depend on the thickness of the protective coating, which can serve as a criterion for determining the control mode. The constants k_1 and k_2 substantially depend on the sequence of microscopic events preceding chemisorption, as well as on the state of the metal surface.

In the first case, this is reflected in the value of the activation energy of chemisorption, in the second, on the accommodation coefficient *S*, which is defined as the fraction of chemisorbed particles in relation to those in contact with the surface. The latter, in turn, depends on the degree of filling of the active centers of the surface θ, on which chemisorption actually occurs, and in the simplest version has the form:

$$S = S_o(1 - \theta^2),$$

S_o — accommodation coefficient at θ=0. Moreover, the value of the heat of chemisorption ΔH_{XA}, and, consequently, the value of the activation energy of the process also depends on the value of θ (**Fig. 3.28**).

Fig. 3.28 depicts the qualitative change in H_{XA} and E_c with an increase in the parameter θ. As θ→1 tends, E_c increases, that is, it becomes more and more difficult for H_2 molecules to «incorporate» into the metal surface, since less active adsorption centers remain on the surface over time. This entails a decrease in the accommodation coefficient, and hence the efficiency of chemisorption.

A decrease in the heat of adsorption leads to a change in j both in case (1) and in case (2). Therefore, reference books usually give the value of the initial heat of adsorption (at θ=0), which is a qualitative characteristic of the intensity of the chemisorption process at an early stage. The more H_{XA}, the stronger the chemical relationship between the metal and hydrogen, the more intense the chemisorption.

A similar characteristic (2) at the initial stage can, apparently, be the value of the activation energy of dissolution $E_p=\Delta H_{XA}+(\Delta H_p+E_M)$. The more E_p, the more difficult it is for chemisorbed hydrogen atoms to penetrate into the surface layer of the metal. Therefore, the good adsorbed properties of the metal do not mean at all that the penetrating ability of hydrogen into the surface layer of the metal is just as great.

Large values (ΔH_p+E_M) can greatly complicate the process of penetration and make stage (2) a controlling stage of water penetration. Consequently, when predicting the material for a protective coating, it is not enough to classify them according to the ΔH_{XA} value, without taking into account the E_p value:

T_{sec}, $\tau_{ag} \ll \tau_D$ — diffusion-controlled case.

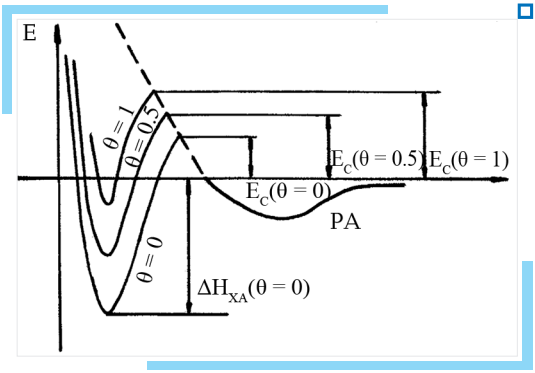

Fig. 3.28 Change in the heat of chemisorption of hydrogen H_{XA} and the activation energy of the transition from molecular to chemisorbed state E_c

Here, in the «surface» layer at the inlet, an equilibrium concentration of hydrogen C_p is rapidly established at a given pressure and temperature. At the outlet, the removal of hydrogen across the metal-protected material interface has time to take place. Therefore, the hydrogen concentration can be considered zero. Under these conditions, there is a stationary diffusion flow of hydrogen through the protective coating, the density of which is given by the expression:

$$J \sim DC_p/l;\ D=D_0\exp(-E_m/RT),$$

$$C_p=\Delta_0\sqrt{P}\ exp(-\Delta H_p/RT).$$

Accordingly, for water penetration, according to the definition, there is:

$$\rho=DC_p/\sqrt{P}.$$

When choosing a material for a protective coating, one can compare not the absolute values for specific materials, but the value in relation to other applicants. Hence it follows that sufficient information for this is provided by the estimate DC_p, since:

$$\rho_i/\rho_j=D_iC_p^i/D_jC_p^j\ (i\neq j).$$

It should be noted that the pure water penetration is understood as the diffusion-controlled mode, when the equilibrium concentration determined by the Sieverts law is maintained in the surface layer. Therefore, graphs of the permeability of metals to hydrogen are usually given in variables $l_n\rho$ (ρ in $cm^2/s\cdot bar^{1/2}$) — $1/T$. The presence of a straight line on the graphs means the diffusion controllability of the process. Deviations from a straight line are associated with surface action.

τ_{ag}, $\tau_D \ll \tau_{sec}$ — the process is controlled by the removal of hydrogen from the coating metal, while the equilibrium concentration C_p is maintained throughout the entire depth of the coating.

A qualitative characteristic of the efficiency of this stage, apparently, can be the value ($E_m+\Delta H_p$) on both sides of the coating boundary — the protected material (**Fig. 3.2**). It follows from **Fig. 3.2** that the difficulties in the transition of hydrogen from the coating to the protected sample can be associated with overcoming an additional barrier:

$$\Delta H=(E_m^{(3)}+\Delta H_p^{(3)})-(E_m^{(1)}+\Delta H_p^{(1)}).$$

Then the sign ΔH would determine the character of such a transition. It is interesting to note that the quantity ($E_m^{(1)}+\Delta H_p^{(1)}$) also appears in the formula for the permeability in the diffuse case. Moreover, the requirement

to slow down diffusion processes means the choice of a material with a maximum value ($E_m^{(1)} + \Delta H_p^{(1)}$). But this deliberately facilitated the penetration of hydrogen into region III (**Fig. 3.29**). Thus, effectively combining the latter two modes is perhaps difficult, if possible.

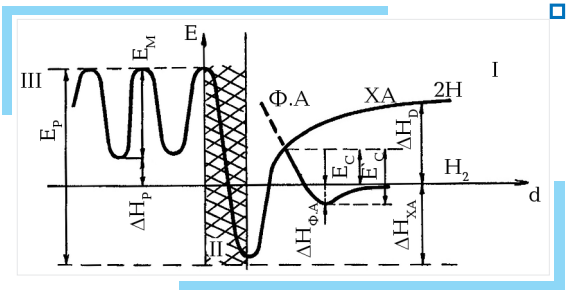

Fig. 3.29 Diagram of hydrogen energy change during diffusion in the «coating — protected material» system: I — matrix of the coating metal; II — transition layer; III — matrix of the protected material

If to take into account the ability to inhibit the process of saturation with hydrogen of the surface coating (max E_p), then, of course, the real way of creating effective protective coatings can only be associated with the inhibition of surface or diffusion actions, and better both at once.

2. Analysis of experimental data on the effect of the characteristics of various metals on their water resistance.

As shown above, the surface properties or the degree of interaction with hydrogen, as well as the values of the diffusion coefficient and solubility of hydrogen in the material under consideration, should be attributed to the number of characteristics of a material that can most affect its water resistance. If we consider the surface properties of materials in connection with the possibility of using them as protective coatings in hydrogen-containing media, then the materials of greatest interest are those whose hydrogen chemisorption is minimal.

According to [88, 89], Au, Zn, and Cd seem to be among the elements least active with respect to hydrogen. There are no quantitative data on their heats of adsorption in the literature, probably due to the smallness of surface activated adsorption. Concerning Cd, this is a direct indication [90]. Hydrogen does not dissolve noticeably in either solid or liquid gold and cadmium.

The data on the solubility of hydrogen in Zn are contradictory. According to Sieverts, at T<600 °C, hydrogen does not dissolve in either solid or liquid zinc. Also, no interaction was found between Zn and activated hydrogen. Other authors [91, 92], on the contrary, classify zinc as one of the metals capable of enclosing hydrogen.

However, this ability, even if it takes place, is at temperatures above T_m. It should also be noted that there are no data on the diffusion of hydrogen in Au, Zn, and Cd, which may indicate the low solubility of hydrogen in these metals.

Among the metals that practically do not interact with hydrogen at temperatures close to room temperature, aluminum should be attributed, for which there are also no data on the heat of hydrogen adsorption. It is only indicated that the processes of dissolution and permeability of hydrogen in solid aluminum are highly complicated and limited by the state of the surface: the permeability of hydrogen in an ordinary atmosphere is scarce and increases by a factor of 100–1000 when hydrogen is activated, for example, by a glow electric discharge [93].

Silver and copper are also metals that interact very weakly with hydrogen, although the adsorption of hydrogen on these metals has been observed experimentally [94–97]. The listed metals form a series for which the surface processes of interaction with hydrogen are rate-determining, and which, according to this parameter, can be considered as one of the most effective metals for coatings that prevent flooding of protected materials. According to the degree of efficiency, in decreasing order, these metals can be placed as follows: Au, Cd, Zn, Al, Ag, Cu.

For other metals, chemisorption processes are experimentally recorded, proceeding with greater or lesser intensity [95], or by their properties, for example, such as potassium, pure tin, and some others that are not very suitable for use as coatings, which makes it possible to exclude them from the above series of metals.

Comparative analysis of experimental data on such characteristics as hydrogen solubility and diffusion coefficients of various materials in the range of room temperatures is rather difficult to carry out, since practically for most materials of interest in this consideration, these characteristics were determined at higher temperatures. Therefore, only estimates can be made by extrapolating the available data to the room temperature range.

Among the materials that can serve as effective diffusion barriers for hydrogen, first of all, one should include Au, Cd, Zn, which, as mentioned above, practically do not dissolve hydrogen. Comparison of the values of permeability $\rho = DC_p/\sqrt{P}n_2$, calculated on the basis of the available literature data for less diffusion-permeable metals (**Table 3.13**) shows that W, Mo, Al, Ag, Cu should be included among those already mentioned.

Assuming that hydrogen penetration is controlled by diffusion, it is possible to estimate the time it takes to reach the boundary hydrogen concentration n_0 through the protective coating, which critically affects the properties of the protected material. In this case, we will assume that all surface processes proceed rather quickly, and an equilibrium hydrogen concentration is established at the surface layer of the metal.

Table 3.13 Comparative characteristics of some metals [94–97], which determine their protective properties in hydrogen-containing media

Metal	Hydrogen diffusion				Solubility			Permeability, ρ, cm/s·bar$^{1/2}$	t_n^D, s (year)	t_n^p, s (year)
	Temp. interval (T, °C)	D_0, cm^2/s	E_m, kJ/mol	$D=D_0\exp(E_m/RT)$, cm^2·s (at 20 °C)	Temp. interval (T, °C)	Temp. dependence	C_n (at 20 °C)			
Cu	200–300	$1.06\cdot10^{-2}$	38.4	$2\cdot10^{-9}$	500–1083	2.65–2650/T	$6.6\cdot10^{-12}$	$1.3\cdot10^{-20}$	$2.4\cdot10^{8}$ (~7.5)	10^{-4}
Ag	200–850	$4.9\cdot10^{-3}$	30.8	$2.1\cdot10^{-8}$	550–961	2.72–3600/T	$1.9\cdot10^{-15}$	$4\cdot10^{-23}$	$7.9\cdot10^{10}$ ($\sim2.5\cdot10^{3}$)	$4\cdot10^{-4}$
Al Al	360–630 450–600	$1.1\cdot10^{-1}$ $2.5\cdot10^{-2}$	40.9 90	$2\cdot10^{-9}$ $5\cdot10^{-18}$	400–630	3.01–3300/T	$9.8\cdot10^{-15}$	$8\cdot10^{-23}$ $5\cdot10^{-23}$	$4\cdot10^{10}$ ($\sim1.3\cdot10^{3}$)	$3.2\cdot10^{7}$ (~1)
Mo	250–2000	$0.89\cdot10^{-2}$	58.6	$8.5\cdot10^{-13}$	900–1500	2.87–2730/T	$1.1\cdot10^{-12}$	$9.4\cdot10^{-25}$	$5.8\cdot10^{11}$ ($\sim1.8\cdot10^{4}$)	$1.5\cdot10$
W	400–1000	62	103.8	$3.5\cdot10^{-19}$	900–1750	2.55–5250/T	$8.9\cdot10^{-21}$	$3\cdot10^{-39}$	$3.2\cdot10^{24}$ ($\sim10^{17}$)	$1.6\cdot10^{11}$ ($5\cdot10^{3}$)
Ti Ti	133–415 227–900	$2.1\cdot10^{-3}$ 10^{-2}	46.6 51.5	$1.6\cdot10^{-11}$ $1.1\cdot10^{-11}$	–	–	up to 0.1	– –	10 s/C_p %	– –

Then $D_n C_p S t_n / d$ — the number of hydrogen atoms reaching the metal surface at the outlet during t_n, (d — thickness of the coating); on the other hand, their max allowable amount in the protected metal is equal to Vn_0 (their uniform distribution is assumed; V — volume:

$$Vn_0 = D_n C_p S t_n / d,$$

that is, all the hydrogen that has reached the limit is immediately absorbed by the sample and distributed over the volume V. Hence:

$$t_n^D = dL / D_n \cdot n_0 / C_p,$$

where $L = V/S$ — characteristic scale of the sample.

In the calculations, let's take $l = 0.1$ cm; $d = 10$ μm $= 10^{-3}$ cm, $n_0 = 10^{-5}$ % (at.). The results of calculating t_n^D for some metals are given in **Table 3.13**. Based on them, it is possible to again write a series: Au, Cd, Zn, W, Mo, Al, Cu, Ti (coinciding with a similar comparison obtained), in which the saturation time increases from right to left. These estimates show that Ag, Al, Mo, W can serve as effective diffusion barriers to hydrogen.

Let's now estimate the saturation time, assuming that the rate-determining stage is the penetration of hydrogen from the chemically adsorbed state into the surface layer.

In this case, the diffusion stage proceeds much faster, and all the hydrogen penetrating into the surface layer of the protective coating is immediately delivered to the metal to be protected, so that the hydrogen concentration in the surface layer is maintained at zero.

Then $NC_n \exp(-E_p / RT) S t_n$ — the number of hydrogen atoms penetrating into the surface layer of the metal, overcoming the barrier E_p — the activation energy of dissolution; N — vibration frequency of the H atom in the surface potential well. In addition, the max allowable amount of hydrogen in the leveling sample Vn_0.

Here,

$$t_n^p = Ln_0 / V C_n \cdot \exp(E_p / RT),$$

C_n — surface density of hydrogen; $E_p = \Delta H_{XA} + E_m + \Delta H_p$.

It should be borne in mind here that ΔH_{XA} depends on the degree of filling of surface active centers with hydrogen, and ΔH_{XA} tends to zero at $\theta \to 1$. Taking this into account, to estimate t_n^p as C_n let's take the saturation density, that is, the maximum number of particles in the sample area, which can be accommodated there. But in this case, ΔH_{XA} can be neglected, and t_n^p takes the form:

$$t_n^p = Ln_0 / VC_n^{\max} \exp((E_m + \Delta H_p) / RT).$$

The data for determining t_n^p will be taken as follows:

$l = 10^{-1}$ cm; $n_0 = 10^{-7}$ particles/cm$^3 \cdot 10^{23} = 10^{167}$ particles/cm^3;

$N = 10^{13}$ s^{-1};

$C_n = 10^{15.7}$ particles/cm^2;

E_m and H_p/R are given in **Table 3.13**.

The estimates of t_n^p (**Table 3.13**) indicate that the values of t_n^p can be much less than t_n^D. However, here it should be borne in mind that for all metals C_n~10^{15} particles/cm^2 was taken. This is true for those metals that adsorb hydrogen well, and Al, Ag and Cu do not belong to them.

Estimates of the characteristic times of hydrogen saturation of the protected material through a coating of the metals under consideration at temperatures close to room temperature show that even thin ~10 μm coatings can serve as reliable barriers for metals very sensitive to hydrogen, for which the maximum permissible concentration was taken in the calculations equal to 10^{-5} at. %

No data have been found on direct experimental results on measuring the water impermeability of the materials under consideration at room or close to room temperatures. At higher temperatures (>200 °C), the experimental data on water penetration [96] are in qualitative agreement with the results obtained on the degree of efficiency of using various materials as protective materials in hydrogen-containing media. Note that there is a wide scatter in the measured values of the water penetration of coatings and materials, which is associated with a strong influence on the measurement results of the coating method and its quality.

Taking into account the estimates obtained for the protective ability of metals, from which it follows that for a number of metals in the range of room temperatures the saturation times are so long that practically any of them could provide the highest requirements for stability in hydrogen, it should be concluded that when choosing a material for protective the quality of the resulting coatings and the choice of the method of their application can become decisive.

For example, it was shown in [97] that a plasmid-sprayed coating even 150 μm thick made of Ni, Cu, W, Mo, Ti has practically the same effect on the water penetration of stainless steel membranes. The reason for this is the high (15–30 %) porosity of the coatings, and it is this porosity, as shown by the analysis of the temperature dependence of coatings made of different metals, that determined the magnitude of the hydrogen flux through the coating. Similar results were obtained for electroplated coatings made of Cu and Ni [97].

The highest quality coatings are obtained by plasma-chemical and ion-plasma methods [85]. Experimental studies of the water penetration

of various coatings [100] obtained by condensation from plasma flows of an electric arc vacuum discharge and crystallization from the gas phase showed that the best protective properties were possessed by gas-phase coatings of Mo and Cr, which were practically impermeable to hydrogen at a thickness of about 1 μm.

For electric arc molybdenum coatings of the same thickness, the experimental and calculated values of water penetration differed by more than an order of magnitude [101], which is apparently due to their increased porosity as compared to gas-phase coatings. Arc coatings with Cu and Ti with a thickness of 1...10 μm also have lower protective properties in hydrogen as compared to gas-phase coatings.

Thus, the data show that the best results on the use of coatings for protection against interaction with hydrogen can be achieved with an integrated approach to the choice of the coating material and the method of its application. When analyzed from this standpoint, possible coating materials and methods of their deposition, gas-phase coatings of Mo and W appear to be one of the most promising. This is due to the fact that these metals are among the most effective diffusion barriers for hydrogen, the processes for obtaining such coatings have been studied in sufficient detail, and the technologies are quite simple, environmentally friendly and well developed.

3. Experimental studies of the protective ability of gas-phase molybdenum coatings in hydrogen.

The analysis of experimental data on the influence of the characteristics of coatings on their protective ability showed that the method of obtaining coatings has a great influence on the results of studies of the water resistance of various metals. First of all, this is due to the differences in such characteristics of coatings as their structure and porosity.

Having chosen the gas-phase method of deposition of molybdenum for the deposition of protective coatings, studies were carried out of the influence of the conditions for the formation of coatings on their structural features, which can affect the protective ability of coatings in a hydrogen environment. The studies were carried out on stainless steel samples coated with molybdenum, obtained by thermal dissociation of molybdenum hexacarbonyl in the temperature range of 400...700 °C.

The performed studies have shown that, depending on the conditions of the process of deposition of molybdenum and the method of surface preparation, during the growth of the coating, macrostructures of the globule type, fan-shaped structures with looser grain boundaries, micropores at the contact points of growing grains and dome-shaped growths can form. Such «macro defects» are certainly undesirable for protective coatings.

Taking these studies into account, the modes were selected and prototypes were obtained from a material that actively interacts with hydro-

gen (Ti), with molybdenum coatings deposited on them. Before the coating was applied, the surface of the samples was subjected to ion-plasma cleaning followed by the application of a Mo sublayer with a thickness of 1...2 μm. Protective molybdenum coatings were applied at a temperature of 450 °C. The thickness of the coatings was 10...15 μm.

The samples were tested in a hydrogen atmosphere at a pressure of 600 mm Hg. The temperature of the samples during the tests was regulated by a thermostat and maintained within 60±2 °C. The temperature was measured using a X-A thermocouple. The test results were evaluated by the change in the weight of the samples, determined with an accuracy of 10^{-5} g, as well as by visual inspection at a magnification of 20x. The change in the weight of the samples during the tests is given in **Table 3.14**.

Table 3.14 Change in weight of samples during testing

No. sample	time, h					
	0	215	455	954	1314	3090
1	35.5769	35.5768	35.5767	35.5767	35.5767	35.5767
2	35.6317	35.6316	35.6314	35.6314	35.6314	35.6313
3	35.6151	35.6150	35.6147	35.61475	35.6147	35.61475

Tests carried out for 3000 hours showed that there were practically no changes in the weight and appearance of the samples during the entire campaign. The obtained experimental results confirm the conclusions made on the basis of theoretical studies about the high protective properties of such a material as molybdenum in hydrogen-containing media. The gas-phase method for the formation of such coatings ensures the required quality and can be recommended for practical use in the protection of materials sensitive to the action of hydrogen.

Thus:

1. The mechanisms of hydrogen penetration through metallic materials are considered and the influence of the characteristics of less waterproof metals: Au, Zn, Cd, W, Mo, Al, Ag, Cu on their protective ability in hydrogen-containing media is analyzed. The effect of moisture and radiation on the protective properties of metals is estimated.

The studies carried out and the estimates made allow to physically reasonably approach the choice of coatings designed to protect units and structures that are sensitive to the effects of hydrogen.

2. The analysis of experimental data on water-impermeability of coatings made of various metals has been carried out, showing that the method of their application has a significant and sometimes decisive effect on the protective properties of coatings. In this respect, plasma-chemical methods

should be considered as the most promising for the formation of high-quality protective coatings.

3. Experimental studies on the production of molybdenum coatings by thermal dissociation of molybdenum carbonyl on materials sensitive to hydrogen have been carried out, and their protective ability has been tested in hydrogen-containing media. It is shown that gas-phase molybdenum coatings are highly stable in hydrogen and can be recommended for the protection of materials sensitive to hydrogen.

4

Criteria for the stability of the microstructure of multicomponent materials

The progress of many scientific and technical areas is associated primarily with the development and design of new functional materials with a set of specified properties, and effective technological processes for their preparation.

Let's take a closer look at the process of designing new materials. As noted earlier, we are talking about the creation of materials only for individual particularly critical structural units, the rate of failure of which determines the service life of the entire product.

Schematically, the design algorithm is as follows.

Based on a preliminary assessment of the factors influencing the material, economic indicators, requirements for dimensions and weight, the appropriate material is selected and a preliminary design of the corresponding unit is developed. Obviously, for the material indicated in the reference book, methods of production have been developed in detail and its properties during operation are known. Therefore, the construction technology of the unit is carried out according to an abbreviated scheme. A different situation arises in the absence of a material with the desired properties. In this case, the process of designing a node is significantly lengthened. Since the dimensions of the product are, as a rule, limited, a microscopic analogue of the composition is built that meets the specified requirements, and its properties are calculated. Then, possible ways of creating the material are analyzed and its models are tested in conditions that are close or simulate operational ones. If the methods for obtaining the composition are traditional and it is possible to calculate its properties during operation, then, in the future, the work proceeds in the traditional way. However, unfortunately, in the overwhelming majority of cases, new materials require new methods of their preparation. Exposure to high temperatures and various radiation fields can significantly change the properties of materials compared to the original ones. The prediction of the behavior of materials can be provided by modeling the evolution of the microstructure under the influence of operational factors.

It is obvious that the creation of new materials is the result of many years of efforts by large teams of specialists in various fields. Considering

the large material and time costs of this work, it is necessary to find ways to reduce these costs. One of the most promising is the theoretical construction of model structures, reflecting the properties and structure of the proposed composite material, the calculation of the characteristics of such a structure and the issuance of recommendations for optimizing the processes of creating a material at each stage. Of course, the lack of reliable data on the microscopic properties of materials and compounds, the insufficient development of ideas about the evolution of the microstructure do not allow predicting quantitative characteristics with sufficient reliability; in most cases, we are talking only about qualitative trends. But even such qualitative conclusions significantly narrow the range of options under consideration and allow obtaining positive results within an acceptable time frame.

As evidenced by numerous literature data on the effect of production and operation conditions on the stability of the structure and properties of multicomponent materials. Destabilization of multicomponent materials is a serious problem.

Crystal lattice defects play a decisive role in the formation of the structure and composition of functional materials. Consequently, the structurally sensitive physical and mechanical properties significantly depend on the conditions for obtaining and using the material. By directionally changing the parameters of the processes, primarily high-temperature heat treatment, it is possible to change the characteristics of the materials obtained.

One of the main physical processes that determine the stability of multicomponent materials is the diffuse decomposition of supersaturated solid solutions, which leads to the formation of heterogeneous structures in a solid with a certain distribution of macrodefects or to an undesirable violation of optimized structures. Understanding the distribution, interaction and kinetics of defects, mechanisms of formation and stability of the structure is important for understanding the behavior of materials under various external influences and allows to propose ways to design new materials.

A consistent theory of diffusional decomposition of supersaturated solid solutions at a later stage, when the supersaturation of the material with point defects causing diffuse mass transfer becomes small, and the growth of large macrodefects occurs due to dissolution («eating») of small ones — the coalescene stage itself — built by Lifshits and Slezov [102, 103].

It turns out that the characteristics of diffuse decomposition at the stage of coalescence caused by the diffusion interaction of macrodefects are universal in nature, independent of the initial distribution function. The distribution function of precipitates by relative size asymptotically in time takes on a universal form, and the evolution of the characteristics of a dispersed system (the number and size of precipitates, saturation) is determined by universal power laws.

The theory was generalized to the case of diffuse decomposition of multicomponent solid solutions in [104—107]. The main regularities of

diffusion decay — the universality of the distribution function and decay characteristics — are also preserved for multicomponent systems.

Diffuse decomposition of multicomponent systems with precipitates of complex chemical composition, covering most of practically important structural materials, is characterized, as follows from the theory, by a number of features that decisively determine the thermal dimensional and phase stability of the microstructure of materials.

These features due to chemistry occur, and consist, first of all, in the fact that the equilibrium concentrations of the components, and with them the main characteristics of decomposition, are significantly determined by the thermodynamics of chemical reactions occurring at the interphase boundaries and the laws of conservation of the substance of the components.

The existing theory of diffuse decomposition of supersaturated solid solutions makes it possible to formulate general criteria for the thermal and phase stability of multicomponent multiphase systems, which can be useful for predicting the stability of thermal materials.

In a multicomponent system, additional external characteristics appear, which make it possible to more fully optimize the technology for creating materials with an overestimated resistance to particle growth and to predict their characteristics at high temperatures.

Based on the general theory of diffusion decomposition of multicomponent systems, analysis [104–107] of numerous experimental data on the kinetics of precipitation growth in various systems — steels, heat-resistant alloys based on nickel, aluminum, strengthened by precipitates of the V′-phase, dispersion-strengthened, etc. etc. has convincingly shown that the theory of diffuse decay has reliable experimental confirmation and is in very good agreement with experiment both qualitatively and quantitatively.

This allows, based on the general theory of diffusional decay of multicomponent systems [104—107], to formulate the fundamental foundations of predicting the evolution of complex multicomponent systems in the process of diffusional decay depending on various external conditions. These criteria can be useful in developing recommendations for creating materials with increased dimensional and phase thermal stability of the microstructure.

When choosing alloying and reinforcing elements to increase the stability of materials, the approach, naturally, should be comprehensive and include various requirements for the physical (necessary linear expansion coefficients, strength, plasticity, impact strength, etc.), technological (the possibility of creating parts of the required shape, mechanical processing, welding, soldering, etc.) and chemical compatibility (interaction at interphase boundaries, surface tension, etc.). Here we will only touch upon issues related to the increase in the thermal dimensional and phase stability of materials.

4.1 Dimensional stability

Let's first consider the criteria for the stability of the size of precipitates during the diffuse decay of multicomponent systems:

1. High enthalpy of dispersed phases. One of the most important thermodynamic requirements for the dispersed phase from the point of view of increasing the thermal stability of the material is the high heat of formation of the phase. The higher the heat of formation of the dispersed phase, the slower the growth of the size of the precipitates.

The highest thermodynamic stability is possessed by refractory oxides — SiO_2, ZrO_2, Al_2O_3, MgO, BeO, ThO_2, etc. Therefore, it is not surprising that when creating composite materials by strengthening metals with particles of various compounds — intermetallic compounds, oxides, carbides, etc., the introduction of oxides is most effective, allowing to increase the working temperature of metals up to $0.9T_m$ [108].

Well-known examples are the strengthening of copper with aluminum oxide, tungsten — with thorium dioxide, nickel — with thorium dioxide (TD-nickel), aluminum — with aluminum oxide (SAP), etc. Such composite materials at high temperatures have significantly higher heat resistance than the best casting alloys based on these metals, and retain high structural stability up to $0.8–0.9\ T_m$.

A comparative study of the thermal stability of Al_2O_3, ZrO_2, SiO_2, HfO_2 particles dispersed in a nickel matrix shows that the tendency to growth of particles at all temperatures studied (1000 — 1350 °C) decreases in the series γ'-Al_2O_3>SiO_2>α-Al_2O_3>ZrO_2>HfO_2.

As expected, the more refractory and higher enthalpy hafnium dioxide is the most stable in this series at all temperatures [109]. The extremely low growth rate of thorium dioxide particles in TD-nickel is due to the very high stability of ThO_2 [110].

2. Low diffusion coefficients. One of the ways to increase the thermal stability of the material is to properly alloy the matrix material. Of the possible alloying elements (of course, these elements must form at least limited solid solutions with the matrix), those that reduce the rate of diffusion and self-diffusion to the greatest extent will be more effective.

The further way in this direction is the use of alloying with several components. Alloying nickel alloys with the γ'-phase with such elements as Ti, Nb, Ta, increasing the thermal stability of the γ'-phase and reducing the diffusion coefficients, leads to an increase in the structural stability of the alloys and a decrease in the creep rate.

The use of complex multicomponent alloys as a matrix, alloyed with correctly selected components, makes it possible to slow down diffusion processes and, consequently, to increase the thermal stability of the material. It is no coincidence that many modern high-temperature alloys contain a large amount (sometimes up to 10 or more) alloying elements.

Complex alloying, along with the positive effect of reducing the diffusion coefficient, can lead to undesirable changes in strength, a decrease in the melting temperature, phase stability, and an increase in interfacial energy. Therefore, the choice of alloying additions to the matrix must be consistent with the possible harmful effect of these elements on the dimensional and phase stability of precipitates. Improper doping can reduce the stability of the [111] structure.

3. Low solubility. The low solubility of precipitates in the matrix is of great importance for increasing thermal stability during diffuse decomposition. Systems with complete insolubility should have the highest stability. This was experimentally proved for tungsten-reinforced copper [112]. Such a composite retains a high structural stability up to $0.8–0.9T_m$.

The solubility of oxides decreases in the series SiO_2-Al_2O_3-ZrO_2-ThO_2 [113, 114] and it is in this sequence that the stability of the particles of these oxides in the metal matrix increases.

4. Initial concentrations of components. As follows from the theory, the lower the excess initial concentrations of the components, the closer they are to the equilibrium concentrations, the lower the growth rate of the precipitates and the higher their stability. Physically, this is due to the fact that diffusion fluxes on the precipitates will be minimal. For example, when studying the growth of alumina particles in the Cu-Al alloy, it was noted that alloys with a lower amount of residual oxygen showed a lower tendency to particle growth. Naturally, the initial concentrations should be higher than the equilibrium ones at a given temperature, since otherwise the particles will dissolve.

Alloying far beyond the limits of solubility is also dangerous due to the possibility of fluctuation formation of large precipitates, which can sharply worsen the plasticity and toughness of alloys, as well as their machinability. Thus, the correct choice of the initial concentrations of the components, which are the most effective technological tool, the choice of optimal heat treatment conditions and their matching with the operating conditions are important requirements for increasing the thermal stability of the material.

5. Decrease in interfacial energy. An increase in the dimensional stability of precipitates, as follows from the theory, can be achieved by decreasing the specific surface energy of the precipitate-matrix interface. The lower the value of the specific interfacial energy, the slower the redistribution of substances between particles in the process of coalescence and the more stable the structure of the material at high temperatures. A striking example is non-monic — alloys of the Ni-Ni_3X type, strengthened by the γ′-phase. Exceptionally low values of interfacial energy Ni-γ′ (σ=0.2 J/m^2) provide extremely high stability of the fine structure of nickel alloys. Such alloys, strengthened by precipitates of the γ′-phase, are the most heat-resistant among nickel alloys and have found wide application in technology [112].

By changing the value of the specific surface energy of the interface, it is possible to influence in a directed manner the growth rate of the average size of the precipitates. For example, the interfacial energy in the Ni-Al_2O_3 system is 1830 erg/cm^2, and in the Ni-ZrO_2 system — 970 erg/cm^2. Consequently, one can expect that the Ni-ZrO_2 electrode materials will be more stable, which is in qualitative agreement with experiment [109].

As is known, the specific surface energy of the metal-oxide interface can differ significantly depending on the nature of the metal. To reduce the interfacial energy, interfacial elements can be used in the form of alloying parts of the matrix or in the form of coatings of dispersed particles introduced into composite materials as fillers. It was shown experimentally [9, 7] that the thermodynamic stability of Al_2O_3 in the matrix increases significantly upon the introduction of 1 % titanium into the matrix.

A possible explanation for the sharp slowdown in the growth rate of Al_2O_3 particles consists precisely in a decrease in the interfacial energy of the Al_2O_3-matrix (Ni-1 % Ti) to values of 930 erg/cm^2 due to the segregation of titanium on alumina particles. In this case, it is, of course, necessary to take into account the effect of the interfacial element not only on the surface energy, but also on the chemical interaction with the components of the material, diffusion, etc., as well as on the physical characteristics of the composite — mechanical, electrical, etc. properties.

The use of coatings is promising in terms of creating materials with increased structural stability at high temperatures. In composite materials containing at least two different phases, the issues of ensuring the physical (coefficient of thermal expansion, elastic properties, etc.) and chemical (reactions at the phase boundaries and with the external environment) compatibility of components become especially acute. An effective way to overcome these difficulties is to use appropriately selected barrier coatings for the reinforcing phase (parts, fibers, etc.).

Thus, in the development of nickel alloys reinforced with sapphire fibers, it was shown [114] that the interaction at high temperatures between Al_2O_3 and the matrix reduces the strength of the fibers due to the appearance of defects on their surface, which does not allow the full potential of strengthening such a composite. Sufficient stability at temperatures up to 1200 °C is found by a coating of W and W — 26 % Re.

However, the high interdiffusion of Ni and W reduces the efficiency of these coatings during long-term high-temperature operation. The best protective barrier coating in a sapphire Ni-fiber system, according to [114], is a Y_2O_3 layer of 1–2 μm. Good results were obtained when using silicon carbide coatings on boron fibers when reinforcing tungsten, steels, etc.

The role of protective coatings in composites is usually multifunctional, that is, in addition to the main task of preventing interaction with the matrix, other requirements are often put forward for the coating — ensuring reliable adhesion at the interface, reducing the interfacial energy to increase

the thermal stability of the composite. Since it is rarely possible to satisfy all these requirements at the same time with one coating material, in the development of optimal technologies, complex multi-layer coatings with a different functional purpose of each layer are becoming more widespread. Thus, for the already mentioned composite of Ni-sapphire fiber, preferred results were obtained [114] using a double coating consisting of 1–2 μm Y_2O_3 on sapphire and the next 5–10 μm layer of tungsten to improve wetting during the preparation of the composition by vacuum impregnation.

6. Complication of the composition of the secretions. The stability of the secretions can be increased as a result of the dissolution of some alloying elements in them, which leads to a complication of the composition. Thus, the dissolution of titanium in nickel alloys strengthened by the γ′-phase leads to the formation of a more stable Ni_3(Al, Ti), phase, and at high concentrations in the cobalt alloy, an even more complex compound with increased stability $(NiCo)_3$(AlTi). It is clear that the effective coefficient of mass transfer of such complex compounds is significantly lower than for Ni_3Al, which determines their higher stability. Nitrogen additives to steels containing.

7. Absence of polymorphic transformations. It is desirable that the precipitate and the matrix do not undergo polymorphic transformations under operating conditions, since, in addition to adversely affecting the physical characteristics (strength, plasticity, etc.), the stresses developing during the transformation stimulate diffusion and, therefore, can reduce the thermal stability of the structure. Thus, the decrease in the stability of the Cu-Al alloy strengthened by Al_2O_3 particles during annealing at high temperatures is associated [116] with the polymorphic transformation γ-$Al_2O_3 \rightarrow \alpha$-$Al_2O_3$ occurring at these temperatures.

Acceleration of the diffuse growth of particles, caused by the occurrence of polymorphic transformations in them, was also observed upon annealing of nickel strengthened by particles of zirconium dioxide. These effects are most significant for metals with polymorphic transformations (Ti, Zr, U), especially if they are intended for operation under thermal cycling conditions [117].

8. Monodispersity. Estimates show [105] that the closer the precipitation system is to monodisperse, the longer it remains stable and the later the distribution function takes on a universal form. This conclusion is in qualitative agreement with the experimental results that the stability of particles of different oxides in nickel is the higher, the thinner and more uniformly they are distributed in the matrix.

9. Substructure management. The theory suggests [104–107] that the correct regulation of the substructure of the material can become a rather effective means of increasing the thermal stability of precipitates. In practice, various processing methods are widely used to control the structure and substructure of a material and impart the necessary properties to it.

Reducing the size of the grains and blocks improves long-term strength, creep resistance, etc. One of the promising ways in this direction is the creation of structures with fine precipitates. However, at high temperatures, the question of the stability of such a finely dispersed structure arises.

10. Kinetic stabilization. Interesting possibilities of maintaining dimensional stability in multicomponent systems are associated with the kinetic features of the decay process. By gradually changing the temperature periodically, one can achieve dissolution of some phases and stabilization of the size of precipitates of other phases. The same kinetic stabilization effect is possible through other external parameters. The principle of multistage thermal cycling is widely used in the technology of forming modern materials.

4.2 Phase stability

Considering the phase stability of multicomponent systems under the action of external parameters, the theory allows one to obtain equations that determine the boundaries of the regions of coexistence of different phases. By changing the external conditions (heat treatment temperature, pressure), it is possible to change the position of the boundaries of the regions of coexistence of phases, which changes the conditions of phase stability. A change in the initial concentrations of the components can lead to the same result.

Estimates [118] show that, for example, for a three-component phase, it is sufficient to change the concentration of one of the components (or several) by an amount of the order of 10^{-2} in order to transfer the phase from one element of the phase volume to another, nonequilibrium for the given phase. For a 9-component phase, fluctuations of the order of 10^{-5} are sufficient, and for $N>15$, even a small value of 10^{-9}–10^{-10}, i.e. in practice such phases should be unstable.

In this case, the probability P_N of simultaneous contact of all components or phases in the solid state in a multicomponent system with an increase in the number of components in comparison with the binary (P_2) sharply decreases ($P_N/P_2=2/\mathrm{N!}$). Hence, in particular, it follows that it is practically impossible to achieve complete homogenization of the composition of a multicomponent multiphase system. Difficulties in homogenizing the composition of multicomponent systems are well known to material scientists and technologists.

When precipitates of phases of nonstoichiometric composition precipitates from saturated solid solutions [119], it has been shown in theory that asymptotically stable precipitates of phases are not arbitrary, but only of a certain composition. This composition corresponds to the composition within the region of homogeneity or composition at its boundaries, depending on the ratio of the initial concentrations of the components.

If the kinetic difficulties in the formation of a phase are large (for example, for any of the components D_i is small), and this phase is not realized in real time, then the formation of metastable states is possible, and some phases, asymptotically unstable, can be frozen by artificially creating kinetic difficulties.

As already noted, in the framework of the general theory of diffusion decay, systems of nonlinear differential equations are obtained to determine the asymptotically surviving phases and boundaries of the regions of coexistence of phases. Taking into account the complexity of the nonlinear equations of the theory and the impossibility of obtaining analytical solutions for specific cases, we used methods of numerical simulation of diffuse decay processes. For modeling, the particle method was used, which makes it possible to visualize the process of diffusion decay and the method of direct solution of systems of nonlinear equations by numerical methods [120].

Programs are being developed for modeling multicomponent systems that allow determining the boundaries of the regions of coexistence of phases, determining the evolution of the composition and number of coexisting phases, non-stoichiometric coefficients, etc. It becomes possible to construct kinetic phase diagrams of decomposition of material models using simulation, which allows predicting the thermal stability of real multicomponent SOFC materials. This path is quite fruitful for developing recommendations for the creation of SOFC materials with increased thermal stability of the structure.

5

Development of industrial research technologies for Avinit coating

5.1 Avinit functional coatings with improved tribological properties for use in internal combustion engine friction pairs

For a number of years, together with machine-building plants, work has been carried out to increase the service life of internal combustion engines by using composite reinforcing coatings.

Technological processes have been developed for obtaining multicomponent multilayer metallic and non-metallic coatings by vacuum-plasma and plasma-chemical vapor deposition using nonequilibrium low-temperature plasma to select new generation coating materials for rubbing pairs with significantly improved wear resistance and tribological characteristics. The studies have shown that layered compositions of coatings contain enormous potential in the creation of materials with a wide range of properties due to the possibility of combining various materials in various combinations and varying the thickness of layers, and this is undoubtedly one of the most promising ways of creating materials with a given set of properties.

The developed nanocomposite coatings show a unique set of properties «high stiffness — low friction coefficient — elasticity». In this case, the thermal stability of the coatings is 600–700 °C. This combination of characteristics makes these coatings promising candidates for tribological applications in automotive and gas turbine engines.

Unique structure and properties of ion-condensed materials (nanocrystalline, amorphous, microlayer structures, high purity, ultra-high rigidity, extremely high adhesion strength with a variety of substrates, special physicochemical and other properties), the ability to form products of complex configuration and technologies for their production

Composite materials possess these properties due to the use of coatings from various refractory metals and their compounds in combination with various structural materials, primarily structural steels.

Technologies for applying multi-layer reinforcing coatings Avinit have been developed in order to improve the functional characteristics of parts of transport engineering, which are successfully used in the serial production

of similar parts in other industries (power and general engineering, engine and aggregate construction).

New multifunctional nanocomposite coatings Avinit have been developed for components of internal combustion engines (ICE) and aggregates, in particular, parts of fuel equipment, elements of a cylinder-piston group (CPG), and parts of a crankshaft.

5.1.1 Avinit wear-resistant coatings for parts of fuel equipment

5.1.1.1 Determination of tribological characteristics of materials for parts of fuel equipment of diesel engines

The fuel equipment of diesel engines must ensure the dosage of a strictly defined amount of fuel for each cycle in accordance with the engine loading, fuel supply at a certain moment, optimal fuel injection characteristics in time, and the best fuel distribution in the combustion chamber. Fuel pumps must supply all cylinders with the same amount of fuel when operating in any mode, provide the rated power of the diesel engine with the total fuel supply by all pumps, completely stop the fuel supply to the injectors when the diesel engine stops, start supplying fuel to the injectors at a certain moment with one and the same. the same feed advance angle. The main criterion for the quality of precision vapors of fuel equipment is the hydraulic density, which is characterized by the time of fuel impregnation under a certain pressure into the vapor gap or the time of the liquid pressure drop [121, 122].

During operation, precision parts experience high dynamic loads, high pressures and high speed of fuel movement. Fuel is chemically active and contains hard abrasive particles and possibly moisture. With the wear of precision parts, the geometry of their combinations changes significantly, clearances increase, which leads to a violation of the engine operating modes [122]. Some parts are subject to local wear, possibly the development of tear areas, jamming (freezing) of friction units. Abrasively worn surfaces have significant irregularities and depressions in the form of grooves that form microchannels, due to which the size of the combined gap increases. All of the above factors, which are a consequence of the wear of parts, reduce the hydraulic density of precision pairs, and lead to a loss of tightness.

Thin-layer coatings obtained by the ion-plasma method are very promising for increasing the wear resistance of parts of fuel equipment [123–125].

In works [126, 127], comprehensive studies were carried out on the application of composite coatings on friction pairs, in particular, plungers of fuel pumps, shut-off and control valves, and tribotechnical tests of materials and coatings for parts of friction units of fuel equipment «plunger pair» sprayer body were carried out « diesel engines with friction of multi-

component coatings based on Ti-Al-N, as well as bearing steel 1.3505 and tool high-speed steels HS18-0-1 and 1.3343 з with a lower tungsten content, used for the manufacture of parts for fuel diesel engines. The purpose of these studies is to select the optimal combinations of seize resistance and coefficient of friction of thin solid vacuum-plasma coatings to increase the wear resistance of precision parts of diesel engine fuel equipment.

To obtain hardening coatings, a widespread method was chosen among the group of methods for forming materials from ionized and molecular flows, namely, the method of vacuum arc spraying. This method has ample opportunities in the formation of multicomponent materials, both by using alloyed cathodes of the appropriate composition or simultaneous deposition from different single-component cathodes, and by the plasma-chemical formation of compounds during the condensation of metals in an atmosphere of various reactive gases.

In a number of materials science problems to be solved, the most important problem is the choice of coating materials for rubbing pairs. The main efforts are focused on the formation of nano- and microlayer multicomponent reinforcing coatings as the most promising for achieving the necessary tribological characteristics, which opens up extremely wide opportunities for creating new materials. To implement the processes of controlled formation of multicomponent nano- and microstructural coatings, which ultimately makes it possible to closely approach the issue of micro-design of coatings with specified characteristics, we have developed Avinit vacuum-plasma technologies. are based on the integrated use of vacuum-plasma (PVD) and plasma-chemical (CVD) processes in the Avinit cluster.

The following variants of friction pairs were selected for testing:

1. Steel 1.3505 — steel 1.3505.
2. Steel 19CrNi8 (non-cemented) — steel 1.3505.
3. TiN coating — steel 1.3505.
4. TiAlN coating — steel 1.3505.
5. MoN coating — TiC coating.
6. TiAlN coating — TiC coating.
7. TiN coating — MoN coating.

Samples of steel 1.3505 were subjected to volumetric quenching with low tempering, hardness 59...60 HRCE. Samples of steel 19CrNi8 passed carburizing to a depth of 0.7...1.0 mm (after machining — 0.4...0.9 mm), normalization and low-temperature tempering, the hardness of the working surfaces was 63...65 HRCE.

The investigated coatings were applied to the Avinit vacuum-plasma cluster, which allows programming to obtain multilayer nanocomposite coatings with an improved set of characteristics. The calculated thickness of the investigated coatings was 3...5 μm. Samples of steel X155CrVMo12-1, heat-treated to a hardness of 60–61 HRCE, were used as substrates for the coatings.

The roughness of samples without coatings corresponded to Ra 0.32–0.16 μm, samples with coatings Ra 0.16 μm.

The tests were carried out on a 2070 SMT-1 friction machine according to the «disc-shoe» scheme at a sliding speed of 1.3 m/s. Lubrication was carried out with diesel fuel by the immersion method, as well as once before the start of the tests (when determining the seize resistance of the mates). Movable samples «disks» were made of steel 1.3505 with a diameter of 50 mm and a height of 12 mm, «shoes» were made of steels 1.3505, HS18-0-1 and steel SKD11 with Ti-Al-N coating in the form of a cube with dimensions of 10×10×10 mm. The value of the friction coefficients (F_{fr}) was determined at a step load in the range of total loads of 0.2–0.6 kN, the seize formation and the amount of wear of a stationary sample — «shoe» along the width of the produced hole after testing at a load of 0.2 kN for 1 hour.

The results of tests to determine the coefficients of friction of the investigated compounds (with a single lubrication) are given in **Table 5.1** and **Fig. 5.2**. The analysis of the results obtained indicates that the combination of case-hardened steel 20X2H4MA with steel 1.3505 can provide a higher seize resistance and preferable characteristics of friction of joints of parts of fuel equipment. Tests of ion-plasma coatings have shown that they can provide even lower values of the friction coefficients, and the combination of TiAlN coating with steel1.3505 also provides an increase in the seize load.

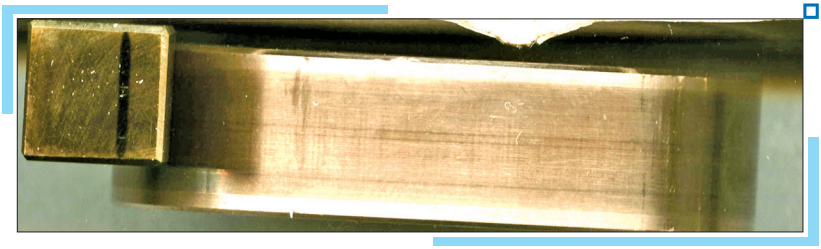

Fig. 5.1 Test according to the scheme «disk (1.3505) — «shoe»

Table 5.1 The value of the coefficients of friction (F_{fr}) and the seize resistance of the mating materials of the parts of the fuel equipment of diesel engines (with a single lubrication)

Counter-materials		Coefficient of friction F_{fr}, at loading of P, kN		
«disc»	«shoe»	0.2	0.4	0.6
1.3505	1.3505	0.130	0.125	0.125
1.3505	HS18-0-1	0.120	0.118	0.123
20X2H14A	1.3505	0.140	0.130	0.216
TiN	1.3505	0.120	*	—
TiAlN	1.3505	0.120	0.120	0.153
1.3505	Ti-Al-N	0.110	0.115	0.110

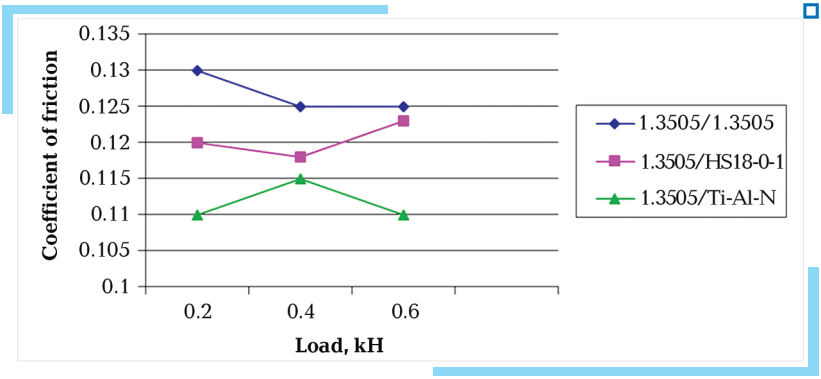

Fig. 5.2 The value of the coefficients of friction (F_{fr}) for different pairs of friction

The data obtained indicate that the use of the investigated coatings makes it possible to reduce the friction loss in the rubbing joints of the fuel equipment and, consequently, the heat release in contact, which should have a positive effect on the dimensional stability and operation of the parts.

Tests to determine the seize resistance of joints showed that during friction of shoes made of 1.3505, a sharp increase in the friction moment and the onset of seize occurs at a total load of 0.6 kN, with friction of shoes made of steel HS18-0-1 — at a load of 0.4 kN. With friction of the coating with a load of 0.8 kN, burrs do not occur (further increase in loads is limited by the danger of fuel ignition).

The amount of wear of the coating, determined by the width of the produced hole on the working edge of the shoe after testing for 1 hour. when loading 0.2 kN, it is 0.35 mm. For comparison — wear of HS18-0-1 steel — 0.99 mm; steel 1.3505 — 1.53 mm. The microhardness H50 of the coating, measured along the friction track, is 1495 kg/mm^2, and for steel HS18-0-1 and steel 1.3505, respectively, 1225 kg/mm^2 and 991 kg/mm^2. The results of these studies are presented in graphical form in **Fig. 5.3**.

To determine the efficiency of using various coating compounds applied to both parts of the interface, tests were carried out in the lubrication mode by the method of immersing a movable counterbody. This made it possible to expand the range of investigated loads due to better removal from the contact zone. The results of these tests are presented in **Table 5.2**.

An analysis of the obtained values of the friction coefficients indicates that the combination of MoN and TiAlN coatings with a TiC coating has relatively preferable antifriction properties in comparison with the used joint of steel 1.3505 with steel 1.3505. At the same time, an unfavorable combination of coatings is also possible. This is evidenced by the test results of a TiN coating with a MoN coating. In this case, tear formation occurs already at the first stage of loading.

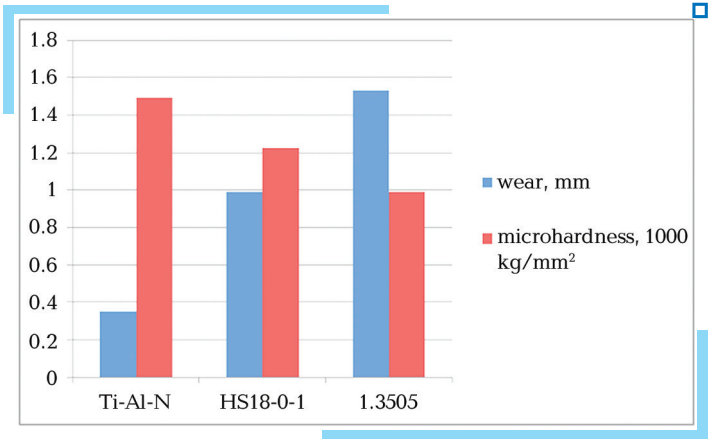

Fig. 5.3 Values of wear of shoes paired with steel 1.3505 and value of microhardness of friction tracks

Table 5.2 Test results for various combinations of coatings for fuel equipment parts (immersion lubrication)

Counter-materials		Coefficient of friction F_{fr}, at loading of P, kN						
disc	shoe	0.2	0.4	0.6	0.8	1.0	1.2	1.4
MoN	TiC	0.067	0.062	0.053	0.050	0.052	0.055	0.070
TiAlN	TiC	0.070	0.068	0.080	0.090	0.098	0.102	0.108
1.3505	1.3505	0.130	0.125	0.125	*	—	—	—
TiN	MoN	*	—	—	—	—	—	—

The relatively low seize resistance of the combination of TiN coatings with a MoN coating can be explained by the tendency of the coating components to adhesive interaction in the presence of uncompensated interatomic bonds; this is facilitated by favorable structural and dimensional factors. At the same time, the relatively high seize resistance and antifriction properties of the combination of MoN-TiC coatings may be explained by the formation of protective suboxide or oxide structures during friction by the reaction:

$$2TiC + 3O_2 \cdot 2TiO_2 + 2CO.$$

The TiN compound does not interact with oxygen, in contrast to the TiC compound; therefore, when a TiN coating is combined with a MoN coating, the effect of the formation of secondary protective structures during friction may not appear.

The obtained research results, as well as the known data [2–7] on a multiple increase in the wear resistance of parts and tools when using vacuum

ion-plasma coatings, make it possible to recommend a combination of MoN-TiC and MoN-TiC coatings on parts of precision friction pairs of fuel equipment of diesel engines under bench conditions and tests on prototype engines.

As the results of the tests carried out show, the combination of case-hardened steel 20X2H14A, as well as the TiAlN coating with steel 1.3505, can provide a higher seize resistance and preferable antifriction characteristics of the joints of the parts of the fuel equipment.

The combination of MoN and TiAlN coatings with TiC coating has relatively preferred antifriction properties in comparison with the used joint of steel 1.3505 with steel 1.3505. According to the data obtained, the lower values of the friction coefficients are provided by the connection of the coatings MoN and TiC.

The data obtained show the possibility of increasing the performance and durability of parts of the fuel equipment of diesel engines due to a significant improvement in the tribotechnical characteristics of combinations of parts of fuel equipment when using vacuum composite coatings. This makes it possible to reduce the accepted values of the gaps in the rubbing joints and, accordingly, to improve the quality of the fuel equipment by reducing fuel leaks and increasing the injection pressure.

The studies performed have shown that multicomponent multilayer rigid and superhard coatings of the new generation have significantly higher wear resistance and tribological characteristics and are very effective for increasing the efficiency and durability of parts of the fuel equipment of diesel engines.

5.1.1.2 Coating plunger dummies and plunger full-scale batches

During the development of pilot technological processes, the work was carried out on mock plungers in the form of samples of steel X162CrMoV12 with a spherical surface, heat treated to a hardness of 62...64 HRC and polished to V 11, — analogs of full-scale plungers.

Corresponding technological modes of heating the models of plungers to a predetermined temperature, their ionic cleaning and subsequent ionic treatment and coating have been worked out.

Optimization of the technological parameters of deposition of strongly adhered nanocomposite coatings on spherical and cylindrical surfaces of plunger dummies was carried out and the modes of deposition of coatings of various compositions — (Ti-N; Mo-N) and multilayer compositions based on them [(Ti-N)-Ti; (Mo-N)-Mo)] (**Table 5.3**).

All experiments were carried out with a straight-line separator, temperature — 150–200 °C.

According to the worked-out modes, coatings were applied to the plunger dummies.

Table 5.3 Technological parameters for applying coatings to pilot plunger models and characteristics of the original samples

No.	Cathode	Composition	Process parameters		Initial parameters		
			Time, hours.	Pressure. Nitrogen, mm	HRC	Class	Roughness
2.1	Ti	Solid TiN	4.0	$(1.5–2)\cdot10^{-3}$	60–62	13	0.018
2.2	Ti	Nanolayers TiN-Ti	2.5	$5\cdot10^{-4}$; work 48 s, pause 48 s	60–62	12c	0.020
2.3	Ti	Solid TiN	4.0	$(1.5–2)\cdot10^{-3}$	60–62	13	0.015
2.4	Ti	Solid TiN	4.0	$(1.5–2)\cdot10^{-3}$	60–62	12c	0.020
2.5	Ti	Microlayers TiN-Ti	2.0	$1.8\cdot10^{-3}$; work 12 min, pause 12 min	60–62	12c	0.020
2.6	Mo	Macrolayers Mo_2N-Mo	2.0	$5\cdot10^{-4}$; Mo — 0.5 h, Mo_2N — 1 h, Mo — 0.5 h	60–62	12c	0.020

Fig. 5.4 Sample-witness and dummy plunger with nanolayer coating based on Ti

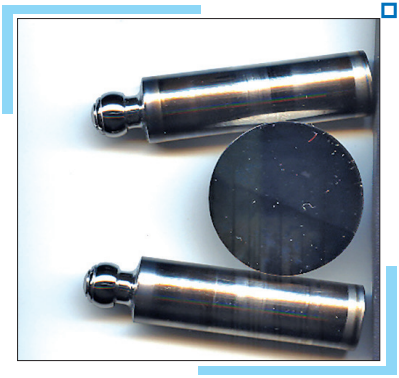

Fig. 5.5 Sample-witness and models of plungers with microlayer coating based on Mo

Fig. 5.6 Spherical plunger surface with Ti-based Avinit nanolayer coating

Metallographic studies of the deposited coatings have been carried out.

According to research data (**Table 5.4**), the developed processes of strengthening the spherical and cylindrical surfaces of the plunger on the experimental parts retain the hardness of the material within the required limits, the thickness of the coatings is 0.5–1 μm. The coatings have a homogeneous structure and are evenly distributed over the entire surface to be coated.

Table 5.4 Characteristics of the studied samples-witnesses and prototypes of plungers with coatings

No.	Composition	Finite. Parameters			
		Thick-ness, μm	Microhardness, $H_{v(50\ g)}$	Class	Rough
2.1	Solid TiN	1	1150	10c	0.10
2.2	Nanolayers TiN-Ti	0.5	894	11	0.040
2.6	Macrolayers Mo_2N-Mo	0.2	894	12b	0.026

Metallographic studies of samples of the investigated coatings on plunger models (roughness, base hardness, microhardness, coating thickness) confirmed that the developed coatings have high tribological characteristics.

Avinit multi-layer antifriction wear-resistant coatings have been developed to improve the tribological characteristics of friction pairs to reduce wear and friction of parts of fuel equipment:

- plunger pairs (with surface hardening or for plunger restoration);
- nozzle needles;
- spray nozzles.

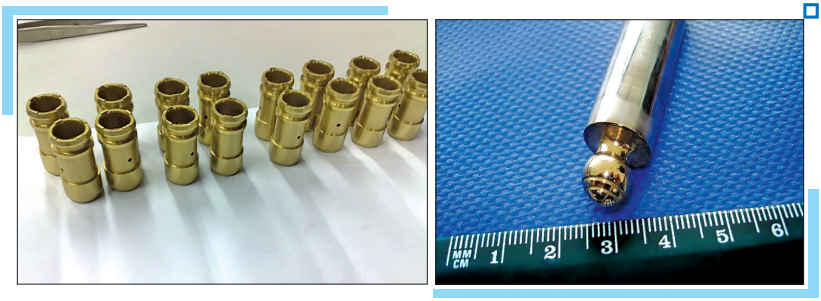

Fig. 5.7 Strengthening the surfaces of the plungers

Features of nanocomposite anti-friction wear-resistant coatings Avinit to improve the tribological characteristics of friction pairs.

The coatings have a nanolayer structure and consist of layers of various metals and compounds with a thickness of ~ 5–10 nm.

Microhardness 8000–45000 MPa (depending on the composition of the coating).

Preservation of the surface purity class Ra=0.025–0.036 μm.

Coating thickness 2–3 μm.

The coefficient of friction is 0.005 to 0.02.

Low-temperature coating processes with good adhesion to the substrate ($T \leq 200$ °C).

Fig. 5.8 Reinforcement of sliding and rolling raceways of bearings with Avinit nanocomposite wear-resistant anti-friction coatings

Thus,

1. The optimization of the technological parameters of the deposition of strongly adhered nanocomposite coatings on the spherical and cylindrical surfaces of full-scale plungers has been carried out, and the regimes for the coating of the selected compositions have been tested.

2. Processes of applying reinforcing coatings on spherical surfaces of full-scale plungers have been worked out.

The data obtained show the possibility of increasing the performance and durability of parts of the fuel equipment of diesel engines due to a significant improvement in the tribotechnical characteristics of combinations of parts of fuel equipment when using vacuum composite coatings. This makes it possible to reduce the accepted values of the gaps in the rubbing pairs and, accordingly, to improve the quality of the fuel equipment by reducing fuel leaks and increasing the injection pressure.

Successful experience in the industrial implementation of the latest technologies developed by us for applying wear-resistant antifriction coatings using nanotechnology to increase the resource of friction pairs (sliding bearings, plunger pairs, rods and bushings of high-pressure control and stop valves) convinces of the great prospects for the use and life of precision engine parts and gas turbine technology

5.1.2 Multi-component coatings for CPG parts (pistons, rings)

5.1.2.1 Avinit anti-seize coating for engine pistons

One of the reasons for the rapid destruction of the contacting surfaces in the friction units is the formation of scoring. This may be due to a violation of the lubrication conditions, overload, or non-conformity with the selected operating conditions. In the latter case, the problem arises of choosing a material that can satisfy the specific working conditions of a given university.

The use of aluminum-based alloys for the manufacture of diesel pistons with high power to improve the weight, size and other promising parameters of the engine is a very important direction in engine building. A typical example is the heat-resistant aluminum alloy EN AW-AI with a tempering temperature of 180–200 °C. Aluminum alloys of this group combine strength and satisfactory tribological indicators that explain their use. necessary, alloys of this group are created in the manufacture of pistons for internal combustion engines.

At the same time, their use is associated with certain difficulties due to insufficient wear resistance and seize resistance of these alloys. Under heavily loaded engines, the possibility of seize limits their use. Better wear resistance is also desirable. Such a material can be a typical structural material in mechanical engineering with the characteristic conditions of the permissible heating temperature, which does not reduce its mechanical properties after that, as well as the disadvantages of the headset and limitations in use.

In connection with a sharp difference in the requirements for the material properties of parts of friction units in the volume and in a thin near-surface layer containing the parameters of friction and wear, it is more urgent to use new technologies for applying protective, wear-resistant, antifriction and seasoning coatings that ensure expansion. the possibilities of forming working layers, differing in the criteria of compatibility [4], as well as achieving maintenance-free machine with a comprehensive solution to the problems of a sharp multiple increase in parts.

The piston coating is affected by mechanical and corrosive fuel and gas, which are provided by gas combustion, oxidizing carbon, nitrous oxide, sulfur dioxide, concentration, depending on the composition of the fuel. The coating must be chemically resistant, and no films or deposits must appear in it.

The coating must have good thermal conductivity, which does not change during engine operation. Should be observed in comparison with the corresponding standard pistons in terms of wear resistance and piston wear rate, the running-in of coated pistons should not be carried out when using standard pistons.

5.1.2.1.1 Development of multifunctional composite coatings Avinit

We have developed new multifunctional composite coatings Avinit [128, 129] for the elements of the cylinder-piston group (CPG):

- pistons;
- piston pins and bushings;
- oil scraper and compression piston rings.

In work [130], the development of low-temperature processes of deposition of wear-resistant, anti-seize coatings of various compositions on the EN AW-AI alloy was carried out.

When working out the coating processes, the main task was to select the parameters of the installation, which would ensure the receipt of fortress coatings of the selected compositions without violating the strength of the base material. For the heat-resistant aluminum alloy EN AW-AI, such modes should not have reduced its hardness below 110 units on the Brinell scale.

The study of the formation processes of coatings of different compositions was carried out under conditions that did not lead to an increase in the temperature of the samples above 200 °C. At the stage of vacuum-plasma cleaning, this was achieved through the use of a pulsed processing mode and the choice of the ratio of the intervals of operation and pause of arc sources, as well as the total processing time. When forming coatings using titanium or aluminum cathodes, as shown by experiments, it is close to the optimal operating mode of the arc source 2 sec. and a pause of 4 seconds. with a total processing time of 3–5 minutes with a gradual increase in the accelerating potential from 30...50 V to a maximum value of 1000 V. When working with a molybdenum cathode, the pause increased to 6 seconds. At the stage of deposition of coatings based on titanium, aluminum and their compounds with nitrogen, it was possible to maintain the temperature in the range of 180–200 °C in the mode of continuous operation of the vacuum-arc source at a potential of 30–40 V. In the case of the deposition of coatings based on molybdenum and its compounds, even at a potential of 25 V, it is impossible to keep the temperature of the samples within the applied limits with the constant operation of the vacuum arc source; therefore, a pulsed operating mode with a cycle of 6 s — work, 4 s — pause was applied.

The methods of plasma cleaning in a glow discharge of argon plasma and in a high-density argon plasma created by a gas plasma generator of the Avinit installation have been developed during the deposition of coatings on prototypes made of aluminum alloy. Pre-bombarding the substrate prior to coating is beneficial to both adhesion and coating quality. The parameters of ion bombardment have been determined, which provide the necessary temperature regime, which makes it possible to prevent overheating of the base material and to ensure the application of fortress coatings.

The high-temperature aluminum alloy EN AW-AI with a tempering temperature of 180–200 °C was chosen as the material for the prototypes.

The work [131] investigated the tribological characteristics of coatings on samples under conditions simulating the operation of the piston group of the D80 engine.

Table 5.5 shows the compositions of the investigated coatings, the value of their microhardness, thickness.

Table 5.5 Investigated coatings

Composition	Microhardness, GPa	Thickness, μm
Mo	4.0	4÷5
AlN	30	5÷6
TiN	22	5÷6
Mo + Mo_2N	25	(~ 0.3) + (4÷5)
AlN + Al	30	(5÷6) + (0.1)
Mo + Mo_2N + Mo	–	(~ 0.3) + (2÷2.5) + (2.5)
(AlN-Ti) nanocomposite	20	5÷6
(TiN-AlN) nanocomposite	35	5÷6
(TiN-AlN) nanocomposite + Mo	–	(5÷6) + (2.5)

Optimization of the technological parameters for the deposition of firmly adhered high-quality coatings and the development of modes of ion-plasma deposition of coatings of different compositions (Al-N; Ti-N; Al, Ti-N; Mo-N; Mo) and multilayer compositions based on them (Al-(Al-N)-Al; Al-(Al-N)-Al-(Al, Ti-N); (Mo-N)-Mo; -(Al, Ti-N)-Mo) for samples of aluminum alloy EN AW-AI provide sufficient adhesion of coatings and preservation of the hardness of the EN AW-AI alloy within the specified limits. The measured values of the stiffness of the base were not less than 125 kg/mm^2 for the studied samples. Metallographic studies of samples with coatings confirmed the continuity and uniformity of the thickness of the coatings over the entire surface of the samples.

The coatings of the above compositions were applied to the samples for tribotechnical tests according to standard factory methods on friction machines of the SMC-2 and 2070 S SMC-1 types according to the «disc-shoe» scheme with a step load in the Central Factory Laboratory of the State Enterprise «Malyshev Plant «(Kharkiv) [131, 132,].

Wear tests are critical because wear increases the amount of gases escaping through the piston grooves and the engine power decreases.

Table 5.6 shows the results of measuring the value of the wear of the coatings under study, applied to the «disks» of the EN AW-AI alloy, as well as the «shoes» of cast iron sleeve after tests at a step load of up to 6 MPa. For comparison, samples of uncoated «discs» were tested.

Table 5.6 Results of measurements of wear values during loading up to 3 MPa (dick EN AW-AI, shoe — sleeve cast iron)

No.	Coating	Disc wear, g	Shoe wear, g,	Relative increase in stability
1	uncoated	0.0343	+0.0004	1
2	Mo	0.0632	0.0001	2.1
3	AlN	0.0006	0.1233	64.2
4	TiN	0.0023	0.0476	28.7
5	Mo + Mo_2N	0.0180	0.0497	56
6	(TiN-AlN)	0.0006	0.0340	87.9
7	(AlN-Ti)	0.0716	0.0007	0.7
8	AlN + Al	0.0008	0.0295	47.6
9	Mo + Mo_2N + Mo	0.0064	0.0003	20.6

The analysis shows that the samples of the EN AW-AI alloy without coating wear out intensively.

The coating of pure Mo has a lower linear wear rate compared to the EN AW-AI alloy and wears out the counterbody quite insignificantly, but, in general, showed low wear resistance and was almost completely worn out to the base during the tests. Comparison of the test results of Al, Ti, and Mo nitrides shows that the AlN coating is the most wear-resistant, however, when it is tested, the greatest wear of the counterbody occurs, which can characterize the abrasive properties of this coating. MoN and TiN coatings showed approximately the same wear performance results.

The coating (TiN-AlN) showed the highest wear resistance, but it also has the highest wear resistance in relation to the counterbody.

Examinations of the nanocomposite coating (TiN-AlN) showed that its wear resistance is the same as that of the AlN coating, but the ability of the wearing counterbody is significantly lower (more than 3 times). The nanocomposite coating (AlN-Ti) showed an even lower wear capacity in relation to the counterbody, however, when friction with a load of up to 3 MPa, adhesion occurs with destruction of the coating and surface layers of the metal, which explains such high values of disk wear.

Table 5.7 shows the results of subsequent repeated tests of some variants of the investigated coatings up to a load of 10 MPa, the maximum possible during examinations according to the chosen scheme.

The wear of the samples after repeated tests was to some extent influenced by the running-in processes that took place during the examinations at the first stage. So, the amount of wear of the uncoated EN AW-AI alloy turned out to be less than during the first examinations, this is also true for the TiN coating. All investigated coatings withstood the maximum load

without destruction. The Mo + Mo_2N + Mo coating, as in the first series of examinations, showed the lowest wear capacity in relation to the counter-body, and the nanocomposite coating (TiN-AlN) turned out to be the most wear-resistant. Since the magnitude of the load is limited by the capabilities of the mechanism loading the friction machine, in order to assess the limiting performance of the Mo + Mo_2N + Mo coating, a repeated load was performed up to 10 MPa. With repeated loading, the coating worn out to the base material at a load of ~8 MPa, however, tear and seize were not detected, as evidenced by the course of change in the friction coefficient (F_{fr}) up to a maximum load of 10 MPa (**Table 5.7**).

Table 5.7 Results of measurements of wear values during loading up to 10 MPa (disk EN AW-AI, shoe — sleeve cast iron)

No.	Coating	Disk wear, g	Shoe wear, g	Coefficient of friction F_{fr}, at loading of 6 MPa
1	—	0.0113	+0.0002	0.03
2	AlN	0.0014	0.1228	0.12
3	TiN	0.0013	0.0496	0.14
4	Mo + Mo_2N	0.0032	0.0815	0.12
5	AlN + Al	+0.0010	0.0614	0.11
6	(TiN-AlN)	0.0007	0.1188	0.12
7	Mo + Mo_2N + Mo	0.1934	0.0014	0.1

Dependences of the friction coefficient on overload are presented in **Table 5.8** (load up to 3 MPa) and **Table 5.9** (repeated loading up to 10 MPa).

Table 5.8 Dependence of the friction coefficient (F_{fr}) on the load up to 0.6 kN (disk EN AW-AI with coatings, shoe» — sleeve cast iron)

No.	Coating	Coefficient of friction F_{fr}, at loading of P, kN		
		0.2	0.4	0.6
1	—	0.15	0.16	0.14
2	Mo	0.14	0.15	0.14
3	AlN	0.12	0.15	0.146
4	TiN	0.05	0.15	0.14
5	Mo_2N	0.1	0.135	0.14
6	AlN + Al	0.02	0.05	0.093
7	(AlN-Ti)	0.024	0.085	0.097
8	(TiN-AlN)	0.054	0.05	0.08
9	Mo + Mo_2N + Mo	0.04	0.033	0.027

Table 5.9 Dependence of the friction coefficient (F_{fr}) on loading when loading up to 2.0 kN («disk» EN AW-AI with coatings, «shoe» — sleeve cast iron)

No.	Coating	Coefficient of friction F_{fr}, at loading of P, kN										Notes
		0.2	0.4	0.6	0.8	1.0	1.2	1.4	1.6	1.8	2.0	—
1	—	0.03	0.015	0.014	0.012	0.012	0.03	—	—	—	—	—
2	AlN	0.06	0.095	0.12	0.12	0.12	0.12	0.114	0.115	0.113	0.115	—
3	TiN	0.17	0.15	0.14	0.14	0.13	0.14	0.13	0.135	0.137	0.135	—
4	Mo_2N	0.09	0.1	0.12	0.12	0.12	0.12	0.12	0.126	0.13	0.124	—
5	AlN + Al	0.016	0.02	0.07	0.11	0.11	0.11	0.11	0.11	0.11	0.11	—
6	(TiN-AlN)	0.03	0.075	0.12	0.12	0.12	0.12	0.12	0.12	0.116	0.115	—
7	Mo+ +Mo_2N+Mo	0.022	0.04	0.06	0.11	0.11	0.1	0.11	0.11	0.116	0.114	I load.
8	— » — » —	0.02	0.005	0.005	0.006	0.007	0.007	0.008	0.005	0.008	0.008	II load.

Analysis of the data obtained shows that the uncoated EN AW-AI alloy with repeated loading withstands a load of up to 6 MPa, the subsequent load leads to a sharp increase in the friction moment and the beginning of setting. The level of values of the coefficient of friction under repeated loading has significantly decreased, which can be explained by attaching the working surfaces. The decrease in the friction coefficients of the investigated coatings under repeated loads is less pronounced, which may be associated with the relatively higher rigidity and wear resistance of the investigated coatings. However, under one more load of the Mo+Mo_2N+Mo coating up to the ultimate load of 10 MPa, a significant decrease in the friction coefficients was recorded, which characterizes the possibility of using this coating as wear-resistant and antifrictional under appropriate operating conditions.

The results of examinations of the selected options for coatings according to scheme 2 with a load of up to 10 MPa are presented in **Tables 5.10, 5.11**.

Table 5.10 Wear of the coating at a step load of up to 10 MPa («disk» — sleeve cast iron, «shoe» EN AW-AI)

No.	Coating	Shoe wear, g	Disk wear, g	Notes
1	—	0.0075	0.0023	load up to 8 MPa
2	Mo + Mo_2N + Mo	0.0002	0.0034	load up to 8 MPa
3	Mo + Mo_2N + Mo	0.0005	0.0062	—
4	(TiN-AlN)	0.0002	0.0290	—
5	(TiN-AlN) + Mo	0.0002	—	—

Table 5.11 Dependence of the friction coefficient (F_{fr}) on the load («shoe» EN AW-AI with coatings, «disk» — sleeve cast iron)

No.	Coating	Coefficient of friction F_{fr}, at loading of P, kN									
		0.2	0.4	0.6	0.8	1	1.2	1.4	1.6	1.8	2.0
1	—	0.042	0.02	0.013	0.01	0.011	0.01	0.011	0.016	—	—
2	Mo + Mo_2N + Mo	0.094	0.105	0.115	0.114	0.11	0.107	0.106	0.106	0.107	0.098
3	Mo + Mo_2N + Mo	0.13	0.125	0.113	0.099	0.092	0.085	0.086	0.09	0.092	0.093
4	(TiN-AlN)	0.1	0.127	0.137	0.133	0.127	0.125	0.121	0.121	0.121	0.12
5	(TiN-AlN) + Mo	0.16	0.155	0.145	0.135	0.13	0.127	0.125	0.125	0.124	0.123

The tests of the EN AW-AI alloy without coating showed a sharp increase in the friction moments and the beginning of the formation of scoring at a load above 8 MPa. Coated specimens withstand maximum loads without burr or breakage. The highest wear resistance in these examinations, as in the previous ones, was shown by the coating (TiN-AlN), but it also had the greatest wear resistance in relation to the counterbody. In this regard, the Mo+Mo_2N+Mo coating turned out to be better, for which, as exams up to a load of 8 MPa showed, the wear of the counterbody is not much higher than this indicator in the examinations of the EN AW-AI alloy without a coating, with a sufficiently high wear resistance of the coating itself. However, nanocomposite coatings of the (TiN-AlN) type are undoubtedly interesting as a promising option for strengthening parts made of aluminum and other metals and alloys.

The Mo+Mo_2N+Mo coating has the lowest wear capacity in relation to the counterbody (the wear of the counterbody is slightly higher than this indicator when testing the EN AW-AI alloy without a coating), but the wear resistance of the coating itself is quite high. When loading the Mo+Mo_2N+Mo coating up to the ultimate load of 10 MPa, a significant decrease in the friction coefficients was recorded, which characterizes the possibility of using this coating as a wear-resistant and antifrictional one under appropriate operating conditions.

The analysis of the obtained results showed [131] that the Mo+Mo_2N+Mo coating, which has the lowest ability in relation to the counterbody in comparison and very high wear resistance, has the best combination of wear resistance, wear capacity in relation to liner cast iron and antifriction properties of the studied coatings. These coatings were selected for application as anti-seize wear-resistant coatings on full-scale pistons made of deformed heat-resistant aluminum alloy for diesel engines of the D80 type for bench tests.

Thus, tests of various coatings obtained by the method of vacuum ion-plasma spraying on samples of heat-resistant deformed alloy EN AW-AI were carried out under sliding friction under conditions of extreme lubrication.

The test results show that the developed nanocomposite vacuum-arc coatings on the EN AW-AI alloy of the corresponding compositions prevent

seize when working in tandem with liner cast iron under sliding friction conditions under lubrication boundary conditions corresponding to the operating conditions of the parts of the cylinder-piston group of engines. In this case, the relative increase in resistance reaches 20–80 times, and the wear of the counterbody decreases by 4–5 times.

The highest wear resistance of the investigated coatings is possessed by a coating of the composition Ti-Al-N. The multilayer coating of the (Mo-N)-Mo composition has the lowest wear capacity in relation to the counterbody in comparison with other coatings.

The coatings of these compositions withstood the tests at maximum loads without the formation of burrs; their coefficient of friction during the test tended to decrease in value.

The Mo + Mo_2N + Mo coating has the best combination of wear resistance, wear capacity in relation to liner cast iron and antifriction properties of the studied coating options. This coating is recommended for pilot testing as an extreme pressure wear resistant coating for pistons made of aluminum alloys.

5.1.2.1.2 Avinit C220 coating on full-scale pistons

The adaptation of the process of applying anti-seize and wear-resistant coatings to aluminum pistons of D80 diesel engines has been carried out.

The development and manufacture of the necessary technological equipment for the application of ion-plasma coatings on full-scale pistons was carried out.

Corresponding technological modes of piston heating to a predetermined temperature, their ionic cleaning and subsequent ionic treatment and coating have been worked out.

Optimization of technological parameters of deposition of strongly adhered ion-plasma coatings Mo + Mo_2N + Mo on the surface of full-scale aluminum pistons of D80 diesel engines has been carried out.

Metallographic studies have confirmed the preservation of the stiffness of the piston material within the required limits. The thickness of the applied coatings is 3–5 μm. The coatings have a homogeneous structure and are evenly distributed over the entire surface of the piston to be coated.

The worked out modes provide sufficient adhesion and preservation of the hardness of the EN AW-AI alloy within the specified limits. Metallographic studies of samples with coatings confirmed the continuity and uniformity of the thickness of the coatings over the entire surface of the samples.

The technical process of applying Avinit anti-seize coatings on natural cuttings of the D80 piston has been worked out.

The Mo + Mo_2N + Mo coating was applied to the full-scale aluminum pistons of diesel engines of the D80 type for bench tests according to the worked-out modes (**Fig. 5.9**).

Fig. 5.9 Anti-seize and wear-resistant Avinit nanocomposite coatings on pistons made of aluminum alloy of D80 diesel engines (State Enterprise «Malyshev Plant», Kharkiv)

5.1.2.1.3 Bench tests of pistons made of EN AW-AI aluminum alloy with anti-seize wear-resistant coatings Avinit C220 for diesel engines of type D80

Bench tests of pistons made of deformed heat-resistant aluminum alloy EN AW-AI with developed anti-seize wear-resistant coatings Avinit C220 for diesel engines of D80 type were carried out at the SE «Malyshev Plant «(Kharkiv). The tests were carried out as part of a diesel engine according to a single-cylinder scheme with the maximum approximation to full-scale operating conditions.

The test results show that nanocomposite vacuum-arc coatings have been developed on the EN AW-AI alloy of the corresponding compositions (Al-N; Ti-N; Al, Ti-N; Mo-N; Mo) and multilayer compositions based on them (Al-(Al-N)-Al; Al-(Al-N)-Al-(Al, Ti-N); (Mo-N)-Mo; (Al, Ti-N)-Mo) completely prevent seize when working in steam with sleeve cast iron under sliding friction conditions at boundary conditions of lubrication corresponding to the operating conditions of parts of the cylinder-piston group of engines. Depending on the type of coating, the relative durability of coated samples in relation to uncoated ones increases by 20–80 times, and the wear of the counterbody decreases by 4–5 times. The $Mo + Mo_2N + Mo$ coating has the best combination of wear resistance, wear capacity in relation to liner cast iron and antifriction properties of the studied coatings.

The developed anti-seize coatings Avinit C220 for diesel engines of the D80 type have been fully certified at the factory.

This coating is recommended for pilot testing as an extreme pressure wear resistant coating for pistons made of aluminum alloys.

The test results confirmed the high efficiency of the developed coatings, and they were recommended instead of the factory running-in coating VAP-2.

Testing of pistons D80.0406-1 with a multilayer nitride-molybdenum coating was carried out on a 2-cylinder in-line diesel engine with a cylindrical power of 187 hp. at 1000 rpm.

The diesel engine has passed rolling tests and acceptance tests.

By the time of disassembly, it worked with the indicated pistons for 64 hours and 50 minutes. During the tests, there were no comments on the operation of the cylinder-piston group.

Inspection of the piston cuttings revealed that there are no signs of wear, damage or destruction of the coating. No traces of oxidation of the lubricant were found on the piston cuttings. The pistons are in working order and are suitable for further operation. There are no comments on the condition of the cylinder liner sliding surface.

The work performed to increase the service life of diesel locomotive engines of the D80 type by expanding the scope of possible use of coatings of a new generation can serve as the basis for creating a «maintenance-free engine».

5.1.2.2 Avinit hardening coating for compression rings in diesel engines

Avinit reinforcing nano-coatings have been developed for compression rings of diesel engines, which have shown high efficiency while reducing the total number of piston rings.

In [133], studies were carried out to strengthen the edges of the oil scraper piston rings of the D80 diesel engine with nanocomposite coatings based on Ti-Al-N.

The technical and economic characteristics of internal combustion engines largely depend on the features of the work of the parts of the cylinder-piston group and, above all, the piston rings. Reducing the frictional losses of these parts to the greatest extent determines the possibility of increasing the mechanical efficiency and, accordingly, reducing the fuel consumption in operation.

The consumption of lubricant for waste in internal combustion engines is determined by many factors, the most important of which is the size of the gap between the mirror of the liner and the surface of the ring. The resistance to wear of the ring determines the lubrication consumption during engine operation, which is an important characteristic of the engine. In diesel engines D80, the surface of the oil scraper ring, facing the sleeve, is made in the form of a wedge with an angle of 45° and a belt 0.2÷0.3 mm wide at its apex in contact with the sleeve. The belt is the most loaded part of the ring and it is on its wear resistance that the stability and the amount of lubricant consumption during engine operation depend to the greatest extent.

Various methods are used to increase the resistance of friction surfaces. One of the widespread and relatively simple methods used at machine-building enterprises to strengthen surfaces, including at the manufacturer of the D 80 engine, are electrolytic coating methods. However, attempts to apply these methods to strengthen the oil scraper ring belt did not give a positive

result, since it turned out to be impossible to provide the required geometry of the ring belt working surface due to the very large unevenness in the coating thickness. This unevenness is typical for electrolytic coating methods on products with sharp edges on the working surface.

In [131], studies were carried out to determine the tribological characteristics in friction pairs with liner cast iron of a number of coatings obtained by the vacuum arc method in relation to the problem of creating anti-seize reinforcing coatings for the piston shaft of the D80 engine. Studies have shown that nanocomposite coatings of the Ti-Al-N system showed the highest durability when tested in tandem with cast iron. These studies served as the basis for choosing the type of coating for applying hardening coatings on the oil scraper piston rings of diesel locomotive engines of the D80 type.

The nanocomposite coating of the Ti-Al-N system was chosen as the main coating. To assess the effectiveness of using this coating as a reinforcing coating, comparative tests for the wear resistance of coatings of the Ti-N system that are widely used to strengthen various products were carried out.

The application of reinforcing nanocomposite coatings by vacuum arc spraying was carried out on the Avinit vacuum plasma cluster. The coatings were applied according to a specific program, in which the time, sequence and mode of operation of the evaporators, the system for supplying reaction gases, and a high-voltage source were set, which made it possible to obtain a multilayer and multicomponent coating with a given composition in thickness. When working out the coating processes, the main task was to select parameters that ensure the formation of strength layers of the selected compositions without compromising the strength of the base material — special cast iron according to D100004.DT-62. The piston ring sliding surfaces were pre-lapped prior to coating. Measurements of the stiffness of the rings showed that the selected modes of coating do not change the rigidity of the latter, which was in the range of 101–104 HRB units both before and after coating.

The ratio of Ti to Al in the coatings depended on the ratio of the currents of the corresponding arc sources at other constant process parameters. For testing, prototypes of piston rings with coatings of two compositions were obtained at currents of arc sources Ti and Al corresponding to a ratio of 1:1 and 2:3 (respectively Ti-Al-N (I) and Ti-Al-N (II)). The pressure of the reaction gas was chosen so as to obtain typical values for the microhardness of the respective compounds.

During the deposition of coatings, a layered structure was formed from layers of the corresponding compositions with a thickness of ~10–15 nm.

Ti-N coatings were applied to two batches of rings under the same conditions, but different thicknesses.

Table 5.12 shows the characteristics of the investigated coatings.

The tests were carried out on samples cut from coated piston rings on a reciprocating friction machine RFM in a mode simulating the operation of an oil scraper ring, with a total load of 5 kg and a sliding speed of 0–1 m/s.

As a counterbody in the tests, we used samples cut from the cylinder liner of a D80 diesel engine while maintaining the working surface.

The results of tests carried out for 1 hour and 7 hours are shown in **Table 5.13**. For comparison, the table also presents the test results of samples of oil scraper piston rings without coating.

Table 5.12 Characteristics of the investigated coatings

Composition	Microhardness, GPa	Total thickness, μm
TiN (I)	22	16
TiN (II)	22	4
Ti-Al-N (I)	35	6
Ti-Al-N (II)	30	6

Table 5.13 The results of measurements of the wear values of oil scraper piston rings (PR) when working in tandem with samples of cylinder liners (GL)

No.	Coating	Wear of samples of the piston rings, $g\times10^3$ during tests, h			Wear of samples of cylinder liners, $g\times10^3$ during tests, h			Relative increase of stability
		1	7	S (8 h)	1	7	S(8 h)	
1	TiN (I)	0.90	0.55	1.45	–	–	67.7	–
2	TiN (II)	0.45	0.15	0.60	–	–	15.9	2.3
3	Ti-Al-N (I)	0.20	0.10	0.30	–	–	3.6	4.6
4	Ti-Al-N (II)	0.15	0.25	0.40	–	–	2.3	3.4
5	Without coating	–	1.2	–	–	–	10,2	1.0

TiN (I) coating with a thickness of 16 μm showed low resistance in tests. Microscopic studies of the surface of such samples after testing showed that wear occurs with the chipping of individual fragments of the coating, which affected the high wear values of the ring on the one hand and, to an even greater extent, the wear capacity of such a coating. This result confirms the numerous data on tool strengthening, according to which coatings of TiN and other similar types of joints are effective up to a thickness of about 6 μm. Due to the high brittleness of such joints, a further increase in thickness does not lead to an increase in the resistance of coated parts, but, on the contrary, begins to decrease. Therefore, subsequently, the thickness of the coatings did not exceed 6 μm. Coatings with TiN (II) with a thickness of 4 μm showed high resistance compared to an unreinforced PC sample and a significant slowdown in the wear rate after 7 hours of testing compared to the first hour of testing. The introduction of Al into titanium nitride and the formation of a nanolayer structure for coatings of the Ti-Al-N system had a positive effect both on increasing the resistance of the coating and on reducing the wear of the counterbody. Coatings with a higher Al content

(Ti-Al-N (II)) showed slightly lower resistance compared to the Ti-Al-N (I) coating, but, on the other hand, and less wear capacity in relation to the counterbody. The obtained differences in the tribological characteristics of coatings with different aluminum contents fit into the general character of changes in the properties of coatings of this system, depending on the ratio of Ti to Al. Thus, the hardness of the coating in the Ti-Al-N system increases with an increase in the Al content in the coating, reaching a maximum in the region of ~40–50 at % aluminum and then, with its further increase, decreases. According to this coating, with higher rigidity, they showed both higher resistance to wear and faster running-in of the surface of the cast iron counterbody, showing less total wear in the next 7 hours compared to an hour in the initial period. Coatings based on Ti-Al-N, having a higher rigidity compared to TiN coatings, at the same time, as compared with the latter, as shown by studies [131], lower values of the coefficient of friction in a wide range of loads. This was reflected in the amount of wear of the counterbody during tests, which, when using a TiN coating to strengthen the prototypes, exceeded the wear obtained during tests with coatings based on Ti-Al-N by more than 4–6 times.

Tests have shown that nanocomposite coatings based on the Ti-Al-N system have 1.5–2 times higher wear resistance compared to TiN coatings and more than 4–6.5 times lower in wear capacity. Thus, it can be expected that the wear resistance of rings with nanocomposite coatings based on Ti-Al-N coatings will be 3–4 to 10 times higher compared to rings without coatings.

Studies of the characteristics of friction and wear of ion-plasma coatings under the operating conditions of parts of the cylinder-piston group of highly accelerated diesel engines, as well as the experience of operating aluminum pistons with a composite coating MoN + Mo indicate high characteristics of these coatings in terms of tear resistance and antifriction.

In [133], the characteristics of friction of such composite ion-plasma coatings in relation to the operation of piston rings of diesel locomotive engines were determined, as well as an assessment of the effect of these coatings on the technical and economic characteristics of the engines produced. The results of tests to determine the effect of the composition of composite vacuum ion-plasma coatings on the magnitude and nature of the change in the friction coefficient depending on the load are presented in the range of piston ring loads of diesel locomotive engines.

The following coating options were selected for testing:

1. TiN coating.
2. TiAlN coating.
3. MoN + Mo coating.
4. MoCuN coating.

The calculated thickness of the investigated coatings was 3...5 μm. Samples of X12Ф1steel, heat-treated to a hardness of 60...61 HRC, served as substrates for the coatings. For comparison, samples of piston rings of a 10Д100М1 diesel engine with a chrome coating applied by an electrolytic method were examined.

The results of tests to determine the coefficients of friction (F_{fr}) are given in **Table 5.14**.

The analysis of the results obtained indicates that the use of the investigated composite coatings for piston rings can provide a higher tear resistance and better friction characteristics of the liner – piston ring interface in comparison with the used electrolytic chromium coating. However, it should be noted that with an increase in the total loads, the friction coefficients of the investigated coatings slightly increase, while the friction coefficient of the chrome-plated piston ring decreases. This indicates that in order to achieve a greater effect of using the studied promising coatings of piston rings, it is advisable to simultaneously process the possibility of lowering the acting loads in combinations.

To assess the efficiency of using various coatings, **Table 5.15** shows the average values of the coefficients of friction (F_{fr}) in the range of total loads of 0.2–1.0 kN, typical for the operating conditions of compression piston rings.

Table 5.14 Test results of the investigated coatings

Coating	Coefficient of friction F_{fr}, at loading of P, kN						
	0.2	0.4	0.6	0.8	1.0	1.2	1.4
Ti	0.025	0.033	0.040	0.051	0.085	0.097	0.086
TiAlN	0.020	0.023	0.028	0.034	0.040	0.057	0.086
MoN + Mo	0.020	0.23	0.032	0.038	0.049	0.060	0.065
MoCuN	0.020	0.025	0.030	0.036	0.044	0.050	0.080
Chrome ring	0.120	0.105	0.093	0.92	0.096	↑*	–

Table 5.15 Average values of friction coefficients (F_{fr}) in the range of total loads 0.2–1.0 kN and microhardness of the investigated coatings

Coating material	Value F_{fr}	Microhardness, HV50, kg/mm^2	
		Initial	Friction tracks
Avinit C310	0.029	1503	1720
Avinit C220	0.032	1507	2335
Avinit C240	0.031	2022	2212
Chrome ring	0.101	1057	755

Analysis of average values shows that TiAlN, MoN + Mo and MoCuN coatings give approximately the same friction coefficients in the range of 0.029–0.032, which is more than three times less than the values of the friction coefficients of chrome-plated piston rings. TiN coating reduces the coefficient of friction by about half compared to chrome coating. The lowest values of the friction coefficients in the considered range of loads were obtained during testing of the TiAlN coating.

The studies carried out to determine the tribological characteristics in friction pairs with liner cast iron showed that Avinit C310 nanocomposite coatings have the highest stability (**Table 5.15**).

To determine the effectiveness of the application of the investigated coatings on the manufactured piston rings of diesel engines, a preliminary calculation of the power losses for friction of the cylinder-piston group of the 10D100 engine was carried out when using compression piston rings with such coatings. Taking into account the higher efficiency of coatings in reducing the friction coefficients at lower loads, the calculation considered the possibility of reducing the acting loads by reducing the axial height of the piston compression rings.

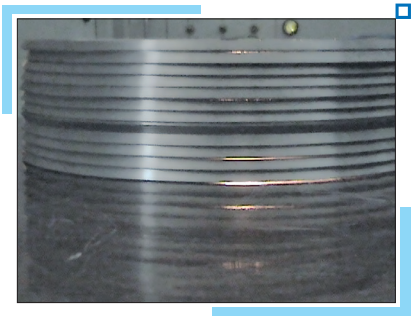

Fig. 5.10 Oil scraper piston rings with reinforcing Avinit C310 coatings

The efficiency of using the investigated coatings with a decrease in the total number of piston rings, which is a general trend in modern piston engine building, is also considered.

The calculation results show that a decrease in the frictional losses of the piston rings leads to a significant increase in the rated engine power, as well as to a decrease in specific fuel consumption. Thus, the results obtained show an increase in the rated power, a decrease in specific fuel consumption due to a decrease in friction losses of the compression rings.

Conclusions.

1. Tests were carried out to determine the tribotechnical characteristics of coatings obtained by the method of vacuum ion-plasma spraying in comparison with an electrolytic chromium coating for the manufactured piston rings of diesel engines.

2. TiN coating reduces the coefficient of friction by about half compared to chrome coating. Coatings with TiN (II) with a thickness of 4 μm showed high durability compared to the unreinforced PC sample.

3. Tests of various reinforcing nanocomposite coatings obtained by the method of vacuum ion-plasma spraying on oil scraper piston rings (PC) have been carried out.

4. The TiAlN, MoN + Mo and MoCuN coatings give approximately the same friction coefficients, which in the load range of 0.2–1.0 kN are more than three times less than the values of the friction coefficients of the chromium electrolytic coating of the piston rings of the 10D100M1 diesel engine.

5. Multilayer coatings such as TiAlN and AlTiN exhibit higher tribological characteristics. The introduction of Al into titanium nitride and the formation of a nanolayer structure for coatings TiAlN (I), TiAlN (II), AlTiN (II)

had a positive effect both on increasing the resistance of the coating and on reducing the wear of the counterbody. On the basis of the tests carried out, one can expect an increase in the wear resistance of rings with such coatings from 3–4 to 10 times when operating the engine during the part-time period and during the period of the beginning of operation.

6. The research results, as well as the known data on the multiple increase in the wear resistance of parts and tools when using vacuum ion-plasma coatings, make it possible to recommend the coating of MoN + Mo, TiAlN and MoCuN on the manufactured piston rings of diesel engines for testing under the conditions of bench tests and tests on experimental engines.

5.1.2.3 Composite coating for crankshaft parts

At present, the most promising antifriction materials for plain bearing shells of the crankshaft of an internal combustion engine are aluminum-tin feet of the AMO1-20 type. Such inserts are distinguished by the highest corrosion resistance and resistance to wear and tear destruction and durability. However, their use for bearings of highly accelerated diesel engines is restrained due to the threat of tear formation due to possible violations of operating conditions, as well as due to possible deviations in the technologies for manufacturing parts, assembly, etc. Therefore, the creation of an anti-friction anti-seize coating on the working surfaces is of great importance for a significant increase in the reliability and durability of the ICEs produced.

For steel-bronze and steel-aluminum main and connecting rod bearings, Avinit running-in coatings and Avinit quasi-crystalline coatings have been developed (**Fig. 5.11**). Technological equipment (dies, sockets, etc. parts), which are used in the process of making liners, operate under conditions of increased friction and require reinforcing and anti-friction coatings (**Fig. 5.12**).

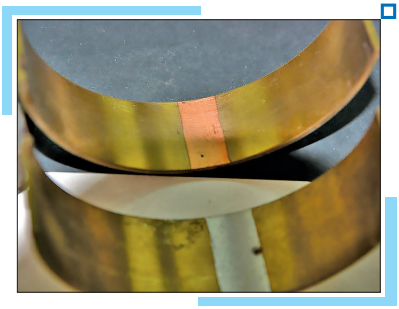

Fig. 5.11 Anti-friction Avinit coating on the working surface of plain bearings (liners) for internal combustion engines (Melitopol Plain Bearing Plant)

Fig. 5.12 Technological equipment for the formation of liners with a hardening anti-friction coating (Melitopol Plain Bearing Plant)

5.1.2.4 Coating for corrosion protection of power steel parts

Corrosion of structural elements is one of the factors that reduce the service life of mechanisms and machines [78, 79].

One of the ways to combat corrosion and improve the reliability of parts is to apply protective coatings on their working surface that improve their anti-corrosion properties. In mechanical engineering, different methods of coating are used: spraying, vacuum-plasma, plasma-chemical, high-temperature diffusion, galvanic, etc. Each method and applied coating has some disadvantages and advantages, as well as its own field of application. Vacuum-plasma and plasma-chemical methods of coating deposition are the most promising among the methods that ensure the production of strongly adhered, practically non-porous coatings from any metals, alloys and compounds.

In work [134], a protective coating obtained using vacuum-plasma technologies was proposed, which it was decided to test on the load-bearing part «Press nut 457.81.027-1» made of 40 carbon steel.

The operating conditions of steel parts «Press nut 457.81.027-1» and the nature of corrosion are such that the most probable causes of corrosion damage to the oxidized surface of a part made of steel 40 are electrochemical processes of metal dissolution and oxidation during the formation of a moisture film on the surface due to adsorption forces or a capillary, which can occur even at a relative humidity of less than 100 %. Under conditions of large temperature drops in the sealed volume, condensation of supersaturated water vapor can simply occur. In addition, chemically active products released during engine operation can accumulate in the sealed volume. All this taken together suggests that the conditions in which the steel parts «Press nut 457.81.027-1» are operated can be attributed to the group of severe or especially severe operating conditions.

The work [134] analyzes the stability of various coating materials, adapts vacuum-plasma technologies for producing fortress coatings, worked out technological regulations and applied a coating to an experimental batch of parts «Press nut 457.81.027-1» for carrying out accelerated corrosion tests of these nuts.

According to the terms of reference for the work, additional machining of the surface of the nuts was not allowed, as well as the tempering of the material of the part during coating. Therefore, to obtain a higher quality coating, other methods of preliminary surface preparation were used: chemical digestion, ultrasonic cleaning, treatment in a gas discharge plasma and molybdenum ions in the saturation mode. According to the selected modes, the test coating was applied to the surface of the nuts, which differed in the initial state of the surface, its preliminary treatment, and the thickness of the applied coating.

It is well known that non-porous coatings made of corrosion-resistant materials can provide reliable protection against corrosion in such conditions. Practice shows that absolutely non-porous metal coatings can be

obtained under optimal conditions for their formation and at a thickness of, as a rule, more than 20–50 μm, while the surface to be coated should not have rough surface defects (cavities, microcracks, nicks, etc.). the fact that the surface of the side faces of the steel parts «Press nut 457.81.027-1» when tightened or unscrewed can be subjected to sufficiently large mechanical loads, the coatings must also have the necessary adhesion and a reserve of plasticity and strength, so that in the process of such operations the coating can maintain its integrity (do not flake off, do not crack, do not peel off).

The requirements for corrosion resistance of coatings in combination with rather high requirements for mechanical properties complicate the choice of materials for the coating and methods of their application. In addition, according to the existing technology, steel parts «Press nut 457.81.027-1» are made from a hexagonal blank without additional processing of edges containing many rough surface defects, which makes it practically impossible to obtain metal coatings without through porosity at reasonable thicknesses.

The protective properties of coatings with through pores during electrochemical corrosion are determined by many factors (composition and concentration of ions in the electrolyte, temperature, degree of electrolyte renewal, its aeration, etc.). Coatings that have a more negative potential in contact with the base metal during electrochemical corrosion processes will serve as an anode and inhibit corrosion of the protected metal in the places of its contact with the electrolyte due to pores or other violations of the integrity of the coating, that is, in principle, they can also provide sufficient a high degree of protection and, on the contrary, with reverse polarity in the «coating-metal» pair, the base metal will corrode faster.

The standard electrode potential of iron is –0.43 V. Its electrode potential in different electrolytes can be «upgraded» (according to [78] to –0.135 V), but it does not reach positive values. Comparison of data for other metals shows that most of the metals commonly used in practice in contact with iron (carbon steel) can have a more noble potential than iron, including those having a more negative standard potential with respect to iron (for example, chromium, titanium). Even classic zinc coatings, widely used for the protection of carbon steels as anodic ones, at temperatures above 70 °C can acquire a potential more positive than iron. This behavior of a number of metals is due to their ability to passivate (inhibit the anodic dissolution process) when immersed in electrolytes of a certain composition. The transition to a passive state can also be caused by the passage of current from an external source, including due to the current due to the contact potential difference arising between two dissimilar metals in the electrolyte. Therefore, the selection of a suitable anodic type coating to protect a particular metal in the general case can be quite difficult.

In this particular case, when the composition of the corrosive medium and its possible changes during the operation of the part are unknown, it is not possible to foresee in advance the ratio of the potentials of the protected

metal and the probable coating. Therefore, the preliminary selection of the coating material in this case will be of a probabilistic nature, and the possibility of its use as an anode one in a pair of «carbon steel-coating» can be assessed only by the results of tests of coated parts (samples). However, despite certain difficulties in choosing a coating material, in this work, the solution to the problem of protecting a part from corrosion using an anode-type coating is the best.

The presence of an anode-type coating does not completely remove the question of its porosity as such, and in any case, it is necessary to strive to ensure that the number of pores and their sizes are as small as possible, since the service life of such a coating largely depends on this.

In work [78] data of studies of electrochemical behavior of samples of carbon steel with different porous galvanic coatings, in particular, with coatings based on nickel and chromium, in 0.1-n. NaCl solution depending on their thickness, varying from 1 μm to 50 μm. Common to all coatings is a change in the potential of the samples with a change in the thickness of the coating from a value close to the value of an uncoated sample to a potential close or equal to the potential of the coating material with almost complete absence of through pores. The potential of the samples with nickel coatings shifted to the region of more positive values in comparison with the potential of the uncoated sample, i.e. Nickel plating was run as a typical cathode plating at all thicknesses investigated. The time dependence of the potential of the coated samples is also noted. For example, for thin (up to 10 μm) nickel coatings, the potential of the samples became «ennobled» with time, while for thicker ones, on the contrary, it was ennobled, which indicated, respectively, the acceleration and deceleration of the anodic reaction in the pores. The electrochemical behavior of the samples with chromium coatings turned out to be more complex. Thus, the potential of samples from a freshly deposited coating was more negative than that of uncoated samples. The change in its value depending on the thickness of the coating was of a non-monotonic nature. The maximum deviation from the potential of the uncoated sample was observed at a coating thickness of 20 μm, then it decreased at a coating thickness of 30 μm (approximately to the value of the potential at a coating thickness of 10 μm) and increased again at a coating thickness of 50 μm.

It is possible that this anomalous behavior of the chrome coating is associated with internal stress in it and possible flooding. Low-temperature annealing of the coated samples in an air atmosphere for 2 hours at 150–200 °C led to the fact that, as a result of annealing, the potentials of the chromium-plated samples became more positive than those of the original samples, that is, the chromium coating began to behave like a cathode in relation to the protected material. As for the dependence of the deviation of the potential of the coated samples on the coating thickness, its general nature did not change, except that these deviations were in the positive

direction and the maximum deviation was observed at a coating thickness of 10 μm. In general, the absolute changes in the potential of the coated samples were much less than the potential difference between the uncoated sample and pure chromium, which, apparently, is associated with the high porosity of chromium coatings, which actually took place. The abnormal behavior of the potential of the coated samples on the thickness of the coating could be caused by cracking of chromium coatings (characterized by high brittleness) upon reaching a certain thickness and the accumulation of the corresponding level of internal stresses. This led to a sharp increase in the number of through defects in the coating against the background of the general regularity of a decrease in through porosity with an increase in the coating thickness and, accordingly, to a dip in the curve of the potential versus coating thickness. This assumption can also explain the shift in the maximum deviation of the potential towards a decrease in the coating thickness after annealing of the samples, since upon heating, the total stress of the coating increases due to the difference in the coefficients of thermal expansion of the coating and the base, and the critical stress values causing cracking of the coating are achieved at a smaller thickness.

The change in the ratio of the electrode potentials of the chromium coating and carbon steel after annealing of the samples in air can be related to the observed tendency for the potential of nickel coatings, as well as bonded copper, chromium, and other coatings, to be improved over time [78], both with polar and with the accumulation of products corrosion in the pores. In this regard, the oxidations of chromium and iron inevitably occurring during annealing can be considered as the cause of the change in the ratio of the potential of the chromium coating and carbon steel.

The analysis of the behavior and properties of coatings on carbon steel in various electrolytes makes it possible to determine the range of metals (taking into account their mechanical properties, testing as coatings, availability, etc.), which with sufficient probability could be considered as the most optimal for solving problems of corrosion protection of parts made of black and stainless steel.

Excluding from consideration of possible coating materials metals that have more positive stationary potentials in various electrolytes than iron (copper and some others, including, of course, noble metals), as well as those that, although they have large negative potentials, do not They are distinguished by the most sufficient corrosion resistance in harsh and especially harsh operating conditions (beryllium, magnesium, manganese, cadmium, zinc, aluminum), there remains a relatively small group of more or less widely used metals (alloys), which are more negative than that of iron, standard potential

These materials, apparently, include titanium, zirconium, chromium. Of this group of metals, titanium is the most accessible, has good mechanical properties (with an appropriate level of purity for impurities) and has

been sufficiently tested as coatings for various purposes. From zirconium, as a metal that is more negative than titanium, one can expect higher protective properties as an anode-type coating on the steels under consideration, although it is less common than titanium. Chromium is widely used as an anticorrosive coating on carbon steels, but it is highly fragile and prone to cracking, especially at increased thicknesses.

More negative than that of iron, the standard potential has a group of metals - stainless steel, nickel, molybdenum and some others. The high corrosion resistance of this group under conditions of wet corrosion and the presence of sufficiently aggressive chemical elements and compounds is due to the formation of dense, poorly conductive and stable films or adsorbed layers in such media, which inhibit oxidation processes.

Molybdenum has high rigidity, sufficient strength, high resistance in particularly aggressive environments. Its use as coatings has been less studied in comparison with the aforementioned metals, which can be associated with its lower availability and the need to use modern coating methods that have been developed only in recent years.

In [82], a comparison is made of the protective ability of coatings on steel 3 from some materials of the above group, namely: stainless steels 1.4563 and X10CrNiTi18-9, as well as titanium. Coatings with a thickness of 6–10 μm were applied by the vacuum-plasma method on samples with a roughness of Rz=40 and Rz=10 μm. Tests of the protective ability of the coatings were carried out by immersing the samples in various electrolytes (5 % solutions of sulfuric and orthophosphoric, as well as 10 % nitric acid) at room temperature.

Studies have shown that on samples with coatings made of steels 1.4563 and X10CrNiTi18-9, an intense dissolution of the substrate was observed in all investigated media, while the coatings of steel 1.4563 themselves are completely preserved, and coatings from steel X10CrNiTi18-9, are cracked. In samples with a titanium coating in a nitric acid solution, rapid local (at the pore sites) corrosion of steel was also observed, followed by the propagation of a corrosion center under the coating, while the protective film itself was completely intact. In solutions of sulfuric and orthophosphoric acids, a more uniform corrosion of steel along the pores in the titanium coating was observed. Thus, all investigated coatings proved to be cathodic in relation to steel 3, and the coating of steel 1.4563 even led to an acceleration of the overall corrosion rate of steel 3 (in terms of weight loss) up to 10 times. The presence of coatings made of steel X10CrNiTi18-9, practically did not change the total corrosion rate of steel 3 based on 72 hours of testing. Titanium coatings, in spite of the fact that they did not provide suppression of corrosion processes in the places of through porosity as a metal with a more negative standard potential than iron, nevertheless, on the whole, reduced corrosion losses by weight of samples up to 5–10 times in all studied solutions at test duration up to 144 hours.

In [83, 84], studies of the protective ability of a number of coatings (W, Mo, Nb, Ta, Cr) on structural steels in media that are mixtures of inorganic and organic acids and other chemical compounds were carried out. The highest corrosion resistance was shown by tungsten, molybdenum and tantalum coatings. The corrosion resistance of chromium coatings was several orders of magnitude lower than the resistance of the above-mentioned three metals. This is partly due to the increased porosity of chromium coatings in comparison with other coatings; on the whole, their stability correlated with the value of the normal electrochemical potential in the studied media. **Table 5.16** presents some data on their value, obtained in the work [84].

Table 5.16 Electrochemical normal potential of samples from different materials

Sample substrate/coating	USt 37-2/W	USt 37-2/Ta	USt 37-2/Mo	1.0503/without coating	Ti/without coating
Potential in corrosive environment (*v*)	0.19	0.21	0.12	−0.215	0.07

Comparative tests of coatings on samples with different roughness and obtained at different angles to the applied flow of the coating material confirmed that their protective ability correlates with porosity. The latter increases with an increase in the surface roughness and the angle of inclination of the sample with respect to the flow of the sprayed material.

Summing up this consideration, it seems reasonable to use a titanium coating as an initial (basic) coating option for testing, not excluding the possibility of using the above metals both independently and in combination with each other.

If everything related to the above coatings is considered from the standpoint of the choice of the method of their application, then the method should ensure the production of fortified coatings with the minimum possible number of through pores at the minimum possible thicknesses. In this respect, vacuum-plasma and plasma-chemical methods of coating are unmatched, providing strong adhesion, practically pore-free coatings on suitably prepared surfaces, starting from a thickness of 10–15 μm (for gas-phase plasma-chemical — from a thickness of ~1 μm) and practically from all metals, alloys and compounds. Obtaining non-porous coatings at the lowest possible thicknesses is not an end in itself or is dictated by economic considerations due to their cost, although the latter is also important. The thinner the coating, the easier it is to provide a combination of sufficient strength and its ability to deform under load without destruction and peeling, which is important when working with a coated material under conditions of heat changes, dynamic sign-changing loads, etc.

An important point, which largely determines not only adhesion, but also the protective properties of coatings, is the treatment before coating the surface of the protected material. In vacuum-plasma and plasma-chemical methods of coating deposition, surface finishing is carried out by exposing it to ions with energies from 5–10 eV to several keV. In this case, surface cleaning can be carried out both due to the occurrence of plasma-chemical reactions with reactive gases that form light compounds with the substrate material, and due to the processes of physical sputtering of the substrate material at ion energies above the sputtering threshold (> ~20 eV).

When using the method of vacuum-arc sputtering, which is most widely used in mechanical engineering for the application of coatings for various purposes, including protective ones, usually the surface treatment before coating is carried out with metal ions, from which the coating is then formed. This makes it possible not only to ensure effective cleaning of the surface from oxidizing films and other contaminants, but (with an appropriate choice of the cleaning mode) to form a transition layer in the surface layer to a depth of several to tens of microns with a varying concentration of coating metal atoms from 0 to 100 %, yes called a pseudodiffusion layer. The presence of such a transition layer allows for a smoother transition from the base material to the coating and reduces the stress level at the interface between the base and the coating due to differences in the coefficients of thermal expansion of the latter. There is one more point concerning the possibility of the formation of such a transition layer, which has practically not been reflected in studies yet, but, in our opinion, is quite important. This fundamental possibility of influencing the electrochemical potential of the surface of the material to be protected from the standpoint of proper matching of electrochemical potentials at the «coating — protected metal» interface, as shown above, is extremely important.

Considering the latter, when applying titanium coatings, cleaning the surface of steel parts «Press nut 457.81.027-1» with titanium ions may turn out to be suboptimal for several reasons. Firstly, titanium is more electronegative than iron, in order to increase the electrode potential of its surface during treatment with titanium ions and, thereby, to make the ratio of electrode potentials «protected metal-coating» more favorable. In addition, what is much more important, the treated surface of the part contains a large number of surface defects, which during ion-plasma treatment will be sources of increased gas release, which, due to interaction with titanium, leads to the formation of nitrides and oxynitrides in these regions. The sputtering rate of these titanium compounds is much less than the sputtering rate of pure metal and iron, including, which will complicate the cleaning of local surface defects of the part surface and subsequently cause increased defectiveness of the molded coating. In this regard, the preferable option may be the surface treatment of parts with molybdenum ions, since it forms weakly bound compounds with nitrogen, and with oxygen — volatile MoO_3 oxide,

i.e. preventing the cleaning of defective areas of the surface of the part. It can also be expected that cleaning the surface of carbon steel with molybdenum ions in modes that ensure the formation of a pseudodiffusion layer will enhance the electrochemical potential of the part material (molybdenum has a more positive standard electrochemical potential than iron) and, thereby, create better conditions for the formation of a coating namely the anode type.

Pretreatment of the surface with metal ions, which differs from the composition of the coating material, undoubtedly complicates the technological process of applying a protective coating. Therefore, if we restrict ourselves to the task of improving the quality of cleaning the surface of the part and preventing the formation of hard-to-spray compounds in the area of surface defects, then this can also be achieved by preliminary cleaning the surface with ions of an inert gas in a glow discharge, followed by a transition to treatment with titanium ions and applying a titanium coating. This technique insignificantly complicates the technological process and practically has little effect on the productivity and cost of the vacuum-arc coating operation.

5.1.2.4.1 Technological adaptation of coating conditions

When applying a coating to specific products, a number of issues are resolved, related both to the choice of the design of the tooling for fixing the products in the coating chamber, and to the preliminary surface treatment and the choice of the modes of the coating process, which together should provide the necessary properties of the coating. given parameters of the original product (base hardness, uncoated surface areas, etc.).

Press nut 457.81.027-1 has an oxide coating on the outside, the inner surface of the threaded nut is phosphated. The hardness of the nut material is 255–302 HB. When applying an additional protective coating, changes in the state of the thread surface are not allowed, the stiffness of the steel must remain within the above limits.

For coating, nuts were obtained that went through a full technological cycle of manufacturing, including their oxidation and phosphating, as well as nuts that did not undergo the last two treatments. Some of the supplied nuts were already in use. Accordingly, the initial surface of the nuts to be coated was extremely varied: relatively clean, after mechanical operations, its manufacture; oxidized without visible friable corrosion products; the surface with a significant number of areas with friable corrosion products on the nuts in use or were not subjected to oxidation, but remained in the warehouse for a long time. Common to all nuts was the presence of surface cavities, streaks, nicks and other surface defects on the lateral faces of the nut that were not machined during their manufacture. This state of the surface significantly complicates the application of a protective coating and is unacceptable for a number of coating technologies. However, taking

into account the desire not to introduce additional operations into the existing technological cycle of manufacturing the nut, except, in fact, the very operation of coating, so that there are no real additional measures to reduce the level of defectiveness of the coated surfaces. This prevented the development of «individual» surface preparation of each product before coating, depending on its initial state, which could include the operations of digestion and ultrasonic washing, treatment in a gas discharge plasma at different pressures and different potentials, as well as treatment with ions of various metals from vacuum plasma arc discharge.

To fix the nuts in the coating chamber, a planetary-type tooling was made, which made it possible to obtain coatings uniform in thickness on specified surfaces, prevent coating on the nut threads and uniform heating of the coated surfaces during coating.

The issue of thermal conditions during preliminary ion-plasma treatment of a product and subsequent formation of a coating is one of the important points in ion-plasma technologies. In some cases, the permissible heating temperature is limited by the properties of the article to be coated, in particular, in order to prevent a decrease in the strength of the article material. At the same time, properties such as adhesion, coating density, internal stress level and a number of other characteristics are highly temperature dependent. The implementation of their optimal values requires elevated process temperatures or is easier to achieve at them (the requirements for the «cleanliness» of the vacuum conditions of the process and the degree of preliminary cleaning of the product surface become less stringent, the boundaries for the permissible densities and energies of the ionic component in the sprayed substance flow are expanding, etc.).

In this regard, the modes of preliminary ion-plasma treatment of the surface of the nuts and the application of coatings on them were worked out, which ensured the production of serfs, without chips and peeling of coatings at temperatures not higher than 190–240 °C. This temperature was kept within these limits due to the pulse mode of the ion-plasma treatment process, limiting the rate of coating deposition and the energy of the ionic component in the flow of the sprayed substance. Titanium Ti2 was used as a coating material.

5.1.2.4.2 Obtaining experimental coated parts

According to the worked out modes, a pilot batch of products with coatings was obtained, which differed in the initial state and processing before applying the coating. The range of coating thickness was selected in the range of 10–20 μm and was set by the deposition time based on the data on the deposition rate determined on the witness samples in the specified modes. Data on prototypes of nuts are given in **Table 5.17**.

Table 5.17 Summary data on the pilot batch of products «Press nut 457.81.027» with protective coatings

No. sample	Pre-treatment					thick-ness, μm	initial state
	Chem. diges-tion	ultra-sonic wash-ing	plas-ma gas dis-charge	Mo ions in sat-uration mode	Ti ions in heating mode		
10	+	+	+	–	+	18	oxides, after operation
11	–	+	+	–	+	18	no oxides
12	–	+	+	–	+	18	no oxides
20	+	+	+	–	+	15	oxides, after operation
21	+	+	+	–	+	15	oxides, after operation
22	+	+	+	–	+	15	oxides
30	+	+	+	+	+	18	oxides
31	–	+	+	+	+	18	no oxides
32	+	+	+	+	+	18	no oxides
40	+	+	+	+	+	10	oxides, after operation
41	+	+	+	+	+	10	no oxides
42	+	+	+	+	+	10	no oxides

The obtained pilot batch of products with protective coatings was submitted for testing in order to obtain data on the protective ability of the coatings.

5.1.2.4.3 Results of accelerated corrosion tests of coated parts

In order to select the optimal solutions to protect the product «Press nut 457.81.027-1» from corrosion under operating conditions with high values of humidity and temperature, accelerated corrosion tests of parts were carried out.

Pressure nuts 457.81.027-1 were tested, their steel 1.0511 was made and heat-treated for hardness HB 302...255, with an experimental protective coating in the amount of 12 pieces.

Corrosion testing of pressure nuts 457.81.027-1, with an experimental coating was carried out in a heat and moisture chamber — thermostat G-4. The basis was taken by GOST 9.308-85 (method No. 6), which provides for testing metal and non-metallic coatings at elevated values of relative humidity and air temperature with periodic moisture condensation.

Cyclic tests with continuous cycles of 24 hours each. The parts were placed in a chamber and kept at a temperature of 50±2°C for 7 hours, then the heating was turned off until the end of the cycle. The preset temperature in the chamber was maintained automatically, the relative air humidity was 97±3 %. Every hour of testing at an elevated temperature, a fan was turned on for 10 minutes to evenly distribute steam inside the chamber. During the tests, the parts were periodically examined to assess their corrosion damage, determined as a percentage of the total area of the applied coating.

The total test time was 500 hours, of which the parts were kept at a temperature of 50±2 °C for 130 hours. After the end of the tests, an assessment was made of the degree of corrosion damage to the parts.

An external review of the test coated parts showed that corrosion occurred in the main boundary of the hexagon in the form of individual spots, while there was no corrosion on the end surface of the nuts. The irregularity of corrosion damage to the edges of the lateral surface of the nuts is associated with the presence of coating defects such as pores, the appearance of which could lead to an unsatisfactory condition of the original surface. According to the technical documentation, the boundaries of the hexagon are not processed (they remain in the draft version), and the rest of the surface after the manufacture of the nut should be responsible for the cleanliness of processing Rz 40.

The presence of coating defects is confirmed by the results of a metallographic study carried out selectively on individual nuts (No. 12, 22 and 31).

To assess the quality of the application of an experimental protective coating, the study was carried out on samples cut from nuts in the region of the edges and end surface. As a result, it was found that the experimental protective coating is intermittent and uneven in thickness on the edges (**Fig. 5.13**) and continuous and uniform on the end surface (**Fig. 5.14**).

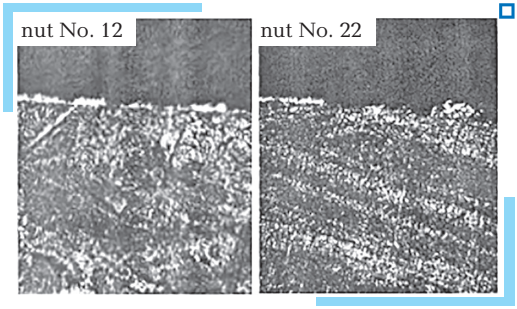

Fig. 5.13 Appearance of the coating on the edges of the nuts (cross section) (×100)

Fig. 5.14 Appearance of the coating on the end surface of the nut No. 31 (×100)

The results of assessing the degree of corrosion damage to parts during testing are presented in **Table 5.18**. The results obtained show that the

degree of surface corrosion damage for most parts after 24 and 500 hours of testing is practically the same. This may be due to the fact that areas of the surface that are not protected by the coating are exposed to corrosion, and over time these processes develop very slowly only in these areas.

Table 5.18 The area of corrosion damage to parts after accelerated testing (% of the total surface of the coating)

No.	Test time, h					
	24	100	200	330	400	500
10	0.1	0.1	0.7	0.75	0.75	0.8
11	2.5	2.9	20	221	21	22.2
12	1.9	2.9	6.0	6.7	10.5	13.5
20	7.0	7.0	7.4	7.4	7.4	7.4
21	17.2	17.2	17.8	17.8	17.8	17.8
22	0.1	0.1	0.1	1.2	2.5	3.4
30	12.5	12.5	13.9	14.5	14.5	14.5
31	8.8	9.4	10.6	11.7	12.2	12.2
32	0	0.1	0.3	0.7	0.7	0.7
40	4.4	4.4	5.9	6.2	6.2	6.7
41	1.3	2.7	5.5	5.5	5.5	5.5
42	43	48.5	49.2	49.2	49.2	49.2

Pretreatment of parts, including chemical digestion, ultrasonic cleaning, the action of a gas discharge plasma, the application of molybdenum ions in saturation mode did not affect the corrosion resistance of the surface of the parts.

Tables 5.19 and 5.20 show data on the dependence of the degree of corrosion damage to parts from their initial state and the thickness of the applied coating.

The data show that oxidized parts have a lower degree of corrosion damage than non-oxidized ones. So, the average size of the area of corrosion damage in the first case is 7.5 %, in the second — 20.5 %.

The data presented in **Table 5.20** show that the dependence of the degree of corrosion damage of parts on the thickness is not observed.

It should be noted that previously conducted similar tests of uncoated nuts (serial oxidized) showed that corrosion damage to the metal is observed after 24 hours of testing. Attempts to protect the surface by applying PF-170 varnish did not give positive results, during the tests the varnish film was swollen and after 72 hours the area of corrosion damage reached 20 % of the total area.

Table 5.19 Dependence of corrosion damage on the surface of the nuts on the initial state

Initial state	No.	Area of corrosion damage, %
Unoxidized	11	22.2
	12	133.5
	31	12.2
	41	5.5
	42	49.2
Oxidized	10	0.8
	20	7.4
	21	17.8
	22	3.4
	30	14.5
	32	0.7
	40	6.7

Table 5.20 Dependence of corrosion damage on the surface of the nuts on the thickness of the coating

No.	Coating thickness, μm	Area of corrosion damage, %
40	10	6.7
41	10	5.5
42	10	49.2
20	15	7.4
21	15	17.8
22	15	3.4
30	18	14.5
31	18	12.2
32	18	0.7
10	18	0.8
11	18	22.2
12	18	13.5

5.1.2.4.4 Study of the effect of titanium coating on the fatigue strength of samples

To assess the effect of a protective anticorrosive titanium coating under specific conditions of its application and surface pretreatment on the fatigue strength of parts, specimens were tested studies of the pressure nut 457.81.027.

Samples of steel 1.0402 were made in quantities of 10 pieces. respectively uncoated and titanium coated.

The tests were carried out on a Brüel & Kjaer vibration stand in the mode of resonant vibrations in the first bending form. For this purpose, sample 1 was installed in a special strain gauge device 2 (**Fig. 5.16**) and the full-scale calibration of strain gauges 3 was carried out according to the bending moment acting on the sample.

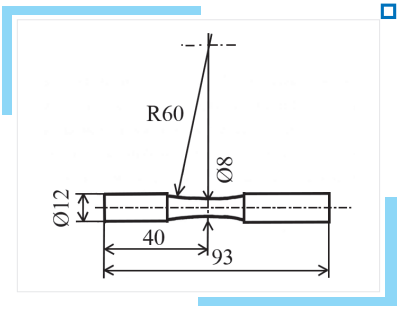

Fig. 5.15 Test sample

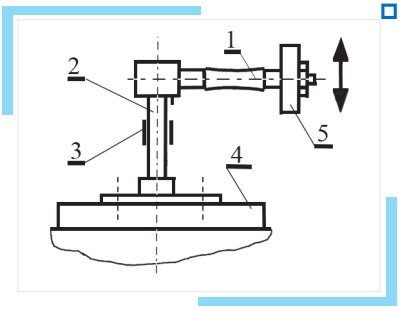

Fig. 5.16 Scheme of testing samples

Then, the device with the tested sample was mounted on the working table 4 of the shaker. After launching the test bench, the resonance mode was set at the first bending frequency. The value of the required load was selected by changing the mass of the load 5 fixed on the cantilever side of the sample.

Four samples (3 uncoated and 1 — with a coating) were used to select the test mode to be determined based on the destruction of uncoated specimens with an operating time of 0.5...1.0 million cycles.

The test results of other (test) samples are presented in **Table 5.21**.

Table 5.21 The test results of other (test) samples

No. of sample	Operating time, thousand cycles	No. of sample	Operating time, thousand cycles
	Samples without coating		Samples with coating
4	762	3	1120
6	435	5	526
8	599	7	3764
1	370	9	1812
12	664	11	3516
14	870	13	3020
16	1196	15	4547
f' av., thousand cycles	690	17	551
—	—	18	4685
—	—	f' av., thousand cycles	2616

Fig. 5.17 Power nuts with developed titanium anticorrosive coatings after prolonged corrosion exposure (in the center, for comparison, a heavily corroded uncoated part)

It follows from the table that specimens with an anticorrosive titanium coating, which have the smallest value in terms of the number of loading cycles, are within the operating time of uncoated specimens. At the same time, the value of «f' av., thousand cycle» for specimens with an anticorrosive titanium coating is more than three times higher than that for specimens without a coating.

Thus, the anticorrosive titanium coating of the fatiguing strength of specimens made of steel 1.0402, at least, does not decrease, but in most cases it significantly increases.

Conclusions.

1. Experimental protective titanium coating possesses high corrosion resistance at elevated temperatures and relative humidity, as evidenced by the absence of corrosion damage on the end surface of all tested nuts.

2. Anticorrosive titanium coating does not reduce the fatigue strength of specimens made of steel 1.0402.

3. The developed titanium protective coating is recommended for implementation on parts with a surface roughness of not more than Ra 6.3.

5.2 Coatings to improve the performance of cutting and shaping tools

The problem of a significant increase in the efficiency of forming parts, especially precision, aerospace, aggregate construction, engine building, power and mechanical engineering and their resource and reliability is becoming increasingly important today, since the resource of aircraft units, for example, should be equal to the resource of the airframe, and the resource of space units — decades. Plunger assemblies and other critical parts require dimensional accuracy of manufacturing no more than 1 μm and surfaces with high tribological properties. Therefore, the efficiency of forming parts, containing the accuracy of the size and shape of the part, surface quality and processing productivity, requires a cutting tool (CT) with extremely high properties. On the other hand, the requirements to improve the tribological properties of the surfaces of parts, in addition to nano-precision, also require the creation of a surface layer with unique properties.

Today there are many methods of strengthening the surface layer of cutting tools and machine parts — vacuum arc coatings, ion implantation

and ion alloying; electron beam, laser processing (strengthening); CVD methods and others, allowing to increase the resource of work of both CT and machine parts. All these technologies independently reached saturation in terms of the possible obtained physicomechanical characteristics (PMC) of materials, but when the conditions for obtaining nanostructures (NS) in the surface layer are created, a new impetus arises for their development.

One of the main drawbacks of existing technologies is the simultaneous failure to take into account the entire complex of problems arising in the processing of both CT and machine parts. These problems include unresolved issues: the most effective conditions for creating emergency situations, adhesion interaction of CT materials and coatings with the processed material, adhesion between the coating and the base material of CT and machine parts, stress state in the contact zone of the coating and the base material, measures to reduce the release from the material of CT (and parts) of alloying materials due to diffusion, design of the composition of the material of the cutting tool, taking into account the possibility of creating an emergency situation both in the surface layer and in the volume of the product for each individual composition of the material.

A significant increase in the PMC of materials is a major challenge for modern mechanical engineering.

5.2.1 The concept and principles of designing parts for aggregate and mechanical engineering, their effective shaping by cutting tools with nanostructures

In works [135–150], a wide range of theoretical and experimental studies was carried out to develop the concept and principles of creating highly efficient high-resource reliable precision parts and cutting tools based on obtaining nano-precision, creating nanocoatings, nanostructures and creating integrated methods and technological processes. fluxes, PVD, CVD, magnetron and femtosecond laser radiation

The concept for parts and tools is based on the following principles:

1. The maximum resource of aggregates, parts and tools is impossible without the creation of nanostructures and nanocoatings.

2. The maximum adhesion interaction, and, consequently, the effective operation of coatings on parts and CT with coatings will be ensured with a maximum difference in the electronegativity of the coating materials and the part (tool), which will also provide maximum adhesion, and, consequently, effective and long-term operation of both tools and parts of the units, and the tools themselves.

3. For blade processing, it is necessary to create coatings that provide a minimum adhesive interaction between the tool and the part.

4. Nano-precision should be observed. Technological criteria should be taken as a criterion for the performance of a tool: critical roughness, ac-

curacy of size or shape (for example, the maximum permissible taper, barrel shape, etc.). So, with an accuracy of manufacturing parts of 1...2 μm, the roughness of the blade edge should be 200...300 nm.

5. The criterion for the effective application of the coating will be the following condition: the grain size in the coating, as a rule, should be smaller than in the base material of the tools.

6. Diffuse wear associated with the diffusion of alloying elements from the material of the tool or part can be reduced through barrier coatings or nanostructured layers on the surface.

7. When choosing multilayer and monolayer coatings, it is necessary to take into account the stress state in the zone of transition from one coating to another and from the coating to the base material.

8. The bending strength of the cutting part of the tools, as well as of the elements of parts working in bending and fatigue strength, should be evaluated taking into account the increase in physical and mechanical characteristics due to reinforcement or coating.

The possibility of surface modification by ion beams, magnetron and laser radiation of the femtosecond range by obtaining nanostructures using femtosecond laser radiation has been proved, and a method for establishing technological parameters has been developed.

On the basis of the model of ion irradiation, the technological parameters of ion fluxes are determined, at which stochastic values of thermophysical and thermomechanical characteristics can be used, if necessary, the thermophysical and thermomechanical characteristics can be calculated using the quantum-mechanical approach. These parameters are summarized and given for a wide range of tools from hard alloys, high-speed steels and polycrystalline superhard materials, as well as parts from aluminum, titanium and magnesium alloys.

It is shown that during the action of ions on the magnesium alloy and hard alloy HS420 with different energies up to 10 %, the stochastic method can be used to determine the thermophysical and thermomechanical characteristics, and the errors for heavy ions (zirconium and hafnium) will not exceed 10^{-1}, under the action of light ions (nitrogen, aluminum, oxygen and yttrium), the error will not exceed 20–25 %. The obtained dependences of the temperature stresses at the boundary of the NS formation zone and the maximum temperature stresses on charge and energy allow for the selection of a wide range of ions C, B, N, Al, Ti, V, Cr, Fe, Ni, Co, Y, Zr, Nb, Mo , Hf, Ta, W, Pt and technological modes when processing steel.

For the selected materials, the dependences of the volume of NS grains on the heat flux density, the time of action of laser radiation and the size of the region of interaction of the heat flux with the material are obtained, and technological parameters are provided, at which it is possible to create NS.

The possibility of significantly increasing the efficiency of shaping due to the design of the composition of hard alloys on the basis of the

proposed concept and principles of the formation of effective cutting tools and high-resource parts has been experimentally proved. It has been proven that the most influential factor in preventing abrasive wear or reducing it is obtaining a grain size of 10...40 nm in the coating or base CT material.

The dependences of the PMC of the X-ray materials and parts on the grain size have been obtained experimentally. For turning and milling, the dependence of the efficiency of shaping, stability of CT and processing productivity on the grain size is obtained.

When using femtosecond laser radiation to obtain nanostructures, the following principles should be adhered to:

1. It is necessary to achieve the minimum spot size of the laser radiation action on the processed material. This leads to obtaining a regime with the lowest possible energy consumption, and at a high frequency of laser operation, the processing performance can be quite high.

2. It is possible to choose technological modes when, due to operation in the main temperature range (1500...500 K) and at rates of temperature rise of more than 107 K/s, modes with lower energy consumption are realized.

Based on the implementation of the concept and principles of creating high-resource parts and ensuring their effective shaping of tools and parts with nanostructures and nanocoatings, a complex of effective ion and laser integrated technologies has been created.

This makes it possible, from a scientific standpoint, to select technological modes of plasma-ion and femtosecond laser systems for obtaining nanostructures. The obtained ratios of the components of the alloys can realize the grain size, which provides the maximum possible efficiency of tool shaping and a high resource of parts for aggregate and mechanical engineering.

It has been proven that modified HG40 hard alloys provide a larger volume of material removed during the RI stability period (when milling the HG40 titanium alloy at a cutter speed n=300 rpm, the material volume is removed for the CT stability period 87–104 mm^3, 2 times more than at traditional processing), while productivity is increased.

The conditions for the combination of layers in coatings have been determined, which provide insignificant differences in temperature stresses during the transition from coating to coating and from coating to the main material of the CT or part (no more than 30 %), which makes it possible to reduce its delamination.

When assessing the adhesive interaction of the materials under study (according to the difference in electronegativity (DEN), it was determined that the material of the CT and coatings with the processed material have low adhesion at a large DEN and a large one at a small DEN).

The obtained dependences of the roughness on the feed and cutting speed make it possible, according to the required roughness, to select cutting modes for the CT with and without coating and provide minimum power consumption.

For a wide range of difficult-to-machine alloys and hardened steels, the dependence of the EF(G) of the part on the grain size and wear along the flank surface of the CT hz was investigated, which makes it possible to predict the resource of the CT when machining with hard alloys (HG40, HS123, HS420, etc.) with one- and two-layer coated. It is proved that a two-layer coating has low adhesion of Al_2O_3 to titanium alloy BT22(Mo 4–5.5 %, V 4–5.5 %, Al 4.4–5.7 % Cr 0.5–1.5 %) and is an order of magnitude higher than the efficiency of shaping.

For turning and milling, the dependence of the shaping efficiency, tool stability and processing productivity on the grain size is obtained. It has been proven that the most influential factor in preventing abrasive wear or reducing it is obtaining a grain size of 10...40 nm in the coating or base material of the CT. A combination of coating layers has been invented, for which the operating conditions are most favorable in dynamic and stationary modes, as well as in mixed operating conditions of tools in the zone of transition from one coating to another and during the transition from the coating to its base material (the principle of tool design). The technological parameters of processing are found, at which the maximum value of the volume of the removed material is realized during the period of stability. This allows this value to be used for efficient machining of BT22 titanium alloy with the first modified HG40 alloy. At the same time, for the second modified HG40 alloy at 300 rpm (4.7 m/min), it is possible to increase the volume of removed material during the stability period up to $8.7 \cdot 10^4$ mm^3. The studies carried out make it possible to predict the volume of steels and cast iron removed during the period of stability, the CT stability and the processing efficiency depending on the grain size in the coating. It is important to select the finish and coating mode for CT. It is proved that when processing cast iron, an important characteristic is the adhesive interaction of the coating with the material being processed, which ensures the value of the volume of the removed material during the stability period of the order of $(1.3...1.8) \cdot 10^7$ mm^3. In this case, the maximum durability of 19...14 thousand s is realized.

The efficiency of shaping and the performance of hard alloys with coatings in the treatment of hardened steels is determined by the grain size in the coating, and a smaller grain size usually (but not always) corresponds to a more efficient shaping and its performance. A decrease in microhardness with an increase in grain size was obtained for HG40, Sandvik Coromant, HS420 coated with 0.2HfN + 0.8ZrN. Microhardness of Sandvik Coromant with a two-layer coating Al_2O_3 + (0.2HfN + 0.8ZrN) changes slightly with grain growth. Experimental studies prove the possibility of obtaining nanostructures in a 0.2HfN + 0.8ZrN coating. The possibility of predicting the grain size taking into account its increase depending on the temperature during cleaning and coating is shown. Comparison of the results of the theoretical calculation and experiment is in good agreement, the deviation is from 16 % to 29 %, from which it can be concluded that the theoretical model makes it possible to obtain this grain size by applying a coating of considerable thickness (10 μm). This can improve the efficiency of tool shaping.

It is experimentally shown that the creation of nanostructures on tools increases the efficiency of shaping by 2.7–3.5 times, with a submicrostructure grain, the efficiency increases only 1.8 times. It is shown that it is possible to predict and sustain a coated plate under specified cutting conditions without a full-scale experiment for hardened steels 66Mn4 and 41Cr4, as well as heavy-work steel 16Cr3NiVWMoNb. Under heavily loaded cutting modes (t=1 mm, S=0.5 mm/rev, V=30 m/min), thermal spalling or elastic spalling of the cutting blade is realized, which does not allow using these modes for processing steel 16Cr3NiVWMoNb. Dependences for roughness Ra and Rz are obtained depending on feed and cutting speed. To obtain the required roughness, it is necessary to select the cutting modes that provide it, as well as to obtain the roughness according to the designated cutting modes.

The life tests of aviation hydraulic units showed that for the EN AW-AI high-temperature alloy under conditions of extreme lubrication, the serviceability increases by 20–30 times, and the wear decreases by 4–5 times. This made it possible to increase the resource of parts to the level of the requirements of modern world needs.

5.2.2 Improving the characteristics of cutting and shaping tools

5.2.2.1 Wear-resistant reinforcing coatings to enhance cutting tool performance

On the basis of the developed concept of creating high-life parts, a wide range of coatings and nanocoatings Avinit-TiC-TiN, Cu-MoS_2) with high tribological properties due to a low coefficient of friction and high microhardness has been theoretically justified and practically obtained.

Ion-plasma coatings with wear-resistant properties, obtained by vacuum-arc deposition, are widely used in mechanical engineering, aircraft construction, metallurgy and other sectors of the national economy when creating structures with protective, strengthening, wear-resistant, erosion-resistant coatings, in particular, to increase the stability of cutting, punching tool.

Known multicomponent wear-resistant coatings and methods of their application to a metal substrate, in particular, coating Ti-N, Zr-N, Cr-N, Ti-CN, Ti-Al-N, Ti-Cr-N, Ti-Zr-N, Ti-Al-VN, Cr-Al-N, obtained by vacuum arc deposition or magnetron sputtering.

There is a known method of vacuum ion-plasma coating on a substrate [151] in an inert gas environment, including creating an electrical potential difference between the substrate and the cathode and cleaning the substrate surface with an ion flow, reducing the potential difference and applying the coating by subsequent annealing the coating by increasing the potential difference to the substrate to 1250–1500 V. When cleaning the surface of the substrate, the ion flow and the flow of the evaporated material

going from the cathode to the substrate are screened, cleaning is carried out with ions of an inert gas, after cleaning the screens are removed and the coating is applied, followed by annealing repeatedly to the required thickness. In this case, the substrate is made of a highly alloyed nickel-based alloy, and nickel is used as the cathode material, along with preliminary cleaning and activation of the substrate surface with ions of an inert gas, increases the adhesion strength of the coating to the substrate.

Known wear-resistant ion-plasma coating based on chromium nitride, applied to a metal product [152] containing vanadium in the nitride (Cr-V) N with the following ratio of chromium and vanadium at %: Cr 28–50, V 50–72.

The coating can be used to increase the wear resistance of cutting and technological tools having a relative wear resistance of 1–3.08, which varies depending on the composition.

A known method of forming a wear-resistant coating on the surface of structural steel products [153], including ion-plasma nitriding in a reactive gas-nitrogen medium, cleaning the surface of the part and applying titanium nitride from the plasma phase. In the known method of nitriding, surface cleaning and the application of titanium nitride is carried out in one vacuum chamber in the plasma of an arc and gas discharge with a strained cathode in a single cycle, forming a three-layer structure on the surface of the parts. In this case, nitriding is carried out using a gas-discharge plasma generator with a strained cathode at a reactive gas pressure of $5{\cdot}10^{-3}-2{\cdot}10^{-2}$ mm Hg, a negative bias voltage on the parts of 300 – 1000 V and an ion current density of 2–8 mA/cm^2 for 30–90 minutes, cleaning is carried out in the plasma of an inert gas – argon at a pressure of $3{\cdot}10^{-4}-7{\cdot}10^{-4}$ mm Hg. and a current density of 3–5 mA/cm^2, also created by a gas-discharge plasma generator, and titanium nitride is applied at a rate of 2 μm/h for 60–90 min with a negative bias voltage on the part of 300–600 V and simultaneous operation of the gas-discharge plasma generator and an evaporator that promotes a more complete course of reactions of synthesis of titanium nitride on the surface of the product. The formation of a three-layer structure, including the first dispersion-hardened nitrided sublayer of the steel base, the second sublayer of solid iron nitride and the third layer (coating) of titanium nitride, provides a smoother transition of hardness from the base to the coating, is crystallographically similar to the second sublayer and is applied. and, ultimately, greater adhesion of the coating to the article and the operability of the entire article-coating composition.

It is also known a wear-resistant ion-plasma coating based on a complex nitride of titanium, aluminum and chromium (TixAlyCrz) N, applied to a metal or ceramic product [154], in which the chromium (z) content depends on the aluminum and titanium content and ranges from 1 up to 1/7 to 1/5 (xy), while $0.05 \le x \le y$, $x/y < 1$.

The coating described above has increased wear resistance.

The known method of combined vacuum ion-plasma treatment of the tool [155]. The method includes processing an article in a gas-discharge

plasma containing argon and hydrogen ions, carrying out its diffusion saturation and applying a wear-resistant coating, and the processing of the article and diffuse saturation are carried out simultaneously in a gas-discharge plasma, additionally containing carbon or carbon and nitrogen ions.

The use of a gas-discharge plasma, additionally containing carbon or carbon and nitrogen ions, makes it possible to form dispersed carbides or carbonitrides in the surface layer of the product in the case of diffuse saturation and, thus, to increase its hardness. Additional bombardment by ions of an inert gas (argon) contained in the gas-discharge plasma created by a plasma generator with a heated emitter increases the diffusion rate and, therefore, increases the thickness of the hardened surface layer.

Known is a multilayer coating containing titanium nitride layers [156], in which titanium nitride is located on a nitrided layer obtained in the usual way and alternates with AlCrN layers 10 to 100 nm thick with a total thickness of 19 μm.

Such a coating provides high rigidity of the coatings and their good adhesion to the substrate to be coated, which makes it possible to increase the wear resistance of the cutting tool.

The work [157] presents the technologies and equipment developed by STC «Nanotechnology» for the deposition of multicomponent (monolayer, multilayer, nanostructured, gradient) Avinit coatings. A series of VPN coatings has been developed for the problems of strengthening cutting tools.

The main characteristics of coatings, conditions of application of cutting tools with VPN-coatings are presented. Comparative production tests confirm the high performance of VPN-coated cutting tools.

The control of the main technological parameters of the processes of applying such coatings and the registration of parameters is carried out using a special automated system.

The coatings have a nanolayer structure and can consist of layers 5–10 nm thick based on aluminum, titanium, chromium, zirconium, molybdenum and their compounds with nitrogen, carbon, oxygen in various combinations.

Key features of VPN coatings:

- microhardness, MPa — 25000–45000;
- coating thickness, μm — 1–5;
- oxidation temperature, T, °C — up to 900;
- coefficient of friction — 0.3–0.64;
- high adhesion of the coating to the substrate;
- preservation of the original surface roughness;
- low-temperature coating processes ($T \leq 200$ °C).

Each type of coating has a specific composition and structure that determine the properties of the coating and its purpose.

Recommended conditions for the use of cutting tools with VPN coatings of different types, developed by the Scientific and Technical Center «Nanotechnology», are given in **Table 5.22**.

Table 5.22 Types of VPN coatings, their properties and conditions of use

Type of a coating	Structure	Foreign analogs	Properties			Recommendations
			H_v, kg/mm^2	Friction coef.	T oxid, °C	
VPN-1	TiAlN monolayer	Duracut (FRAISA), TiAlN (HANITA), Universal (PLATIT), TiAlN (TM Ion Bond)	3300	0.55	800	For high-speed finishing or roughing in stable conditions without cooling or with fog cooling
VPN-1m	TiAlN Multilayer	TiAlN (HANITA), Universal (PLATIT)	2800 – 3000	0.5	800	Same as VPN-1 for intermittent cutting
VPN-2	AlTiN monolayer	Unicut-Duro (FRAISA), TiAlN (TM Ion Bond)	3500	0.6	900	For high-speed dry processing of particularly hard materials
VPN-2m	AlTiN Multilayer	Coverage of the company CARLOY Inc.	3300	0.4	900	Same as VPN-2 for intermittent cutting
VPN-1n	TiAlN nanostructured	Futura-Nano (BALZERS)	3500	0.3	800	For high-speed dry processing of especially hard materials
VPN-2n	AlTiN nanostructured	Futura-Nano (BALZERS)	4000	0.35	900	For high-speed dry processing with the increased temperature stability at processing of especially hard materials
VPNM	TiN Multilayer	Z-Coat (HANITA)	2500	0.4 – 0.5	600	Wide range of the processed materials, increase in processing speed
VPN-02n	AlTiN nanostructured	μAlTiN (PLATIT)	4500	0.3	900	For high-precision machining of particularly hard materials
VPNM-f	TiAlN + AlCrN Multilayer	Alcrona (BALZERS)	2500 – 3000	0.3 – 0.4	700	reduced friction, increased machining speed

Comparative production tests of cutting tools with VPN coatings in an industrial environment have been conducted.

5.2.2.1.1 Application of coatings on the tool of Motor Sich JSC (Zaporizhzhia)

Work was carried out to apply Avinit nanocomposite ion-plasma hardening coatings on cutters manufactured by FRAISA (Switzerland), which are used at Motor Sich JSC for processing (high-speed milling) of molds made of tool steel such as типу 150Cr14, X165CrMoV12, 55NiCrMoV6, with hardness in the range of HRC 50–60.

The material of the cutters is super fine-grained carbide.

Table 5.23 Output cutters parameters

No.	Designation of a mill	∅, mm		R, mm	Modes of cutting for finishing		
			average		Rotations (rpm)	Feeding (mm/min)	Depth of cutting (a_p, mm)
1.1	5280.140	1.962	2	1	42000	1680	0.05
1.2		1.959					
1.3		1.965					
2.1	5280.220	3.96	4	2	42000	4200	0.1
2.2		3.968					
2.3		3.97					
3.1	5280.300	5.968	6	3	42000	5040	0.2
3.2		5.964					
3.3		5.967					

Table 5.24 Coating parameters of cutters

Designation of a mill	No.	Composition	Color	Time, t_Σ, min
5280.140	1.1	Avinit-1 Ti-Al-N	Brown with a violet shade	45
	1.2	Ti-Al-N	Brown with a violet shade	45
	1.3			
5280.220	2.1	Avinit-2 Al-Ti-N	Dark gray with a blue shade	45
	2.2			
	2.3			
5280.300	3.1	Avinit-1n Ti-Al-N with partial separation on Ti and Al	Brown with a violet shade	25
	3.2			
	3.3			

The tests were carried out on milling cutters manufactured by the «FRAISA» company, obtained in a set with the HSM-600 machine. In the initial state, the cutters were not coated. Nanocomposite ion-plasma coatings Avinit were applied by the STC «Nanotechnology» enterprise, Kharkiv, according to the developed technologies.

The tests were carried out by comparing the magnitude of wear on the effective diameter of coated and uncoated cutters operating under the same conditions on a workpiece made of 45 steel with a hardness of 45 HRC.

The amount of wear of the cutting edge H was determined using a microscope at a magnification of 30 times.

The test results of the «FRAISA» cutter are shown in **Table 5.25**.

Table 5.25 Test results of cutters «FRAISA» with nanocomposite ion-plasma Avinit coatings

Cutter designation	Coating	Cutting modes			Operating time, min	Wear rate
		Rotation (rpm)	Feed (mm/min)	Cutting depth a_p (mm)		
5280.140 ∅2 R1	Avinit-1 TiAlN	42000	1680	0.04	53	0.04
	Uncoated	42000	1680	0.04	53	0.12
5280.220 ∅4 R2	Avinit-2 TiAlN	42000	4200	0.05	21	0.03
	Uncoated	42000	4200	0.05	21	0.08–0.1
5280.300 ∅6 R3	Avinit-1n TiAlN	42000	5880	0.12	30	0.05
	Uncoated	42000	5880	0.12	30	0.15–0.2

Comparative tests of carbide cutting tools in production conditions showed that at the same modes of high-speed milling, the wear of cutters coated with Avinit nanocomposite coatings is 2.6–4 times less than that of those not coated.

5.2.2.1.2 Application of coatings on the tool of SE Zoria-Mashproekt (Mykolaiv)

At the SE Zoria-Mashproekt, Mykolaiv, production tests of spherocylindrical cutters R15, reinforced according to the technology of STC «Nanotechnology», were carried out.

The coatings were applied to serially used cutters 9336–1239030 mm; *R* 15 mm; *Z*=6; material — 1.3243 (HRC66).

Test conditions:

1. Operation — milling the blade profile.
2. Equipment — machining center mod. 2204ВМ1Ф4.
3. Workpiece to be processed — straightener blade B90010160.

4. Material — ЕП479 (15Х16Н2АМШ).

5. Rake angle — γ=10°; back angle — α=12°.

6. Cutting modes: number of revolutions — n=200 rpm; feed — S=250 mm/min; processing depth — t=2...3 mm; cooling — oil coolant «Asfol-2».

Table 5.26 Test results of coated spherocylindrical cutters

Mill	Stability
Strengthened STC «Nanotechnology»	5...6 changes (about 45 hours)
Serially applied (not strengthened)	3 changes (about 24 hours)

As shown by the test results, the strengthening of serial tools such as spherocylindrical cutters 9336-1239 using the technology of the Nanotechnology Scientific and Technical Center (Kharkiv) provides an increase in tool life by 1.5...1.8 times with an increase in the quality of the processed surface.

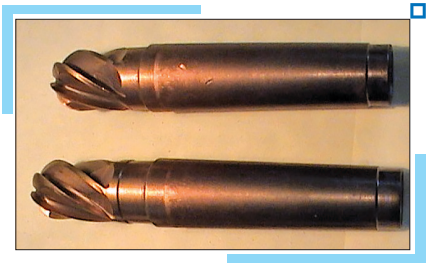

Fig. 5.18 Avinit coated cutters

5.2.2.1.3 Application of coatings on the tool of Illich Steel and Iron Works (Mariupol)

Avinit multilayer coatings have been applied to HG20 carbide inserts to determine improved tool performance in difficult conditions when machining welded pipe ends.

The plates were made at the V. Bakul Institute for Superhard Materials (Kyiv) in two modes:

- mode 1 — sintered in vacuum;
- mode 2 — sintered in vacuum and thermocompression treated (TCT) under argon pressure of 3.0 MPa.

On a part of the plates, multilayer protective coatings were applied from the Scientific and Technical Center «Nanotechnology», Kharkiv.

Comparative industrial tests were carried out at the Illich Steel and Iron Works in the pipe-welding shop when processing the ends of welded pipes (D_p 25–75 mm) made of steel USt 37-2 кп , where Russian-made uncoated HS123alloy plates are used for this operation.

Cutting conditions: processing the end of the welded pipe.

Cutting speed V=20–25 m/min; cutting depth t=3 mm.

The results are shown in the **Table 5.27**.

Table 5.27 Test results for coated carbide inserts

No.	Type and brand of alloy	Cutting resistance
1	HG20, vacuum sintered	170÷180
2	HG20, vacuum sintered with coating Avinit	350÷360
3	HG20, vacuum sintered plus thermocompression hardened	210÷220
4	HS123 uncoated	350÷370
5	Plates of the bucket company «Bucket» with coating Avinit	620÷630

As shown by the results of industrial tests, when processing the ends of welded pipes (∅=25–75 mm) from steel CT3KP in the conditions of production tests of cutting inserts made of HG20 alloy with Avinit multilayer coatings, cutting stability increases 2.6–3 times.

Production tests of cutting tools with VPN-coatings, applied using nanotechnologies, developed by the Scientific and Technical Center «Nanotechnology», have shown their high efficiency.

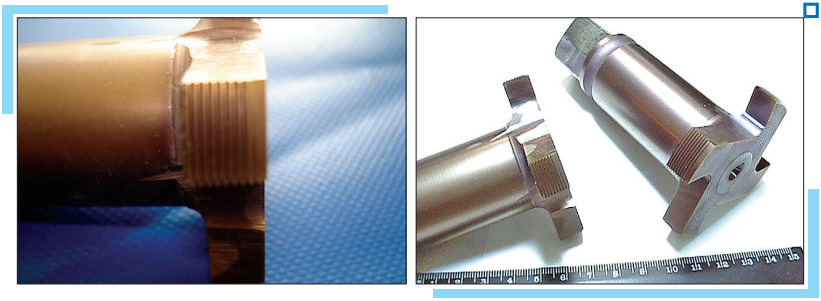

Fig. 5.19 Taps with Avinit coatings (State Scientific and Production Enterprise «Kommunar Association» (Kharkiv))

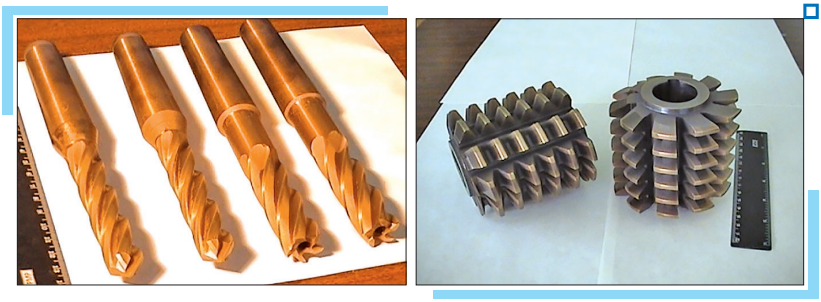

Fig. 5.20 Cutting tool with Avinit coatings («Plant named after Shevchenko», Kharkiv)

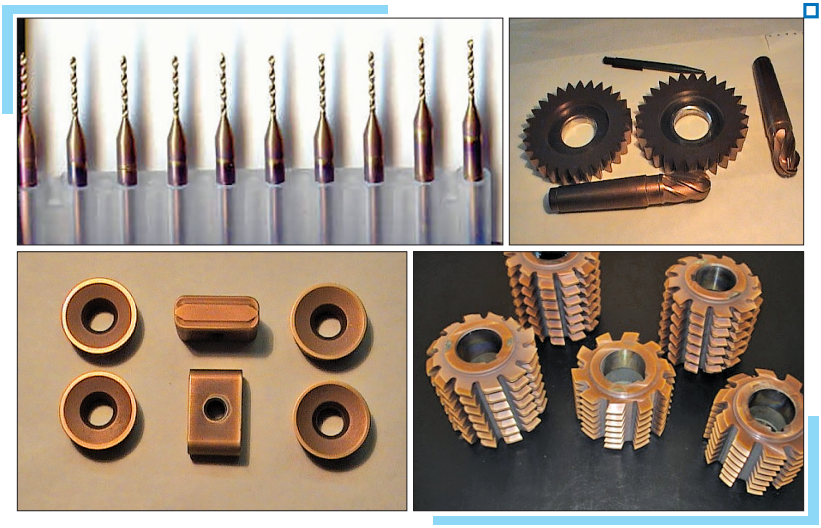

Fig. 5.21 Cutting tool with developed Avinit coatings

The use of Avinit hardening nanocoatings in batch production conditions increases the wear resistance of the cutting tool by 3–5 times.

STC has a positive experience in applying multicomponent coatings not only to the manufactured cutting tool, but also to the tool after regrinding, in particular. application of hardening coatings on reground standard all-metal carbide cutting tools of domestic and foreign manufacturers (FRAISA, HANITA, PLATIT, CARLOY, BALZERS, etc.). It is important to note that when applying VPN coatings, the radius of rounding of the cutting edge remains practically unchanged.

5.2.2.1.4 Reinforced tool for high resource cutting of wood and wood-based materials

Application of wear-resistant coatings on cutting tools is one of the most effective ways to dramatically increase the resource of tools for high-resource processing of cutting wood and wood materials and compliance with international standards.

Increased performance of the tool and improved quality of material processing are ensured by strengthening two-sided processing of the tool by applying wear-resistant coatings, which lead to an increase in the hardness of the tool surface, a decrease in friction forces in the contact between the tool and the processed material, and the absence of chip adhesion due to the antifriction and dielectric properties of the coating.

Reinforcing coatings were applied to a batch of 130×30×3 HSS 18 % W planing knives for wood processing for ENO-Mebli Ltd., Mukachevo, Zakarpattia. (**Fig. 5.22**)

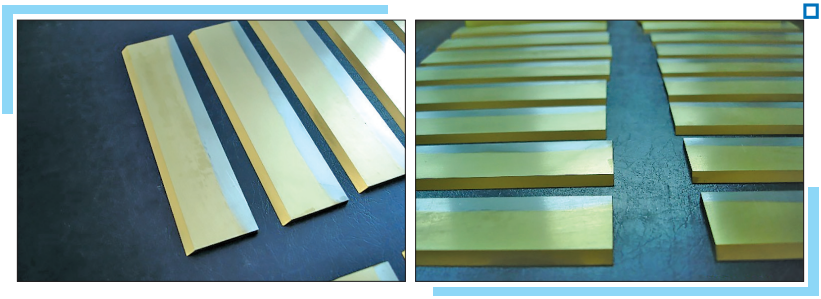

Fig. 5.22 Tool with Avinit coatings

Production tests have shown the high efficiency of the developed strengthening technologies: the wear resistance of the tool increases by 4–5 times, the power consumption for processing is reduced by more than 30 %, and the quality of material processing is increased.

5.2.2.1.5 Removable scalpel blades with protective and reinforcing coatings

Nanocomposite protective and reinforcing coatings on removable scalpel blades reduce the wear rate of the cutting edge by several times, increase the corrosion resistance of medical instruments and make it possible to use not only chromium stainless steel, but also «black» low-alloy steels for making blades. The cutting properties of coated scalpel blades, in contrast to uncoated blades, can be repeatedly restored without regrinding by simple dressing.

Tests of coated black steel blades have shown that in terms of corrosion resistance in sterilization and sterilization environments, they are not inferior and even exceed the resistance of stainless steel blades.

At the Institute of Orthopedics and Traumatology, Kharkiv, clinical and biochemical blood tests, microscopic examinations and assessment of the wound edges of damaged tissues of white rats of the Visteu line, operated with scalpels from steel 1.3542, 66Mn4 and 60MnSiCr4 with coatings and 60MnSiCr4 with coatings, were carried out. As a comparison, we used the results of similar studies obtained on animals operated with scalpel blades made of 1.3542 steel without coatings.

The test data indicate the absence of changes in the analyzes associated with the interaction of the coating material with the living tissues of the animal body during the operation.

Scalpel blades made of steel 1.3542 and low-alloy steel 66Mn4 and 60MnSiCr4 with coatings and 60MnSiCr4 with coatings are recommended for use in medicine.

The developed technology of applying protective and strengthening coatings on removable scalpel blades belongs to low-waste environmentally friendly technological processes.

It can serve as a basic technology for its refinement for other types of medical instruments.

Fig. 5.23 Removable scalpel blades with Avinit coatings

5.2.2.2 Wear-resistant reinforcing coatings to enhance the performance of the shaping tool

In mechanical engineering and a number of other industries, the method of deformation processing of sheet materials is widely used. Modern materials processing technologies require high-performance equipment and the use of appropriate tools. In the field of sheet materials processing, such equipment is offered by a number of well-known foreign machine-tool companies, such as AMADA, BEHRENS, EUROMAC, SALVAGNINI, TRUMPH, FINN-POWER. Buying such equipment (punching, punching, perforating, punching), domestic enterprises, after the end of the tool life, with which the manufacturing firms equip the above-mentioned machines, as a rule, use a tool, which in most cases is non-standard, produced by their own tool sections of production or other enterprises. for individual orders due to the high cost of imported tools. However, the resource of the tool produced, as practice shows, is significantly inferior to the imported tool. As a result, the productivity of the equipment decreases due to the loss of time for reinstalling the tool, the likelihood of obtaining a marriage due to premature failure of the tool increases.

In the metalworking tool market, punching press and die tools occupy a relatively small sector. And if, in the case of a metal-cutting tool, enterprises have the opportunity to choose tools from various manufacturers, both domestic and foreign, with a wide range of characteristics and, thereby, solve, if necessary, the problem of improving the quality and resource of the tool used, then solving such a problem with regard to the press tool, enterprises are often left alone with this problem. Industrial use of tools with hardening coatings can help solve this problem.

The work [158] considers the issues of increasing the service life of punching and stamping tools produced at domestic enterprises. The results

of the industrial use of tools with reinforcing coatings developed by the Scientific and Technical Center «Nanotechnology» are presented. Coatings provide the highest efficiency of hardened punching tools, significantly increasing the tool life and the quality of the processed materials.

Tool steels for punching tools for punching difficult-to-cut materials are subject to high impact loads. They must have such properties as sufficient strength, increased toughness and fatigue strength, good heat resistance, high hardness (45–65 HRC), which together determine the tool's performance.

For punching dies in domestic practice, wear-resistant steels 1.2060, SKD11, X155CrVMo12-1 are usually used, the properties of which do not fully meet modern requirements for a stamping tool.

The solution to the problem of increasing the efficiency and service life of punching and press-stamping tools, as well as for cutting metalworking tools, is possible by applying reinforcing wear-resistant coatings, chemical-thermal and other types of processing of working surfaces. It is the presence of the coating that largely determines the increased durability of the imported press-stamping tool.

Strict requirements are imposed on the properties of coatings for stamping tools, especially those subjected to shock loads.

Naturally, such coatings, having high hardness and wear resistance, should not be brittle and sufficiently crack-resistant, have high adhesion to the tool material, sufficient impact toughness, heat resistance, oxidation resistance, low adhesion activity (adhesion) and reduced to the processed material.

Coating or other surface treatments must not compromise the strength of the tool material. One of the most essential requirements for the technology is the ability to obtain high-quality functional coatings with good adhesion to the substrate at temperatures not exceeding 200–250 °C. These temperatures correspond to the tempering temperatures of steels commonly used in heat treatment of punching and stamping tools.

Among the wide variety of methods, vacuum-plasma and plasma-chemical methods of coating deposition satisfy this complex of requirements to the greatest extent.

The developed [159] low-temperature (T<200 °C) processes of applying reinforcing coatings, which do not lead to a decrease in the hardness of the base, provide coatings with a microhardness 3 – 6 times higher than the microhardness of tool steels in the hardened state, have good adhesion to the base at the level of metal strength, make it possible to form multicomponent coatings of various compositions with an optimal combination of properties in relation to the material being processed and the material of the tool. This preserves and can even increase the strength of the tool by increasing the fatigue strength of the coating.

These coatings provide a high efficiency of the use of hardened punching tools due to a significant increase in its service life and the quality of machined parts.

Production experience shows that when stamping parts made of steels of increased rigidity, punches are the weakest working elements of punching dies. Fractographic studies of the structure of fractures of the cutting edge of punches and the conditions of their operation have established that the fracture is of a fatigued nature. The emergence and propagation of fatigue cracks is due to repeated-replaceable loads acting on the working surface of the punch when it is introduced into the stamped material. Applying a properly selected coating to the working surface of the tool not only reduces the amount of repeated loads during its operation due to the lower coefficient of friction and lack of adhesion to the workpiece, but also increases the overall tedious strength of the base material.

Mechanical fatigue strength tests of coated and uncoated steel specimens showed that coated and uncoated specimens in terms of the number of loading cycles several times exceed the operating time of uncoated specimens, which corresponds to an increase in fatigue strength by about 15–25 %.

The service life of the press-stamping, punching tool and the quality of the processed materials largely depend on the cleanliness of the working surfaces of the punches and dies. This is even more true for coated tools.

When applying reinforcing coatings on press-stamp and punching tools, maintaining the required roughness of the working surfaces and sharpness of the working edges is another of the serious requirements for the technology.

Therefore, when applying coatings to a punching tool, a preliminary thorough preparation of its surface must be carried out, namely:

- traces of scale were removed after heat treatment;
- working surfaces should not have corrosion damage, deep scratches, cavities, cracks, metal rubbing;
- working edges should not have nicks, chips, burrs and burns;
- the tool must be sharpened, and the working surfaces brought to a roughness Ra 0.32...0.16 (9...10 class);
- geometric dimensions, rigidity must correspond to the design documentation.

Compliance with the requirements for the manufacture of tools and coating technology, as experience shows, makes it possible to produce press-stamping and punching tools with characteristics that are comparable and often even higher than those of imported tools.

The work [160] describes the wear-resistant multi-component hardening coatings developed by STC «Nanotechnology» to improve the characteristics of the cutting tool.

Taking into account the specifics of the work of press-stamping and punching tools subjected to shock loads, Avinit VPNM and VPNM-f series reinforcing coatings have been developed [159]. Technologies have

been developed for low-temperature (<200 °C) deposition of high-hard wear-resistant coatings in modes that provide good adhesion to substrate materials without reducing the strength of steel and without deteriorating the purity class of the original surface. allow applying reinforcing coatings on a wide class of tool steels used for the manufacture of punching and stamping tools, including tool carbon steels with low heat resistance, such as 1.1645, 1.1654.

The main characteristics of the coatings:

1. Coatings are applied using nanotechnology.
2. Coating thickness 3–5 μm.
3. Microhardness 20,000–35,000 MPa (depending on the composition of the coating).
4. Maintaining the surface cleanliness class.
5. Excellent adhesion to the substrate (suitable undercoats and ion-plasma pre-cleaning of the surface).
6. Coatings are practically non-porous.

Table 5.28 Types of coatings

Type of coating	Structure	Foreign analogues	Properties	
			H_v, kg/mm^2	Friction coef.
VPNM	Multilayer coating based on Ti-N	Z-Coat (HANITA)	2500	0.4–0.5
VPNM-f	Multilayer coating based on Al-Cr-N	Alcrona (BALZERS)	2500 – 3500	0.3–0.4

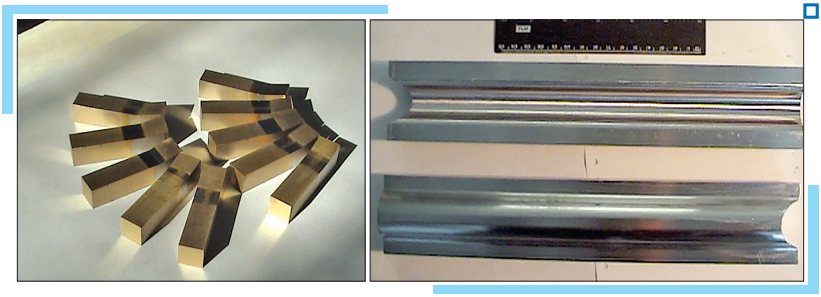

Fig. 5.24 Reinforcing and anti-friction coating on dies and punching tools

To determine the effectiveness of the developed nanocomposite coatings to increase the service life of tools and the quality of the processed materials, tests were carried out in production conditions of tools of various nomenclature and for equipment with developed coatings at a number of domestic enterprises.

5.2.2.2.1 Testing of the hardened die tool produced by the State Scientific and Production Enterprise «Kommunar Association», Kharkiv

A batch of punching die tools with coatings was made and comparative production tests of the hardened die tools produced by the State Scientific and Production Enterprise «Kommunar Association», Kharkiv, were carried out.

Comparative production tests in industrial production conditions of the State Scientific and Production Enterprise «Kommunar» Association in Kharkiv were carried out on dies of ∅12 mm, which are used for the most loaded and hard modes of vibration punching on punching presses with CNC «Behrens».

The tests were carried out by comparing the resistance (number of impacts) and the amount of wear on the effective diameter of coated and uncoated dies operating under the same conditions on workpieces of St 37-2 with a thickness of 3 mm and 1 mm.

The test results are shown in the **Table 5.29**.

Table 5.29 Test results of coated punching tools

Stamp designation	Coating	Thickness of the processed material	Number of blows	Number of blows, mm	Wear rate, mm/blow	Coef. strengthening
Punches ∅12 mm	VPNM	1 mm	161805	0.02	$1.24 \cdot 10^{-7}$	19
	Uncoated		46230	0.11	$2.38 \cdot 10^{-6}$	
Matrix ∅12,07 mm	VPNM		161805	0.004	$2.47 \cdot 10^{-7}$	43
	Uncoated		46230	0.05	$1.1 \cdot 10^{-6}$	
Punches ∅12 mm	VPNM	3 mm	62030	0.03	$4.8 \cdot 10^{-7}$	12
	Uncoated		26140	0.15	$5.7 \cdot 10^{-6}$	
Matrix ∅12,45 mm	VPNM		62030	0.04	$6.4 \cdot 10^{-7}$	5
	Uncoated		26140	0.08	$3.0 \cdot 10^{-6}$	

Thus, the results of comparative tests in industrial production on dies with ∅ 12 mm, used for the most loaded and severe vibration cuts on workpieces St 37-2 thickness of 3 mm and 1 mm on a punch press with CNC «Behrens», showed that under the same conditions and operating modes, the stability of dies with nanocomposite coatings is much higher than without a coating (reinforcement coefficient from 5 to 40 times), while the quality of processed materials.

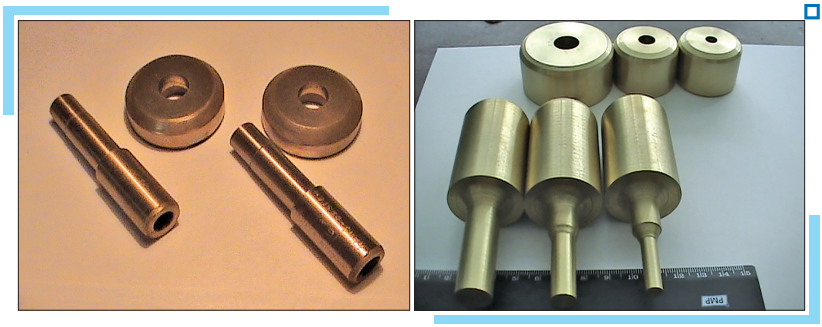

Fig. 5.25 Punching tools with hardening nanocoating (for the «Behrens» sheet-working press)

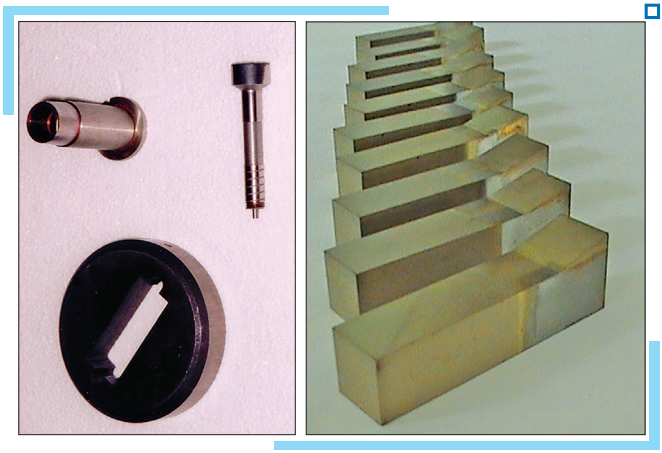

Fig. 5.26 Punching tools for punching press with CNC «Behrens»

5.2.2.2.2 Production tests of the hardened punching tool for the Trumatik 200R sheet-processing press «Plant named after Shevchenko», Kharkiv

The conducted industrial comparative tests of the punching tool for processing sheets of the «Trumatik 200R» press showed that when processing sheet material from stainless and black steel with a thickness of 0.5 to 3 mm, unreinforced dies 5×40 mm and ∅12 mm were made from steel 1.2060 before regrinding thousand strokes. The dies with VPNM hardening coating, when processing the same sheet materials, worked 120 thousand strokes before regrinding. After regrinding, the dies with a hardening coating worked 100 thousand strokes and could continue to work.

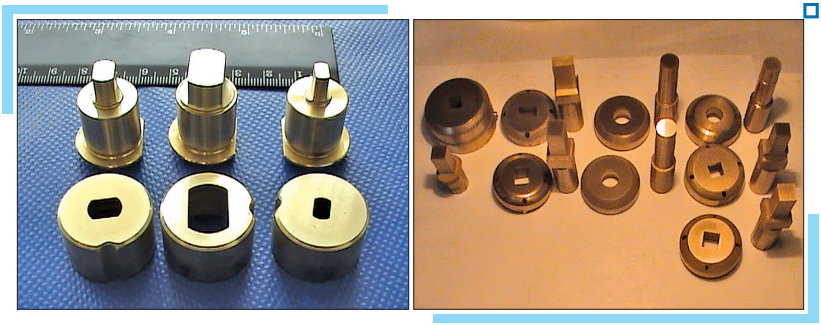

Fig. 5.27 Punching tools with a reinforcing coating (for the «Trumatic 200R» sheet-processing press)

5.2.2.2.3 Testing of punching tools with hardening coating (for sheet-processing center Finn-Power)

When testing the press-stamping tool with the developed coatings used for processing sheets of the FINN-POWER center (JSC «Plant named after Frunze» (Kharkiv), a service life was achieved before the first regrinding, more than 2 times longer than the warranty period indicated the manufacturer of this center.

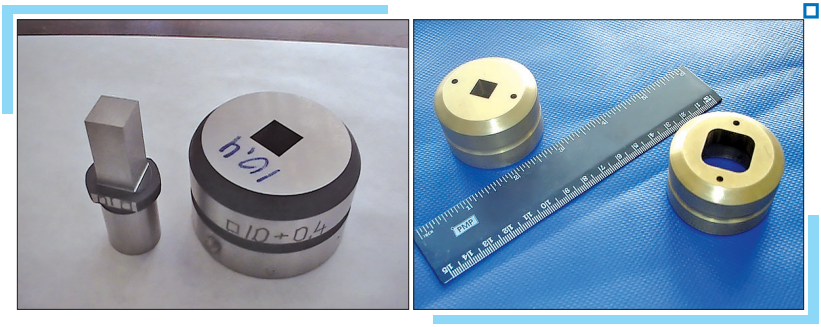

Fig. 5.28 Punching tools with a reinforcing coating for the Finn-Power sheet-processing center (JSC «Plant named after Frunze» (Kharkiv))

It is important to note that during regrinding, the functional properties of the coating are preserved and the coated tool works fine after regrinding without subsequent recoating. So, a punch of square section 10×10 with a coating before the first regrinding worked 91,600 strokes, after the second — 75600 strokes, after the third regrinding it continued to work normally, and therefore a decision was made about the sufficiency of the infor-

mation received about the operability of the coated tool and in the future the control of its operation was not carried out.

When regrinding a coated tool, as shown by tests, to restore the sharpness of the working edge, it is required to remove a layer of about 0.1 mm, while without a coating, it is necessary to remove a layer of about 0.2 mm.

All this as a whole provides a significant increase in the service life of the coated tool.

5.2.2.2.4 Manufacturing of Multitools punching tools with hardening nanocoating

Reinforcing coatings were applied to the punching die tool Multitool of JSC «Electric machine-building plant «SELMA Firm», Simferopol.

Fig. 5.29 Punching tools Multitools with reinforcing coatings (JSC «Electric machine-building plant «SELMA Firm», Simferopol)

Punching tools Multitools with hardening nanocoating applied by STC «Nanotechnology» showed excellent results when working under conditions of serial production at the JSC «Electric machine-building plant «SELMA Firm», Simferopol).

Thus, the experience of working in the conditions of serial production of domestic press tools with our coatings for various sheet-processing centers (Behrens, Trumatic, Amada, Finn-Power) shows a significant increase in its stability (from 3 to 10 times and more) compared to the tool without coatings. With the optimal number of one-time loading of the tool into the chamber of technological equipment for coating, its cost increases from 15–20 % to 30–40 % of the manufacturing cost. This makes it quite competitive both in quality and in price with imported tools.

The use of wear-resistant and antifriction nanocomposite coatings on the mold replacement parts of the dies allows solving the following problems:

- Extension of service life.
- Improving the surface/chrome quality of products.
- Improved product removal.
- Reduced repair and restoration costs.
- Replacement of electroplated coatings.
- Reduced consumption.

The developed coatings demonstrate high application efficiency on the following types of shaping tools:

1. Die cut (recommended VPNM coating). The coating works especially effectively when cutting sheet metals: steel, brass, copper. Resistant to damage at the die edges performs the same function as on cutters under shock loads. The coating protects products from tear formation during cutting, because even with wear of the coating along the cutting edge, it remains for a long time on the adjacent surfaces of the matrix and punch. Increases die durability by 3 or more times. Improves the quality of finished products (eliminates burrs).

2. Bending die (recommended VPNM-f coating with improved antifriction characteristics). The coating on the bending die reduces the friction of the manufactured part against the die. In this regard, a more complete formation of the part occurs, the possibility of scoring is eliminated, the possibility of the part «sticking» to the stamp is reduced.

3. Flaring die, draw die (recommended VPNM-f coating). As in the case of the bending die, reducing the friction between the workpiece and the working surface of the die and simultaneously strengthening it significantly increases the service life of the die and contributes to a better shape of the product.

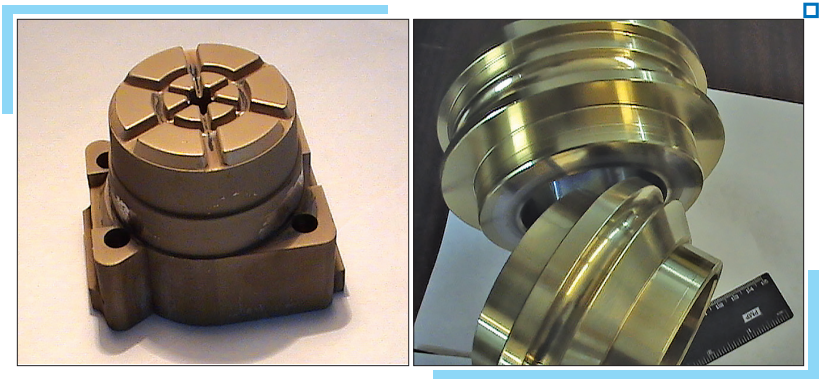

Fig. 5.30 Stamps with Avinit coatings (State Scientific and Production Enterprise «Kommunar Association» (Kharkiv)

5.2.2.3 Wear-resistant reinforcing coatings for improved broaching and piercing performance

Avinit multicomponent coatings reduce abrasive wear, which prevails at low cutting speeds, and adhesive wear at medium to high cutting speeds, and reduce metal adhesion on the back surfaces, which leads to improved surface quality and reduced cutting forces and tool wear.

The covers can be used for both internal and external broaches.

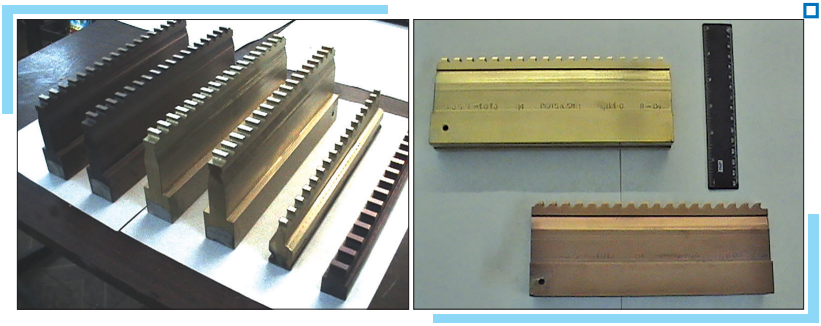

Fig. 5.31 Broaches with Avinit coating (SE Zoria-Mashproekt (Mykolaiv))

Thus, the use of Avinit coatings makes it possible to achieve a manifold increase in the wear resistance and service life of cutting and shaping tools. The effect is achieved by applying very thin (0.1–5 μm) wear-resistant coatings, obtained using nanotechnology, on the working surfaces of parts. Finish coating operation does not affect the preliminary manufacturing process of parts. The small thickness of the coatings does not require a change in the size of the tolerances for their dimensions. Ultra-high rigidity of coatings and extremely high adhesion strength of coatings with a variety of substrates provide an increase in the wear resistance of cutting and shaping tools by 3–30 times, stamps by 5–100 times, rubbing parts against abrasive materials by 10–100 times.

5.2.2.4 Modification of Avinit coatings

We have modified Avinit coatings [161, 162] by developing an improved multi-component wear-resistant ion-plasma coating Avinit for strengthening cutting and shaping tools.

The improved coating contains, along with the elements Ti and Al, molybdenum, chromium, vanadium and silicon in the composition of the coating (Ti-Al-Mo-Cr-V-Si) N.

The introduction of additional alloying elements (Mo, Cr, V, Si) into the composition of the Ti-Al-N coating, capable of forming high-hard,

strong high-enthalpy nitride compounds (Mo_2N, CrN, VN, Si_3N), significantly increases the wear-resistant and mechanical properties of the coating.

The method of forming a coating on a metal substrate is as follows. The coating is obtained by the method of vacuum-arc deposition from the plasma phase in an atmosphere of a nitrogen reaction gas with ion bombardment. Deposition is carried out from two cathodes — alloyed titanium cathode, which contains impurities of molybdenum, chromium, vanadium in the following ratio of components, (%) (**Table 5.30**):

Table 5.30 Content of elements in cathode 1

The content of the element in the cathode, (%)	Ti	V	Cr	Mo
	79.4–86.3	4–5.5	0.5–1.5	4–5.5

and alloyed aluminum cathode, which contains silicon impurities in the following ratio of components, (%) (**Table 5.31**):

Table 5.31 Content of elements in cathode 2

The content of the element in the cathode, (%)	Al	Si
	70.7–76.6	20–22

Before being placed in a vacuum chamber, the products to be coated and the control samples were washed in gasoline, wiped with alcohol, and installed in the sockets of the rotary planetary mechanism of the table of the vacuum-arc unit of the Avinit installation, located in a circle. Fused titanium cathode and alloyed aluminum cathode were used as sputtered cathode materials.

The reaction chamber was evacuated to a pressure of 6.6×10^{-3} Pa, argon was admitted to a pressure of 2×10^{-1} Pa, the glow discharge was ignited, and the discharge current was set at 20 A. 20 V to 1000 for 30 min.

Then the products were processed in a high-density argon plasma. For this, argon was admitted to a pressure of 2×10^{-1} Pa through a gas plasma generator, the gas discharge was ignited, the gas discharge current was set at 20 A, gradually increasing the shear potential on the parts to be coated from 20 V to 400...500 V, the parts were heated to 400...500 °C and purified in an argon gas discharge for 30 min.

After that, argon was replaced with nitrogen at the same operating pressure in the chamber $P_{N2}=(1.33...4.0)\cdot10^{-1}$ Pa and an arc discharge was ignited on both cathodes with the technological parameters given in **Table 5.32**.

Table 5.32 Technological parameters of applying modified coatings, their composition and some properties

Avinit coating	Technological parameters				Composition of a Coating, (%)							Microhard., H_V, kg/mm^2	Thick-ness., μm	Adhesion
	I_p(Ti), A	I_p(Al), A	U_c, V	P_{N2}, 10^{-1}Pa	Ti	Mo	V	Cr	Al	Si	N			
1	80	100	80	1.5	63.0	4.4	4.4	1.4	6.9	2.3	13.6	3500	10	Good
2	90	110	110	2.0	65.0	4.5	4.6	1.5	7.5	2.5	14.4	4200	10	Very Good
3	100	120	120	2.0	66.4	4.6	4.7	1.5	6.1	2.1	14.6	4500	10	Very Good
4	110	130	120	3.0	67.2	4.7	4.7	1.6	4.3	1.5	16.0	4600	10	Good
5 Ti-N	100	–	100	2.0	82.0	–	–	–	–	–	18.0	1800	10	Very Good
6 Ti-Al-N	100	110	100	2.0	74.0	–	–	–	8.0	–	18.0	3000	10	Very Good

When processing titanium in plasma at a discharge current I_p(Ti) = =80–120 A and aluminum at a discharge current I_p(Al) = 90–140 A and a bias potential U_c = 50–150 V in a nitrogen atmosphere at a pressure of P_{N2} = (1, 33...4.0)·10^{-1} Pa, the plasma phase, along with titanium and aluminum ions, additionally contains ions of molybdenum, chromium, vanadium and silicon, which are part of the coating.

The coating was carried out for 120 minutes. The coating thickness reached 8...10 μm.

Table 5.32 shows the dependence of the composition of the obtained coatings on technological parameters and some properties of the coatings.

For comparison in **Table 5.32** shows the characteristics of Ti-N and Ti-Al-N coatings obtained on the same equipment, but not from alloyed, but from pure cathodes.

The optimal technological parameters of the process are as follows: I_p(Ti) = 90 A, I_p(Al) = 110 A, U_c = 110 V, P_{N2} = 2.0·10^{-1} Pa).

In this case, Avinit coatings are formed with the following ratio of components (%) (**Table 5.33**):

Table 5.33 The ratio of the components in the Avinit coating

Ti	Al	V	Cr	Mo	Si	N
65.0	7.5	4.6	1.5	4.5	2.5	14.4

Preliminary tests have shown that the developed coatings make it possible to achieve a manifold increase in the wear resistance and service life of cutting and shaping tools.

References

1. Chaynov, N. F. (2001). Problemy i perspektivy porshnevogo dvigatelestroeniya v Rossii. Dvigatelestroenie, 4, 46–47.
2. Arzamasov, B. N. (Ed.) (1990). Konstrukcionnye materialy. Moscow: Mashinostroenie, 131.
3. Semenov, A. P. (1980). Shvatyvanie metallov i metody ego predotvrascheniya pri trenii. Trenie i iznos, 1 (2), 236–246.
4. Bugas, N. A. (1993). Reshennye i nereshennye zadachi po sovmestimosti tribosistem. Trenie i iznos, 4, 25–33.
5. Tekekbaum, M. M. (1991). Nadezhnost' sel'hozmashin: nedostatki metodologii ee ocenki. Traktory i sel'skohozyaystvennye mashiny, 8, 38–40.
6. Fox-Rabinovich, G., Totten, G. E. (Eds.) (2006). Self-Organization During Friction. CRC Press, 459. doi: https://doi.org/10.1201/9781420017861
7. Francevicha, I. N. (Ed.) (1997). Anodnye okisnye pokrytiya na legkih metallah i splavah. Kyiv: Naukova dumka, 259.
8. Fuks-Rabinovich, G. S., Kacura, A. A., Moiseev, V. F., Dosbaeva, G. K. (1989). Vliyanie fazovogo sostava na iznosostoykost' ionno-plazmennyh pokrytiy iz nitrida titana. Trenie i znos, 10 (4), 742–744.
9. Moiseev, V. F., Fuks-Rabinovichm G. S., Dosbaeva, G. K., Skvorcov, V. N. (1990). Vyazkost' i plastichnost' ionno-plazmennyh pokrytiy iz nitrida titana. Zavodskaya laboratoriya, 1, 57–59.
10. Sal'nikov, A. S. (1993). Iznosostoykost' nitridnyh plenok. MiTOM, 5, 2–5.
11. Byakova, A. V. (1992). Vliyanie strukturnogo sostoyaniya pokrytiy iz nitrida titana na ih prochnost'. Sverhtverdye materialy, 5, 30–37.
12. Derflinger, V., Brändle, H., Zimmermann, H. (1999). New hard/lubricant coating for dry machining. Surface and Coatings Technology, 113 (3), 286–292. doi: https://doi.org/10.1016/s0257-8972(99)00004-3
13. Kaysmasov, L. K. (1991). Povyshenie kachestva iznosostoykih ionno-plazmennyh pokrytiy. Tyazheloe mashinostroenie, 12, 17–18.
14. Antonova, E. A. et. al. (1968). Nekotorye dannye ob ustoychivosti metallokeramicheskih pokrytiy k zadiraniyu. Temperaturoustoychivye zaschitnye pokrytiya. Leningrad: Nauka, 267.
15. Kostyuk, G. I. (2002). Fiziko-tehnicheskie osnovy napyleniya pokrytiy, ionnoy implantacii ionnogo legirovaniya, lazernoy obrabotki i uprochneniya, kombinirovannyh tehnologiy. Kharkiv: AINU, 1030.
16. Aksonov, I. I., Aksonov, S. D., Andrieiev, A. A., Bilous, V. A., Sobol, O. V. (2015). Vakuumno-duhovi pokryttia. Kharkiv, 210.

17. Kostyuk, G. I., Popov, V. V. (2020). Nanotechnology in aviation and general machine building industry. Kharkiv: Planeta-Print Ltd, 688.
18. Lyubchenko, A. P., Macevitiy, V. M., Bakakin, G. N., Beresnev, V. M., Oleynik, A. K. (1983). Issledovanie iznosa vakuumno-plazmennyh pokrytiy iz TiN pri trenii po metallicheskim materialam. Trenie i iznos, 4 (5), 892–897.
19. Lapshin, V. I., Shulaev, V. M., Andreev, A. A. (2002). Vakuumnye tehnologii v proizvodstve instrumenta iz bystrorezhuschih staley s povyshennymi sluzhebnymi harakteristikami. Proc. 3 Int. Conf. «Equipm. and Techn. of Thermal Treatment of Metals and Alloys» (OTTOM-3). Kharkiv, 33–37.
20. Tanaka, Y., Gür, T. M., Kelly, M., Hagstrom, S. B., Ikeda, T., Wakihira, K., Satoh, H. (1992). Properties of (Ti1-xAlx)N coatings for cutting tools prepared by the cathodic arc ion plating method. Journal of Vacuum Science & Technology A: Vacuum, Surfaces, and Films, 10 (4), 1749–1756. doi: https://doi.org/10.1116/1.577742
21. Coll, B. F., Sathrum, P., Fontana, R., Peyre, J. P., Duchateau, D., Benmalek, M. (1992). Optimization of arc evaporated (Ti,Al)N film composition for cutting tool applications. Surface and Coatings Technology, 52 (1), 57–64. doi: https://doi.org/10.1016/0257-8972(92)90371-g
22. Corban', V. F. et. al. (2000). Tribological Characteristics of Multilayer Ion-Plasma Coatings, Based on Chromium and Titanium Nitrides. Proc. 1 Int. Congress on Rad. Phys. High Current Electronics and Modif. Materials. Vol. 3. Tomsk, 494–496.
23. Andrievskiy, R. A., Anisimova, I. A., Anisimov, V. G. (1992). Formirovanie struktury i mikrotverdost' mnogosloynyh dugovyh kondensatov na osnove nitridov. FizHOM, 2, 99–102.
24. Lewis, D. B., Wadsworth, I., Münz, W.-D., Kuzel, R., Valvoda, V. (1999). Structure and stress of TiAlN/CrN superlattice coatings as a function of CrN layer thickness. Surface and Coatings Technology, 116-119, 284–291. doi: https://doi.org/10.1016/s0257-8972(99)00132-2
25. Andreev, A. A. i dr. (2002). Nanesenie vakuumno-dugovyh pokrytiy CrxN — TiN na podlozhki iz chuguna i stali s posleduyuschey termoobrabotkoy. Proc. 3 Int. Conf. «Equipm. and Techn. of Thermal Treatment of Metals and Alloys» (OTTOM-3). Kharkiv, 86–88.
26. Andreev, A. A., Kunchenko, V. V., Sablev, L. P. et. al. (2001). Dupleksnaya obrabotka instrumental'nyh staley v vakuume. Proc. 2 Int. Conf. «Equipm. and Techn. of Thermal Treatment of Metals and Alloys» (OTTOM-2). Kharkiv, 48–56.
27. Vereshaka, A. S. (1993). Rabotosposobnost' rezhuschego instrumenta s iznosostoykimi pokrytiyami. Moscow: Mashinostroenie, 336.
28. Sahalovych, A. V., Kononykhin, A. V., Popov, V. V., Dudnik, C. F., Sahalovych, V. V. (2010). Ustanovka Avinit dlia nanesennia bahatosharovykh funktsionalnykh pokryttiv. Fizicheskaya inzheneriya

poverhnosti, 8 (4), 336–347. Available at: http://dspace.nbuv.gov.ua/bitstream/handle/123456789/98914/8-Sagalovich.pdf?sequence=1
29. Popov, V., Sagalovych, A., Sagalovych, V.; Sagalovych, V. (Ed.) (2020). Improving the performance, reliability and service life of aviation technology products based on the innovative vacuum-plasma nanotechnologies for application of avinit functional coatings and surfaces modification. Tallinn: Scientific Route OÜ, 102. doi: https://doi.org/10.21303/978-9916-9516-1-3
30. Popov, V. V., Sahalovych, O. V., Sahalovych, V. V. (2020). Vakuum-plazmovi nanotekhnolohiyi Avinit. Kharkiv: FED, 241.
31. Sagalovych, A., Sagalovych, V., Popov, V., Dudnik, S.; Sagalovych, V. (Ed.) (2021). Vacuum-plasma multilayer protective coatings for turbine blades. Tallinn: Scientific Route OÜ, 91. doi: https://doi.org/10.21303/978-9916-9516-5-1
32. Sagalovich, A. V., Kononyhin, A. V., Popov, V. V., Dudnik, C. F., Sagalovich, V. V. (2011). Eksperimental'nye issledovaniya pokrytiy tipa Avinit. Aviacionno-kosmicheskaya tehnika i tehnologiya, 3, 5–15. Available at: http://nbuv.gov.ua/UJRN/aktit_2011_3_3
33. Sagalovych, A., Kononykhin, A., Popov, V., Sagalovych, V. (2013). Experimental research of multicomponent multilayer ion-plasma Avinit coatings. Fizicheskaya inzheneriya poverhnosti, 11 (1), 4–17. Available at: http://nbuv.gov.ua/UJRN/Phip_2013_11_1_3
34. Sahalovych, V. V., Popov, V. V., Kononykhin, O. V., Bohoslavtsev, V. I. (2015). Pat. No. 109053 UA. Znosostiyke antyfryktsiyne pokryttia. No. a201313223; declareted: 13.11.2013; published: 10.07.2015, Bul. No. 13. Available at: https://uapatents.com/7-109053-znosostijjke-antifrikcijjne-pokrittya.html
35. Sahalovych, V. V., Popov, V. V., Kononykhin, O. V., Bohoslavtsev, V. I. (2015). Pat. No. 108279 UA. Bahatosharove, znosostiike pokryttia. No. a201308247; declareted: 01.07.2013; published: 10.04.2015, Bul. No. 7. Available at: https://uapatents.com/8-108279-bagatosharove-znosostijjke-pokrittya.html
36. Sagalovich, A. V., Sagalovich, V. V., Popov, V. V., Kononyhin, A. V., Bogoslavcev, V. I. (2013). Pat. No. 141213 RU. Iznosostoykoe antifrikcionnoe pokrytie detaley par treniya. No. 2013152088; declareted: 22.11.2013; published: 27.05.2014. Available at: https://www.lens.org/lens/patent/013-865-821-440-121/frontpage
37. Sagalovich, A. V., Sagalovich, V. V., Popov, V. V., Kononyhin, A. V., Bogoslavcev, V. I. (2013). Pat. No. 2543643 RU. Ploskaya zolotnikovaya para i mnogosloynoe iznosostoykoe pokrytie. No. 2013133367; declareted: 17.07.2013; published: 20.02.2015. Available at: https://www.lens.org/lens/patent/167-445-920-489-979/frontpage
38. Sagalovych, A. V., Babenko, V. A., Dudnik, S. F., Sagalovych, V. V., Cononyhin, A. V., Popov, V. V. et. al. (2007). Multicomponent coatings

for precise tribological pairs working in friction assembly of machine building and aviation. Fizicheskaya inzheneriya poverhnosti, 5 (1-2), 155–164. Available at: http://dspace.nbuv.gov.ua/bitstream/handle/123456789/98803/4-Sagalovych.pdf?sequence=1

39. Sagalovich, A. V., Grigor'ev, A. V., Kononykhin, A. V., Popov, V. V., Sagalovich, V. V., Boguslaev, V. A. et. al. (2014). Pat. No. 2520237 RU. Application of two-component chromium-aluminium coating on gas turbine cooled blade inner cavities and device to this end. No. 2012107601/02; declareted: 28.02.2012; published: 20.06.2014, Bul. No. 17. doi: https://doi.org/10.13140/RG.2.2.25944.32007
40. Sagalovich, V. V., Sagalovich, A. V. (2013). Pat. No. 2555692 RU. Ion-plasma precision nitriding of metal part surface. No. 2013127482/02; declareted: 17.06.2013; published: 10.07.2015, Bul. No. 19. Available at: https://patentimages.storage.googleapis.com/64/70/41/c01b8140a1f302/RU2555692C2.pdf
41. Sagalovich, V. V., Popov, V. V., Boguslaev, V. A. et. al. (2012). Pat. No. 011255 RU. Ustroystvo dlya naneseniya dvuh-komponentnyh hrom-alyuminievyh pokrytiy na vnutrennie polosti ohlazhdaemyh rabochih lopatok gazovyh turbin. published: 16.04.2012.
42. Sagalovich, A. V., Sagalovich, V. V. (2008). Zapornaya armatura v korrozionno-stoykom ispolnenii. Mater. Mezhd. konf. «Ispol'zovanie pnevmaticheskoy energii i oborudovaniya dlya ee polucheniya v gornorudnoy otrasli». Sumy.
43. Sagalovych, O. V., Sagalovych, V. V., Popov, V. V., Dudnik, S. F. (2020). Vacuum-plasma protective coating for turbines blades. Mechanics and Advanced Technologies, 88 (1), 124–134. doi: https://doi.org/10.20535/2521-1943.2020.88.204675
44. Sagalovich, A. V., Sagalovich, V. V., Kononyhin, A. V., Popov, V. V., Oleynik, A. K. (2011). Razrabotka i issledovanie novyh mnogosloynyh pokrytiy Avinit D na osnove sistem «metall-uglerod». Technological Systems, 2, 36–45. Available at: http://technological-systems.net/index.php/Home/article/view/413/421
45. Sagalovich, A. V., Grigor'ev, A. V., Kononyhin, A. V., Popov, V. V., Sagalovich, V. V. (2011). Nanesenie pokrytiy na slozhnoprofil'nye precizionnye poverhnosti gazofaznym metodom (CVD). Fizicheskaya inzheneriya poverhnosti, 9 (3), 229–236. Available at: http://dspace.nbuv.gov.ua/bitstream/handle/123456789/76903/04-Sagalovich.pdf?sequence=1
46. Sagalovich, A. V., Kononyhin, A. V., Popov, V. V., Oleynik, A. K., Grigor'ev, A. V., Sagalovich, V. V. (2012). Izuchenie tribologicheskih harakteristik mnogosloynyh Mo-S pokrytiy, poluchennyh gazofaznym metodom s ispol'zovaniem metallorganicheskih soedineniy. Technological Systems, 1, 10–15. Available at: http://technological-systems.org/index.php/Home/article/view/301/308

47. Sagalovych, A., Sagalovych, V. (2013). Mo-C multilayered CVD coatings. Proceedings of SerbiaTrib'13. Kragujevac, 195. Available at: https://www.yumpu.com/en/document/read/43814103/proceedings-of-serbiatrib-13
48. Sagalovych, A., Sagalovych, V. (2013). Mo-C multilayered CVD coatings. Tribology in industry, 35 (4), 261–269. Available at: https://1library.org/document/oy89d3wq-mo-c-multilayered-cvd-coatings.html
49. Sagalovich, A. V., Kononyhin, A. V., Popov, V. V., Grigor'ev, A. V., Sagalovich, V. V., Oleynik, A. K. (2011). Izuchenie tribologicheskih harakteristik mnogosloynyh Mo-S pokrytiy, poluchennyh gazofaznym metodom s ispol'zovaniem metallorganicheskih soedineniy. Vestnik HNADU, 54, 44–51.
50. Sagalovych, A., Sagalovych, V., Kononyhin, A., Popov, V., Bogoslavcev, V. (2017). The Antifrictional Coatings on the Molybdenum Base. Proc. 15th Intern. Conf. on Tribology SERBIATRIB '17. Kragujevac.
51. Sagalovych, A., Popov, V., Sagalovych, V., Dudnik, S., Popenchuk, R. (2020). Development of the chemical vapor deposition process for applying molybdenum coatings on the components in assembly and engine construction. Eastern-European Journal of Enterprise Technologies, 2 (12 (104)), 6–15. doi: https://doi.org/10.15587/1729-4061.2020.201540
52. Sagalovych, A., Sagalovych, V., Dudnik, S. (2012). Deposition of the stoichiometric coatings by reactive magnetron sputtering. Fizicheskaya inzheneriya poverhnosti, 10 (3), 263–272. Available at: http://dspace.nbuv.gov.ua/bitstream/handle/123456789/98970/3-Sagalovych.pdf?sequence=1
53. Sahalovych, O. V., Kononykhin, O. V., Popov, V. V. et. al. (2012). Formuvannia pokryttiv stekhiometrychnoho skladu pry reaktyvnomu mahnetronnomu napylenni. Tehnologicheskie sistemy, 4 (61), 16–26.
54. Sagalovych, A., Popov, V., Sagalovych, V., Dudnik, S., Dziuba, A. (2021). The effect of obtaining conditions on the structure and composition of Cu-MoS2 coatings upon magnetron sputtering of composite targets. Functional Materials, 28 (1), 55–63. doi: https://doi.org/10.15407/fm28.01.55
55. Valvoda, V., Černý, R., Kužel, R., Musil, J., Poulek, V. (1988). Dependence of microstructure of TiN coatings on their thickness. Thin Solid Films, 158 (2), 225–232. doi: https://doi.org/10.1016/0040-6090(88)90024-7
56. Becofen, S. Ya., Petrov, L. M., Lazarev, E. M. et. al. (1990). Struktura i svoystva ionno-plazmennyh pokrytiy TiN. Metally, 3, 158–165.
57. Belous, V. A., Kartmazov, G. N., Pavlov, V. S. et. al. (1988). Ionno-plazmennye processy osazhdeniya pokrytiy. Metod atomno-ionnogo raspyleniya. Obzor. Moscow: CNIIatominform, 48.

58. Hauert, R., Patscheider, J. (2000). From alloying to nanocomposites — improved performance of hard coatings. Advanced Engineering Materials, 2 (5), 247–259. doi: https://doi.org/10.1002/(sici)1527-2648(200005)2:5<247::aid-adem247>3.0.co;2-u
59. Beresnev, V. M., Fedorenko, A. I., Gritsenko, V. I., Perlov, D. L. (2003). Research of friction properties of composite coatings obtained by a vacuum — ARC method. Fizicheskaya inzheneriya poverhnosti, 1 (2), 180–183. Available at: http://dspace.nbuv.gov.ua/bitstream/handle/123456789/98437/8-Beresnev.pdf?sequence=1
60. Zhou, M., Makino, Y., Nose, M., Nogi, K. (1999). Phase transition and properties of Ti-Al-N thin films prepared by r.f.-plasma assisted magnetron sputtering. Thin Solid Films, 339 (1-2), 203–208. doi: https://doi.org/10.1016/s0040-6090(98)01364-9
61. Efeoglu, I. (2007). Deposition and characteriztion of a multilayered-composite solid lubricant coating. Reviews on Advanced Materials Science, 15 (2). Available at: https://www.researchgate.net/publication/228420023_Deposition_and_characteriztion_of_a_multilayered-composite_solid_lubricant_coating
62. Spassov, V., Savan, A., Phani, A. R., Stueber, M., Haefke, H. (2003). Quaternary-matrix, nanocomposite self-lubricating PVD coatings in the system TiAlCN-MoS2 — structure and tological properties. MRS Proceedings, 788. doi: https://doi.org/10.1557/proc-788-l11.29
63. Holubar, P., Janca, J., Veprek, S. (2003). Development and Industrialization of Novel Superhard Nanocristalline Composite Wear-Protection Coatings. Final Report @Nato Science for Peace Programme. No. SFP 972379.
64. Delplancke-Ogletree, M. P., Monteiro, O. R. (2001). Preparation by pulsed vacuum arc deposition and characterization of DLC/MoS2 nanocomposite thin films. ICMCTF. Available at: https://escholarship.org/content/qt32b0x7d9/qt32b0x7d9.pdf?t=lnq6y2
65. Musil, J. (2000). Hard and superhard nanocomposite coatings. Surface and Coatings Technology, 125 (1-3), 322–330. doi: https://doi.org/10.1016/s0257-8972(99)00586-1
66. Vepřek, S., Reiprich, S. (1995). A concept for the design of novel superhard coatings. Thin Solid Films, 268 (1-2), 64–71. doi: https://doi.org/10.1016/0040-6090(95)06695-0
67. Lahtin, Yu. M., Arzamasov, B. N. (1985). Himiko-termicheskaya obrabotka metallov. Moscow: Metallurgiya, 256.
68. Arzamasov, B. N., Bratuhin, A. G., Eliseev, Yu. S., Panayoti, T. A. (1999). Ionnaya himiko-termicheskaya obrabotka splavov. Moscow: Izd-vo MGTU im. N.E. Baumana, 400.
69. Chatterdzhi-Fisher, R., Eyzell, F. V. et. al. (1990). Azotirovanie i karbonitrirovanie. Moscow: Metallurgiya, 280.

70. Prokoshkin, D. A. (1984). Himiko-termicheskaya obrabotka metallov — karbonitraciya. Moscow: Mashinostroenie, Metallurgiya, 240.
71. Lahtin, Yu. M.. Kogan, Ya. D., Shpis, G.-I., Bomer, Z. (1991). Teoriya i tehnologiya azotirovaniya. Moscow: Metallurgiya, 320.
72. Sahalovych, O. V., Sahalovych, V. V. (2013). Pat. No. 84664 UA. Sposib ionno-plazmovoho pretsyziynoho azotuvannia poverkhon stalei i splaviv Avinit N. No. u201305770; declareted: 16.08.2013; published: 25.10.2013, Bul. No. 20. Available at: https://uapatents.com/10-84664-sposib-ionno-plazmovogo-precizijjnogo-azotuvannya-poverkhon-stalejj-i-splaviv-avinit-n.html
73. Sahalovych, V. V., Sahalovych, O. V. (2013). Pat. No. 107408 UA. Sposib ionno-plazmovoho pretsyziynoho azotuvannia poverkhon detali zi stalei i splaviv Avinit N. No. a201305768; declareted: 07.05.2013; published: 25.12.2014, Bul. No. 24. Available at: https://uapatents.com/11-107408-sposib-ionno-plazmovogo-precizijjnogo-azotuvannya-poverkhon-detali-zi-stalejj-i-splaviv-avinit-n.html
74. Sahalovych, O. V., Sahalovych, V. V., Ostapchuk, D. P. (2014). Pat. No. 95405 UA. Znosostiyke ionno-plazmove pokryttia dlia rizhuchoho i formotvornoho instrumentu. No. u201406981; declareted: 20.06.2014; published: 25.12.2014, Bul. No. 24. Available at: https://uapatents.com/7-95405-znosostijjke-ionno-plazmove-pokrittya-dlya-rizhuchogo-i-formotvornogo-instrumentu.html
75. Sagalovych, O. V., Popov, V. V., Sagalovych, V. V. (2019). Plasma precision nitriding avinit of metals and alloys. Technological systems, 4 (89), 50–56. doi: https://doi.org/10.29010/89.8
76. Sagalovych, A., Popov, V., Sagalovych, V., Dudnik, S., Bogoslavzev, V., Stadnichenko, N., Edinovych, A. (2020). Comparative analysis of the fatigue contact strength of surfaces hardened by cementation and the ion-plasma nitriding Avinit N. Eastern-European Journal of Enterprise Technologies, 6 (12 (108)), 20–27. doi: https://doi.org/10.15587/1729-4061.2020.217674
77. Sagalovych, A., Popov, V., Sagalovych, V., Dudnik, S., Edinovych, A. (2021). Application of Avinit vacuum plasma technologies Avinit to the manufacture of high-precision full-size gears. Mechanics and Advanced Technologies, 5 (1), 79–88. doi: https://doi.org/10.20535/2521-1943.2021.5.1.234484
78. Rozenfel'd, I. L. (1970). Korroziya i zaschita metallov. Moscow: Metallurgiya, 448.
79. Ul'yanin, E. A. (1991). Korrozionno-stoykie stali i splavy. Moscow: Metallurgiya, 256.
80. GOST 9.005-72. Unified system of corrosion and ageing protection. Metals, alloys, metallic and non-metallic coatings. Permissible and impermissible contacts with metals and non-metals. Available at: https://docs.cntd.ru/document/1200007216

81. Mel'nikov, P. S. (1991). Spravochnik po gal'vanopokrytiyam v mashinostroenii. Moscow: Mashinostroenie, 384.
82. Shuyko, Ya. V. (1985). Korrozionnaya stoykost' vakuumnyh ionno-plazmennyh pokrytiy na malouglerodistyh stalyah. Materialy XII konferencii molodyh uchenyh. Lviv, 143–146.
83. Dudnyk, S. F., Sahalovych, V. V. et. al. (1993). Stvorennia koroziyno-stiykoho malotonazhnoho bahatofunktsionalnoho obladnannia dlia khimiko-farmatsevtychnykh vyrobnytstv. Ch. I. Kompozytsiyni koroziyno-stiyki materialy dlia yemkisnoho obladnannia khimiko-farmatsevtychnykh vyrobnytstv. Visnyk farmatsiyi, 1-2, 39–44.
84. Dudnyk, S. F., Sahalovych, V. V. ta in. (1993). Stvorennia koroziyno-stiikoho malotonazhnoho bahatofunktsionalnoho obladnannia dlia khimiko-farmatsevtychnykh vyrobnytstv. Ch. II. Vyvchennia koroziynoi stiykosti konstruktsiynykh stalei z metalevymy pokryttiamy pry syntezi likarskykh zasobiv. Visnyk farmatsiyi, 3-4, 53–59.
85. Ivanov, V. E., Nechiporenko, E. P., Krivoruchko, V. M., Sagalovich, V. V. (1974). Kristallizaciya tugoplavkih metallov iz gazovoy fazy. Moscow: Atomizdat, 264.
86. Nikitin, M. M. (1992). Tehnologiya i oborudovanie vakuumnogo napyleniya. Moscow: Metallurgiya, 112.
87. Dudnik, S. F., Sagalovich, A. V., Sagalovich, V. V. (2003). Application of metal coatings for protecting welded joints prone to electrochemical corrosion. Fizicheskaya inzheneriya poverhnosti, 1 (3-4), 329–333. Available at: http://dspace.nbuv.gov.ua/bitstream/handle/123456789/98454/10-Dudnik.pdf?sequence=1
88. Gel'd, P. V., Ryabov, R. A. (1974). Vodorod v metallah i splavah. Moscow: Metallurgiya, 272.
89. Galaktionova, N. V. (1967). Vodorod v metallah. Moscow: Metallurgiya, 304.
90. Trapnell, B. M. W. (1953). The activities of evaporated metal films in gas chemisorption. Proceedings of the Royal Society of London. Series A. Mathematical and Physical Sciences, 218 (1135), 566–577. doi: https://doi.org/10.1098/rspa.1953.0125
91. Gorshkov, I. E. (1952). Lit'e slitkov cvetnyh metallov i splavov. Moscow: Metallurgizdat, 416.
92. Fromm, E., Gebhardt, E.; Linchevskiy, B. V. (Ed.) (1980). Gazy i uglerod v metallah. Moscow: Metallurgiya, 712.
93. Cochran, C. N. (1961). The Permeability of Aluminum to Hydrogen. Journal of The Electrochemical Society, 108 (4), 317. doi: https://doi.org/10.1149/1.2428079
94. Kagan, Yu. N. (Ed.) (1981). Vodorod v metallah. Moscow: Mir, 475.
95. Kolachev, B. A., Levinskiy, Yu. V. (Ed.) (1987). Konstanty vzaimodeystviya metallov s gazami. Moscow: Metallurgiya, 368.

96. Mihaylovskiy, Yu. N., Strekalov, P. V. (1972). Kinetika nachal'nyh stadiy okisleniya cinka v atmosfere kisloroda i vlazhnogo vozduha. Zaschita metallov, 8 (2), 146–151.
97. Filyand, M. A., Semenova, E. I. (1964). Svoystva redkih elementov. Moscow: Metallurgiya, 913.
98. Pauell, K. (Ed.) (1970). Osazhdenie iz gazovoy fazy. Moscow: Atomizdat, 471.
99. Danilin, B. S. (1989). Primenenie nizkotemperaturnoy plazmy dlya naneseniya tonkih plenok. Moscow: Energoatomizdat, 328.
100. Glazunov, G. P., Svinarenko, A. D., Kosiv, N. L. et. al. (1980). Otkachka vodoroda palladiem s pokrytiem cirkoniy-alyuminievyh splavov. Voprosy atomnoy nauki i tehniki. Seriya «Obschaya i yadernaya fizika», 4 (14), 87–90.
101. Glazunov, G. P., Sagalovich, V. V. Ternopol, A. M., Volkov, E. D., Yuferov, V. B. (1983). Vodorodopronicaemost' palladiya posle obrabotki plazmoy tleyuschego razryada. Voprosy atomnoy nauki i tehniki. Seriya FRPRM, 4 (27), 63–65.
102. Lifshic, I. M., Slezov, V. V. (1958). O kinetike diffuzionnogo raspada peresyschennyh tverdyh rastvorov. ZhETF, 35 (2), 479–492. Available at: http://chair.itp.ac.ru/biblio/papers/ClassicPapersSeminar/LifshitsSlezov1958.pdf
103. Lifshitz, I. M., Slyozov, V. V. (1961). The kinetics of precipitation from supersaturated solid solutions. Journal of Physics and Chemistry of Solids, 19 (1-2), 35–50. doi: https://doi.org/10.1016/0022-3697(61)90054-3
104. Slezov, V. V., Sagalovich, V. V. (1975). Teoriya koalescencii v mnogokomponentnyh mnogofaznyh sistemah. Fizika tverdogo tela, 17, 1497–1499.
105. Slezov, V. V., Sagalovich, V. V. (1977). Theory of diffusive decomposition of supersaturated multicomponent systems. Journal of Physics and Chemistry of Solids, 38 (9), 943–948. doi: https://doi.org/10.1016/0022-3697(77)90193-7
106. Slezov, V. V., Sagalovich, V. V. (1987). Diffusive decomposition of solid solutions. Uspekhi Fizicheskih Nauk, 151 (1), 67–104. doi: https://doi.org/10.3367/UFNr.0151.198701c.0067
107. Slezov, V. V., Sagalovich, V. V., Tanatarov, L. V. (1978). Theory of diffusive decomposition of supersaturated solid solution under the condition of simultaneous operation of several mass-transfer mechanisms. Journal of Physics and Chemistry of Solids, 39 (7), 705–709. doi: https://doi.org/10.1016/0022-3697(78)90002-1
108. Portnoy, K. I. (1968). Dispersno-uprochnyaemye zharoprochnye splavy. Poroshkovaya metallurgiya: Materialy IX Vsesoyuznoy konf. po poroshkovoy metallurgii. Riga: Latv. in-t NTI, 205–208.

109. Sergeenkova, V. M., Berezuckiy, V. V. (1968). Rost dispersnyh okisnyh chastic v metallokeramicheskom nikele. Poroshkovaya metallurgiya: Materialy IX Vsesoyuznoy konferencii po poroshkovoy metallurgii. Riga: Latv. in-t NTI, 219.
110. Footner, P. K., Alcock, C. B. (1972). Growth kinetics of dispersed thoria in Ni and Ni-Cr alloys. Metallurgical Transactions, 3 (10), 2633–2637. doi: https://doi.org/10.1007/bf02644239
111. Martin, Dzh., Doerti, R. (1978). Stabil'nost' mikrostruktury metallicheskih sistem. Moscow: Atomizdat, 280.
112. Kreydera, K. (Ed.) (1978). Kompozicionnye materialy s metallicheskoy matricey. Vol. 4. Moscow: Mir, 503.
113. Mozzhuhin, E. I. (1968). O termicheskoy stabil'nosti dispersnyh okisnyh vklyucheniy. V kn.: Vysokotemperaturnye materialy. Moscow: Metallurgiya, 79.
114. Mehan, R., Nun, M. (1974). Nikelevye splavy, uprochnennye voloknami α-Al_2O_3. V kn.: Kompozicionnye materialy s metallicheskoy matricey. Vol. 4. Moscow: Mir, 165.
115. Balliger, N. K., Honeycombe, R. W. K. (1980). Coarsening of vanadium carbide, carbonitride, and nitride in low-alloy steels. Metal Science, 14 (4), 121–133. doi: https://doi.org/10.1179/030634580790426337
116. Zwilsky, K. M., Grant, N. Y. (1961). Dispersion strenghtening in the copper-aluminium system. Trans AIME, 221, 371.
117. Chuistov, K. V. (1975). Modulirovannye struktury v stareyuschih splavah. Kyiv: Naukova dumka, 232.
118. Berezhnoy, A. S. (1968). O subsolidusnom stroenii mnogokomponentnyh fiziko-himicheskih sistem. UHZh, 9, 920.
119. Kofstad, P. (1975). Otklonenie ot stehiometrii, diffuziya i elektroprovodnost' v prostyh okislah metallov. Moscow: Mir, 396.
120. Kiryuhin, N. M., Sagalovich, A. V., Sagalovich, V. V., Chabanovskiy, V. N. (1991). Chislennoe modelirovanie processov diffuzionnogo raspada. Kharkiv, 15.
121. Simson, A. E., Homich, A. Z., Kuric, A. A. et. al. (1980). Dvigateli vnutrennego sgoraniya. Teplovoznye dizeli, gazoturbinnye ustanovki. Moscow: Transport, 389.
122. Antipov, V. V. (1972). Iznos precizionnyh detaley i narushenie harakteristiki toplivnoy apparatury dizeley. Moscow: Mashinostroenie, 177.
123. Sagalovich, A. V., Dudnik, S. F., Lyubchenko, A. P., Oleynik, A. K., Sagalovich, V. V. (2008). Uprochnenie kromok maslos'emnyh porshnevyh kolec dizelya D80 nanokompozitnymi pokrytiyami na osnove Ti-Al-N. Nanostrukturnye materialy. Mater. Pervoy mezhdunar. Nauchn. Konf. NANO-2008. Minsk.
124. Polyanin, B. I. et. al. (1985). Vakuumno-plazmennaya kondensaciya bronzy. Aviacionnaya promyshlennost', 5, 60–62.

125. Dudnik, S. F., Sagalovich, A. V., Sagalovich, V. V., Lyubchenko, A. P., Oleynik, A. K. (2006). Issledovanie tribologicheskih harakteristik mnogosloynyh pokrytiy. Mater. Mezhd. Konf. po nerazrushayuschemu kontrolyu. Berlin.
126. Sagalovich, A. V., Sagalovich, V. V., Lyubchenko, A. P., Oleynik, A. K. (2008). Issledovanie tonkosloynyh vakuumnyh pokrytiy dlya detaley toplivnoy apparatury teplovoznyh dizel'nyh dvigateley. Mater. XIV Mezhd. konf. «Fizicheskie i komp'yuternye tehnologii v narodnom hozyaystve». Kharkiv, 28–32.
127. Sagalovich, A. V., Sagalovich, V. V., Dudnik, S. F., Oleynik, A. K. (2008). Issledovanie tonkosloynyh vakuumnyh pokrytiy dlya detaley toplivnoy apparatury. Mater. Mezhd. konf. «Ispol'zovanie pnevmaticheskoy energii i oborudovaniya dlya ee polucheniya v gornorudnoy otrasli». Sumy.
128. Sahalovych, O. V., Sahalovych, V. V. (2013). Pat. No. 89830 UA. Kompozytsiyne pokryttia dlia aliuminiu abo yoho splaviv. No. u201315445; declareted: 30.12.2013; published: 25.04.2014, Bul. No. 8. Available at: https://uapatents.com/7-89830-kompozicijjne-pokrittya-dlya-alyuminiyu-abo-jjogo-splaviv.html
129. Sagalovich, A. V., Sagalovich, V. V. (2014). Pat. No. 2585112 RU. Composite coating for aluminium or alloys thereof. No. 2014101978/02; declareted: 22.01.2014; published: 27.05.2016, Bul. No. 15. Available at: https://patents.s3.yandex.net/RU2585112C2_20160527.pdf
130. Sagalovich, A. V., Sagalovich, V. V., Dudnik, S. F., Lyubchenko, A. P., Oleynik, A. K. (2005). Nanesenie antizadirnyh i iznosostoykih pokrytiy na porshni iz alyuminievogo splava dizeley tipa D80. Sovmestnyy nauchno-tehnicheskiy otchet NTC «Nanotehnologiya» i GP «Zavod im. Malysheva». Kharkiv, 27.
131. Dudnik, S. F., Lubchenko, A. P., Oleynik, A. K., Sagalovich, A. V., Sagalovich, V. V. (2004). The investigation of friction and wear characteristics of ion-plasma coatings, received on the aluminum alloy. Fizicheskaya inzheneriya poverhnosti, 2 (1-2), 112–116. Available at: http://dspace.nbuv.gov.ua/bitstream/handle/123456789/98482/16-Dudnik.pdf?sequence=1
132. Sagalovych, A. V., Dudnik, S. F., Lubchenko, A. P., Oleynik, A. K., Sagalovych, V. V. (2006). The Investigation of Friction and Wear Characteristics of Ion-Plasma Coatings, Received on the Aluminum Alloy. Proc. Int. Symp. on Tribology. Amsterdam.
133. Sagalovich, A. V., Sagalovich, V. V., Dudnik, C. F., Oleynik, A. K., Moschenok, V. A. (2009). Opredelenie tribotehnicheskih harakteristik kompozitnyh ionno-plazmennyh pokrytiy dlya porshnevyh kolec dizel'nyh dvigateley. Vestnik HNADU, 46, 111–113.
134. Sagalovich, A. V., Dudnik, S. F., Sagalovich, V. V. et. al. (2001). Nanesenie opytnyh pokrytiy na stal'nye detali «Gayka nazhimnaya 457.81.027-1». Otchet HKBD.

135. Popov, V., Loginov, V., Ukrainets, Y., Shmyrov, V., Steshenko, P., Hlushchenko, P. (2020). Improving aircraft fuel efficiency by using the adaptive wing and winglets. Eastern-European Journal of Enterprise Technologies, 2 (1 (104)), 51–59. doi: https://doi.org/10.15587/1729-4061.2020.200664
136. Kostyuk, G. I., Popov, V. V. (2019). Scientific principles of designing information of a cutting tool with nano coatings and nanostructures. Open Information and Computer Integrated Technologies, 83, 81–97. doi: https://doi.org/10.32620/oikit.2019.83.06
137. Kostyuk, G. I., Popov, V. V., Romanov, M. S., Torosyan, G. D., Kostyuk, E. G. (2019). Machining of hard-to-work alloys with cutting tools with nanostructures. Open Information and Computer Integrated Technologies, 85, 96–110. doi: https://doi.org/10.32620/oikit.2019.85.05
138. Kostyuk, G., Popov, V. (2019). Improving the resource and reliability of details from zirconium alloys during the application of nanocoating and formation of nanostructures. Visnyk Natsionalnoho tekhnichnoho universytetu «KhPI». Seriya: Tekhnolohiy v mashynobuduvanni, 19 (1344), 40–50. Available at: http://repository.kpi.kharkov.ua/bitstream/KhPI-Press/42270/1/vestnik_KhPI_2019_19_Kostyuk_Povyshenie_resursa.pdf
139. Kostyuk, G. I., Popov, V. V., Kostyk, K. O. (2019). Design of the cutting tool material taking into account the type of nanocoating hardening. Technological Systems, 2 (87), 25–37. doi: http://dx.doi.org/10.29010/087.3
140. Kostyuk, G. I., Grigor, O. D., Popov, V. V., Kostyuk, E. G. (2018). Sravnenie temperaturnyh rezhimov i napryazhennogo sostoyaniya splava «VOLKAR» pri ispol'zovanii teplofizicheskih i termomehanicheskih harakteristik. Proceedings of XII International conference on science an deducation. Oslo, 45–48. Available at: http://library.khnu.km.ua/wp-content/uploads/2019/02/konfer_hnu/SE2018.pdf
141. Kostyuk, G. I., Romanov, M. S., Torosyan, G. D., Popov, V. V. (2019). Effektivnost' i rabotosposobnost' rezhuschego instrumenta iz modificirovannogo tverdogo splava VK10 s pokrytiem 0,18HfN+0,82ZrN pri frezerovanii titanovogo splava VT22. Proceedings of XIII Internationalconference on scienceand education. Hajduszoboszlo, 55–57.
142. Kostyuk, G. I., Popov, V. V., Bryika, O. O. (2019). Study of energy ions, their varieties and charge on temperature, rate of temperature rise, thermal stresses for nanostructureson steel materials. Proceedings of XIV International conference on modern achievements of science and education. Netanya, 63–66. Available at: https://er.nau.edu.ua/bitstream/NAU/42327/1/Study%20of%20Energy%20Ions%2c%20

their%20Varieties%20and%20Charge%20on%20Temperature%2c%20Rate%20of%20Temperature%20Rise.pdf
143. Kostyuk, G. I., Popov, V. V., Bruyaka, O. O. (2020). Perspektivy konstruirovaniya materiala RI i ego geometrii s uchetom uprochneniya i obrabatyvaemogo materiala. XIV International conference on science and education, Hajduszoboszlo, 40–42. Available at: http://elar.khnu.km.ua/jspui/handle/123456789/8571
144. Kostyuk, G. I., Popov, V. V. (2019). Nauchnye principy konstruirovaniya rezhuschego instrumenta s nanopokrytiyami i nanostrukturami. XXIX International Conference «New Leading Technologies in Machine Building». Koblevo-Kharkiv, 9.
145. Kostyuk, G. I., Popov, V. V., Yevsieienkova, H. V., Torosyan, G. D. (2020). Prospects for designing the chemical composition of hard alloys, taking into account their hardening due to the formation of nanostructures. Suchasni tekhnolohiyi u promyslovomu vyrobnytstvi: tezy dop. VII Vseukr. nauk.-tekhnol. konf. Sumy, 89–90. Available at: https://essuir.sumdu.edu.ua/bitstream-download/123456789/78515/1/stpv_2020.pdf;jsessionid=F702AFAB446AEFE841A8794C83358AE4
146. Popov, V., Kostyuk, G., Tymofyeyev, O., Kostyk, K., Naboka, O. (2020). Design of New Nanocoatings Based on Hard Alloy. Lecture Notes in Mechanical Engineering, 522–531. doi: https://doi.org/10.1007/978-3-030-50794-7_51
147. Kostyuk, G., Popov, V., Kostyk, K. (2019). Computer Modeling of the obtaining nanostructures process under the action of laser radiation on steel. Proceedings of the Second International Workshop on Computer Modeling and Intelligent Systems (CMIS-2019). Zaporizhzhia, 729–743. Available at: http://ceur-ws.org/Vol-2353/paper58.pdf
148. Popov, V., Kostyuk, G., Nechyporuk, M., Kostyk, K. (2020). Study of Ions Energy, Their Varieties and Charge on Temperature, Rate of Temperature Rise, Thermal Stresses for Nanostructures on Construction Materials. Advanced Manufacturing Processes, 470–477. doi: https://doi.org/10.1007/978-3-030-40724-7_48
149. Kostyuk, G., Popov, V., Kostyk, K. (2020). Volume of the Nanocluster and Its Depth at Effect of Ions of Different Energies, Varieties and Charges on Titanium Alloy VT-1. Advanced Manufacturing Processes, 415–423. doi: https://doi.org/10.1007/978-3-030-40724-7_42
150. Popov, V. (2020). Perspektyvni napriamky rozvytku ahrehatobuduvannia u aviatsiyniy haluzi ta mashynobuduvanni. Proceedings XXX International Conference «New Leading Technologies In Machine Building». Koblevo-Kharkiv, 17. Available at: https://khai.edu/assets/documents/3205/%D0%A1%D0%B1%D0%BE%D1%80%D0%BD%D0%B8%D0%BA%20%D1%82%D0%B5%D0%B7%D0%B8%D1%81%D0%BE%D0%B2%202020.pdf

151. Goloschapov, F. A., Kuznecov, I. A., Petrov, V. P., Pestov, Yu. A., Semenov, V. N., Derkach, G. G., Dodonov, A. I. (2000). Pat. No. 2000109697A RU. Method of ion-plasma application of coatings on a substrate. No. 2000109697/02; declareted: 20.04.2000; published: 10.04.2002. Available at: https://patents.google.com/patent/RU2000109697A/en
152. Karpman, M. G., Fetisov, G. P., Saydahmedov, R. H. (1992). Pat. No. 2025543 RU. Wear resistant ion-plasma coating and method to obtain wear resistant coating. No. 5033556/21; declareted: 24.03.1992; published: 30.12.1994. Available at: https://patentimages.storage.googleapis.com/62/83/93/a293e120913164/RU2025543C1.pdf
153. Shchanin, P. M., Koval', N. N., Borisov, D. P., Goncharenko, I. M. (1998). Pat. No. 2131480 RU. Method of wear-resistant coating formation on surface of articles made of structural steel. No. 97112300/02; declareted: 07.15.1998; published: 10.06.1999. Available at: https://yandex.ru/patents/doc/RU2131480C1_19990610
154. Vajnshtejn, D. L., Kovalev, A. I. (2010). Pat. No. 2405060 RU. (TixAlyCrz)N-Based Ion-Plasma Coar For Cutting Tools. No. 2009137989/02; declareted: 15.10.2009; published: 27.11.2010. Available at: https://yandex.ru/patents/doc/RU2405060C1_20101127
155. Chumikov, A. B., Akif'ev, V. A., Sizyh, Yu. N. (2000). Pat. No. 2210621 RU. Sposob kombinirovannoy vakuumnoy ionno-plazmennoy obrabotki instrumenta. No. 2000123120/02; declareted: 05.09.2000; published: 20.08.2003. Available at: https://www.freepatent.ru/patents/2210621
156. Pat. No. 2009/0123737 US. Coated Surface Coating Resistant to Erosion by Solid Particles. published: 14.05.2009.
157. Sagalovich, A. V., Dudnik, S. F., Sagalovich, V. V. (2005). Mnogokomponentnye nanostrukturnye pokrytiya vpn dlya rezhuschego instrumenta. Instrumentalnyi svit, 1 (25), 15–16.
158. Sagalovich, A. V., Dudnik, S. F., Sagalovich, V. V. (2007). Povyshenie resursa raboty vyrubnogo i press-shtampovogo instrumenta putem primeneniya iznosostoykih pokrytiy. Oborudovanie i instrument, 5, 329–334.
159. Sagalovich, A. V., Dudnik, S. F., Sagalovich, V. V., Zvonik, A. A. (2005). Uprochnyayuschie pokrytiya dlya formoizmenyayuschih chastey shtampov. Oborudovanie i instrument, 10, 1–4.
160. Sagalovich, A. V., Dudnik, S. F., Sagalovich, V. V. (2005). Nanotehnologii-promyshlennye tehnologii XXI veka. Oborudovanie i instrument, 6, 46–49.
161. Ostapchuk, D. P., Sahalovych, O. V., Sahalovych, V. V. (2014). Pat. No. 95071 UA. Sposib formuvannia znosostiykoho ionno-plazmovoho pokryttia dlia rizhuchoho i formotvornoho instrumentu. No. u201406979; declareted: 20.06.2014; published: 10.12.2014, Bul. No. 23. Available at: https://uapatents.com/7-95071-sposib-formu-

vannya-znosostijjkogo-ionno-plazmovogo-pokrittya-dlya-rizhuchogo-i-formotvornogo-instrumentu.html
162. Sahalovych, V. V., Sahalovych, O. V., Ostapchuk, D. P. (2014). Pat No. 111514 UA. Znosostiyke ionno-plazmove pokryttia dlia rizhuchoho i formotvornoho instrumenta i sposib yoho oderzhannia. No. a201406976; declareted: 20.06.2014; published: 10.05.2016, Bul. No. 9. Available at: https://uapatents.com/8-111514-znosostijjke-ionno-plazmove-pokrittya-dlya-rizhuchogo-i-formotvornogo-instrumenta-i-sposib-jjogo-oderzhannya.html